Aus der Universitätsklinik für Radioonkologie mit Poliklinik Tübingen

Heterogeneous impact of hypoxia on cellular radiation sensitivity of three squamous cell carcinoma lines

Inaugural-Dissertation
zur Erlangung des Doktorgrades
der Medizin

der Medizinischen Fakultät
der Eberhard Karls Universität
zu Tübingen

vorgelegt von

Hauth, Franziska Dorothea

2018

Dekan:	Professor Dr. I. B. Autenrieth
1. Berichterstatter:	Professor Dr. D. Zips
2. Berichterstatter:	Professor Dr. C. Petersen
3. Berichterstatter:	Professor Dr. D. Vordermark

Tag der Disputation: 19.03.2018

Table of contents

Abbreviations

ATCC	=	American Type Culture Collection
ATM	=	Ataxia Teleangiectasia Mutated
ATR	=	Ataxia Teleangiectasia and Rad3 - related
BSA	=	Bovine serum albumin
CFA	=	Colony Forming Assay
CHK-1	=	Checkpoint Kinase 1
CTx	=	Chemotherapy
DAB	=	3,3' Diaminobenzidine
DAPI	=	4',6 Diamidino-2-phenylindone
DDR	=	DNA damage response
DMEM	=	Dulbecco's Minimum Essential Medium
DMF	=	Dose- modifying Factor
DNA	=	Desoxyribonucleid Acid
DNA-PK	=	DNA- Protein Kinase
DSB	=	Double Strand Break
DT	=	Doubling Time
ECL	=	Enhanced Chemiluminescence
FCS	=	Fetal Calf Serum
HIF 1α	=	Hypoxia Inducible Factor 1 alpha
HMF	=	Hypoxia Modification Factor
HR	=	Homologous Recombination
hSCC	=	human Squamous Cell Carcinoma
MEF	=	mouse embryonic fibroblasts
NHEJ	=	Non-Homologous End Joining
mmHg	=	mm of Mercury
OER	=	Oxygen Enhancement Ratio
PBS	=	Phosphate Buffered Saline
PE	=	Plating Efficiency
PIKK	=	phosphatidylinositol-3-OH-kinase like family of protein kinases
ROS	=	reactive oxygen species

RT	=	Room Temperature
RTx	=	Radiation therapy
SDS-PAGE	=	Sodium Dodecyl Sulfate Polyacrylamide Gel Electrophoresis
SF	=	Surviving Fraction
SSB	=	Single Strand Break

1 INTRODUCTION

The outcome of a cancer treatment course is mainly determined by the ability of the main treatment modalities, namely surgery, radiation therapy (RTx) and chemotherapy (CTx) to locally and systematically control the tumour expansion. However, the efficiency of the therapeutic options to eradicate tumour cells is hurdled among other reasons by the heterogeneity of the tumour microenvironment (2, 3). Solid tumours maintain their continuous augmentation by becoming insensitive to tissue homeostatic signals and developing their own vascular network. The uncontrolled cellular proliferation coupled with the functional and structural abnormalities of the newly formed tumour blood vessels generate tumour subvolumes that are deficient in oxygen (4, 5). Existence of tumour hypoxia has an adverse treatment outcome mainly because it renders tumour cells more radioresistant due to lower induction of DNA damage (6-8). However, in recent years several lines of evidence from basic and clinical research suggest that hypoxia exposure promotes a more aggressive and resistant cellular phenotype. In the present study, the potential impact of hypoxia on determining cellular survival after treatment with ionizing radiation was functionally assessed in human tumour cells *in vitro.*

1.1 Existence of hypoxia in experimental and human tumours

Tumour growth is enabled due to disturbance of the normal tissues homeostatic mechanisms aiming to maintain a defined number of cells within the context of a given tissue. Tackling tissue homeostasis is empowered to the tumour cells via the progressive acquisition of biological capabilities during the carcinogenesis known as the hallmarks of cancer, namely, evading growth suppression, resisting cell death, sustaining proliferative signaling, inducing angiogenesis, enabling replicative immortality, activating invasion and metastasis, reprogramming of energy metabolism and evading immune destruction initially established and recently reviewed (2). Neoplastic cells under the selection pressure of the induced genetic instability, an enabling characteristic of malignant cells, accumulate mutations in their genome, which renders them insensitive to tissue anti-growth signals and allows them to acquire replicative immortality and to sustain proliferation signals (3). As a consequence, cell production is favored over cell loss

leading to the expansion of tumour cell population. However, the neoplastic cells would have to face oxygen deprivation and nutrient starvation as they progressively move away from the tissue vessels due to the continuous proliferation of the cells adjacent to the blood vessels (5).

In order to support the cellular outgrowth, tumours develop their own vasculature network from already established normal tissue vessels to ensure blood supply and thus nutrient and oxygen availability. The latter occurs via a sophisticated cell-to-cell interaction process, known as angiogenesis, consisting one of the key players in the continuous enlargement of the tumour mass. It is occurring via at least three different mechanisms, namely intussusception, vascular splitting and sprouting angiogenesis, which is by far the most commonly observed process (4). Induction of angiogenesis or turning on the "angiogenic switch" is a crucial step in tumour progression since it not only serves to maintain the continuous tumour growth but also enables the tumour cells to metastasize through vascular dissemination. In the molecular level, it seems to arise as an overexpression of pro-angiogenic factors such as members of the vascular endothelial growth factor (VEGF), angiopoietin (ANG-1), fibroblast growth factors (FGFs) and several classes of chemokines (9) against anti-angiogenic factors e.g. thrombospondin-1 (TSP-1). Upon sensing the pro-angiogenic signal, the quiescent blood vessels respond by degrading their mature structure and initiate a program involving proliferation, vascular elongation through formation of endothelial cell phalanx and migration of the newly formed endothelial cells. As a final step, the migrated endothelial cells resume their quiescent state and under the expression of signaling cascades such as platelet derived factor B (PDGF-B), transforming growth factor–β (TGF-β), ANG-1, ephrin B2 and NOTCH recruitment of pericytes promotes maturation of the newly formed vessels in order to become functional and allow the blood flow (4, 10). The critical role of VEGF as a factor in angiogenesis has been extensively investigated and reviewed (4, 5). However, cancer cells can produce other pro-angiogenic signals, like interleukin-8 or chemokines (CXCL12) through autocrine or paracrine way via stimulation of the tumour-associated stroma or tumour associated bone marrow derived cells to stimulate or further amplify tumour angiogenesis (5, 9). The latter might explain the reason why despite the initial promise, *in vivo* studies have shown that inhibition of angiogenesis either through

VEGF inhibition alone or in combination with other angio-kinase inhibition did not have an impact on local tumour control although vessel area was reduced significantly (11).
In normal tissue, where due to the balanced structure of the inherent vascular architecture the oxygen demand of the underlying tissue is adequately supported by the oxygen supply and maintained at a partial oxygen pressure ranging between 20 and 80 mmHg (12, 13). However, in solid tumours the nascent blood vessels lack the normal tissue architecture causing the rapidly growing tumour mass with an increased oxygen consumption rate to "outrun" the provided insufficient blood supply. In addition, the newly formed tumour vessels are commonly appearing with substantial structural and therefore functional abnormalities causing blind ends, loops and arterio-venous shunts that together result in a heterogeneous and unstable blood flow within the tumour mass, mainly due to lack of sufficient smooth muscle cells support. As a result of these diverse procedures, tumours develop subvolumes that are nutrient and oxygen deprived, rendering hypoxia as a commonly observed phenomenon in most solid tumours. In the clinical setting, hypoxia is generally defined as a state of reduced availability of oxygen resulting in decreased oxygen partial pressures. In this regard, anoxia is characterized as the complete absences of oxygen in tissue, equaling an oxygen partial pressure of 0 mmHg. Critical hypoxic levels, with progressive restrictions to cellular functions and activities, seem to range between 35 mmHg and 0.02 mmHg. For squamous cell carcinoma a median pO_2 of 15 mmHg with a range of median pO_2 between 24 to 66 mmHg for normal tissue has been described (13).

Hypoxia within the tumour emerges as a consequence of the oxygen supply inability to meet the oxygen demand of the growing tumour cell population. This arises mainly through two different mechanisms, which give rise to two distinct types of hypoxia. The insufficient amount of blood vessels to support the expanding tumour mass, coupled with the high oxygen consumption rate of the constantly proliferating tumour cells even in micro-environmental conditions where oxygen or nutrients are diminished, generates oxygen gradients around the perfused blood vessels and in increased distances (greater than 100 μm) oxygen diffusion is reduced giving rise to diffusion-limited or "chronic" hypoxia (14, 15). On the other hand, the structural abnormalities of the tumour blood vessels can cause transient disturbances to the blood flow leading to perfusion-limited or

acute hypoxia. The main difference of the two types of hypoxia lies in the duration of exposure. Acute hypoxia is generally defined as exposure to low intracellular oxygen for minutes to hours followed by rapid reoxygenation, while in chronic hypoxia cells are confronted with low oxygen tension for prolonged periods of time (hours to days). These two diverse effective causes of hypoxia generate a highly dynamic tumour microenvironment where tumour cell subpopulations might be exposed to acute, chronic or cycles of variable extend and duration of hypoxia followed by reoxygenation (cycling hypoxia), implicating that one tumour might contain cell subpopulations with different oxygen tension ranging from anoxia to normoxia and in turn undermine substantial differences in their respective biological behavior (16, 17). Additional pathogenic conditions that might give rise to hypoxia include tumour-associated or treatment-related anemia (anemic hypoxia), resulting in a decreased ability of blood to transport oxygen, or oxygenation might be limited due to pulmonary disease (hypoxemic hypoxia).

The first evidence for the existence of tumour hypoxia as a result of oxygen diffusion distance limitation was reported as early as 1955 by Thomlinson and Gray, who described the occurrence of tumour necrosis as a function of distance from vessels in human tumours (18). Thereafter the existence of hypoxic subareas or hypoxic tumour cell populations in both human and experimental tumours has been demonstrated with numerous different approaches. The most prominent technique, though invasive, for direct assessment of tumour oxygenation has been the polarographic oxygen needle electrodes measuring the oxygen partial pressure (pO_2). They have been extensively used to estimate pO_2 distribution across the same or different tumours and indicated a large intra-tumoural and inter-tumoural heterogeneity of oxygen pressure in a number of experimental and human tumours (8, 19). The presence of hypoxic tumour cells have been manifested and also quantitatively assessed by the means of immunohistochemistry (IMH) in cross-sections from experimental and patient-derived tumours. This method takes advantage of the fact that actively metabolic hypoxic cells overexpress gene and proteins cascades that allows adaptation to the hypoxic microenvironment. Several of these hypoxia-induced genes have been identified and can be visualized when targeted with appropriate antibodies, with the most commonly used being the transcription factor hypoxia inducible factor 1 (HIF1) (20), carbonic anhydrase IX (21) or downstream targets

of these pathways or proteins associated in different ways to hypoxia adaptation e.g. the glucose transporters that mediate the intracellular glucose content during anaerobic glycolysis (22). An alternative way for detecting the presence of hypoxic cells with IMH is to administer exogenous hypoxia markers and then stain the tumour sections. These are chemical compounds that are rapidly diffuse in the tumour tissue and are specifically bio-reduced in hypoxic tumour cells. This method has been extensively used in experimental animal tumours but also in humans, with the most commonly used chemicals being members of 2-nitroimidazoles e.g. pimonidazole and EF5 (23, 24). The limitation of invasiveness of these methods can be overcome when visualizing the whole tumour *in situ* with the use of radiological or nuclear medicine imaging approaches. These methods hold the promise of being rapidly implemented in clinical studies to detect the presence of hypoxia in patient tumours. They mainly include the use of Positron Emission Tomography (PET) and the most widely used hypoxia PET tracers involve Fluor-18 (^{18}F)-labelled 2-nitroimidazole markers e.g. Fluoromisonidazole (FMISO) and have been extensively studied for imaging hypoxia in experimental (25) or cancer patients tumours (26, 27). A more indirect imaging of hypoxia is to evaluate perfusion parameters from dynamic contrast-enhanced MRI (DCE-MRI) (27). Such approaches offer the possibility for repetitive assessment of hypoxia of the same patients in different time points during their treatment.

1.2 Impact of tumour hypoxia in treatment outcome

Tumour hypoxia represents a negative prognostic factor for the outcome of cancer patients. It has been shown for different cancer types, involving the prostate, cervix, breast and head and neck, that patients with tumours containing larger proportions of hypoxic cells have decreased disease-free survival than patients with less hypoxic tumours, confirming the presence of intra-tumoural hypoxia to be a negative prognostic factor for long term survival (8, 19, 28, 29). The latter has been extensively demonstrated from meta-analysis studies especially for squamous cell carcinomas of head and neck region and cervix and it is strongly supported from experimental evidence. A large multi-center study on head and neck cancer patients indicated that low pre-treatment pO_2 was associated with poor prognosis (8). Clinical trials using the PET imaging of hypoxia either

with fluoroazomycin arabinoside (FAZA) (30) or Fluoromisonidazole (FMISO) (31), which have the major advantages that they are non-invasive and can be easily repeated in the same patient at different time points. Furthermore, they can also be applied prospectively and have demonstrated a prognostic potential of hypoxia imaging prior to treatment in HNSCC. Additional studies confirmed that pretreatment tumour oxygenation status is not only highly prognostic for survival and the occurrence of metastatic disease but also a predictive marker of loco-regional tumour control after irradiation treatment (8, 31). Similarly, pre-treatment pimonidazole hypoxic fraction was predictive for the tumour control dose in 10 different human squamous cell carcinoma lines grown as human tumour xenografts (32).

Additional evidence for the impact of tumour hypoxia on the therapeutic outcome arises from the results of clinical trials aiming to counteract the hypoxic microenvironment of solid tumours. Several approaches have been used in the literature intending either to enhance the oxygen deliver from the blood circulation e.g. use of Hyperbaric oxygen (HBO), carbogen and/or nicotinamide breathing, application of oxygen-mimetic compounds e.g. nitroimidazoles, targeting directly the hypoxic cells with hypoxic cell cytotoxins or eliminating the hypoxic cell radioresistance via the use of heavy ions irradiation high linear energy transfer (LET). The outcome of large randomize trials clearly demonstrate that cancer patients benefit from approaches aiming to overcome tumour hypoxia e.g. HBO breathing in cervix carcinomas (Medical Research Council), use of nimorazole in HNSCC (Danish Head and Neck Cancer Study) (33), use of Carbogen and Nicotinamide breathing in an accelerated radiotherapy for HNSCC cancer patients (ARCON) (34). Interestingly retrospective analysis of the randomize trials indicated that patients with more hypoxic tumours had a significantly worse treatment outcome (irrespectively of the endpoint used per study) and that only patients with higher extend of hypoxia either prior or during the treatment benefit from the treatment modification to overcome hypoxia (31, 35). Accumulated evidence supports strategies involving the selection of patients that will benefit from hypoxic modification based on the extent of hypoxia either prior or during therapy. Recently, several hypoxia gene signatures or hypoxia-induced gene expression classifiers have been validated in translation radiation oncology in experimental animal tumours and are prospectively

validated in patient cohorts (36, 37). In experimental human tumour xenografts several approaches to optimize the oxygen diffusion distances through pharmacological inhibition of molecular pathways that are mediated directly from hypoxia activated genes e.g. HIF inhibitors (38) or indirectly controlled by hypoxia e.g. PI3K /mTOR inhibitors (39) have shown promising results in prolonging tumour growth delay or reducing the dose to locally control the tumour (TCD_{50}) either through reduced mitochondria respiration rate to reduce oxygen consumption, or increased oxygenation status of the tumours through vascular normalization.

The poorer treatment outcome of hypoxic tumours is mainly attributed to the hypoxia-induced malignant progression either through systemic changes to the tumour entity or through cellular acquisition of pro-survival signaling and biochemical resistance to radiotherapy damage induction (12, 40). Systemic changes, involve hypoxia induction of angiogenesis and promotion of metastatic phenotype. Through HIF members mediated downstream signaling cascade, angiogenetic factors such as VEGF have been demonstrated to promote angiogenesis e.g. in prostate cancer patients (10, 41). On the other hand, clinical studies indicate that patients with more hypoxic tumours have a higher risk to develop metastatic disease attesting hypoxia to promote a metastatic phenotype in cancers (42, 43). Possible explanations involve the induction of mesenchymal epithelial transition programming through complex cell-cell and cell-extra cellular matrix (ECM) interactions (44, 45).

Hypoxia promotes the development of more “aggressive” tumour cell phenotype through induction of genetic instability, that in turn allows the acquisition of a mutant genotype by compromising either the surveillance machinery of the DNA integrity or the DNA damage response. It mainly occurs through alteration of ATR and ATM mediated checkpoints, induction of ROS during reoxygenation and modification of DNA repair pathways, mainly impairment of HR (46, 47). Recently a prognostic 100 loci DNA signature has been established for the risk of relapse and metastasis in prostate cancer patients, which consists of genes involved in genetic instability and hypoxia (48).
In addition, hypoxia has been implicated in the induction of pro-survival signaling that renders neoplastic cells independent in growth factor abundance (49) e.g. HIF1 induced

over-expression of TGF-β and PDGF and activation of the Phosphatidylinositol 3-Kinase/Akt pathway with subsequent inactivation of Glycogen Synthase Kinase-3 (50, 51). Hypoxia-driven gene activation such as unfolded protein response pathways mediated through PERK, IRE1 and ATF6, the folding capacity of the endoplasmatic reticulum is increased via regulation of transcription and translation (52, 53) while in parallel cellular metabolism is downregulated through the inhibition of the activity of mTOR, the mammalian target or rapamycine, reducing the oxygen demand of the cell and thus preventing more severe hypoxia (54, 55). Over-expression of amino-acid transporters, glucose transporters, monocarboxylate transporters and acid-base regulating carbonic anhydrases mediated via HIF signaling assist the tumour cell to adapt its energy metabolism (56). Evading apoptosis either through loss of p53 or through upregulation of the anti-apoptotic protein IAP-2 (57, 58) or induction of autophagy, another important response machinery to cellular stress, has been reported to be induced in cells exposed to hypoxia, leading to radioresistance (59, 60). An important factor contributing to treatment outcome is the fact that the hypoxic cells can be 2.5 to 3-fold more radioresistant than their well-oxygenated counterparts. Ionizing radiation induces DNA damage in cells, including DNA DSBs, DNA SSBs, base damage and DNA cross-links, either through direct interaction with the DNA or through indirect interaction after induction of reactive oxygen species (ROS). ROS are a group of chemically highly reactive molecules, including superoxide, hydroxyl and peroxyl radicals. Physiologically, ROS are mainly produced during mitochondrial respiration and are immediately eliminated by the enzyme superoxide dismutase (SOD) and other antioxidant defenses after formation (61). The amount of the DNA-damage induction though is highly dependent upon the oxygen tension at the time of irradiation and it has been long demonstrated that irradiation under hypoxia leads to an increase of radioresistance in tumour cells as well as cells of normal tissue as a function of the oxygen tension (62). The mechanism of hypoxia induced radioresistance is commonly explained by the oxygen fixation theory, stating that the indirect effect of radiation is highly reduced under conditions of hypoxia as fewer oxygen-molecules are present and thus less radicals are induced therefore preventing the "fixation" of the DNA damage under these circumstances (63). In order to quantify the magnitude of this effect on cells the enhancement of survival measured by CFA can be calculated as the ratio of radiation doses under hypoxia compared to normoxia that lead

to the same biological effect, e.g. 1% survival. The received value is generally referred to as the Oxygen Enhancement Ratio (OER). These effects have been extensively demonstrated in a variety of *in vitro* experiments, where paired survival curves have been compared under normal air and under hypoxia (64), or *in vivo* with the paired tumour control assays, where tumours were irradiated *in situ* either under ambient conditions or under clamped blood flow (32). Another cause of cellular stress is reoxygenation, which contributes to cellular damage determining cellular survival through induction of reactive oxygen species (ROS) (65). This is generally referred to as reoxygenation injury. During reoxygenation ROS generation exceeds the capacity of these preventive mechanisms, resulting in the formation of hydroxyl radicals which in turn may damage cellular structures, such as enzymes, DNA integrity or the cellular membrane (66).

1.3 The DNA damage response – the role of γH2AX phosphorylation

The cytotoxic action of ionizing radiation arises from its ability to induce DNA damage, including base damage, DNA SSBs and DNA DSBs. Among the different types of DNA damage induced to the cells by ionizing radiation, DNA DSBs are the most crucial lesions as they are complex for the cell to repair and pose a serious threat for the genomic integrity and thus for the survival of the cell (67, 68). Consequently, cells have evolved a complex set of mechanisms to effectively sense and repair DSBs. The DNA damage response (DDR) consists of well-orchestrated signaling pathways that through dynamic interrelation aim to effectively detect and repair DSBs. The process of repairing the DSBs can be subdivided into the sensing, damage signal amplification (signal transduction) and the effector pathways. The whole process is mediated via 3 main kinases, namely ATM, DNA-PKcs and ATR, which are rapidly becoming activated upon DNA DSB induction and each one is active in different parts of the cell cycle and have different interacting partners.

Initial sensing includes the MRN complex (Mre11-Rad50-NBS1) and the Ku70/80 heterodimer (ATR-IP) is mainly acting in repairing DSBs in the S-phase (69, 70). The initial sensing leads to activation of the signal transducing kinases ATM and ATR and DNA-PK, who in turn activate via phosphorylation multiple downstream proteins which

are mainly involved in the amplification of the damage signal and act as template for the DNA repair enzymes e.g. H2AX, BRAC1, 53BP1 and MDC1 (71, 72). The damage signaling then ultimately disembogues in three different effector pathways, including (1) cell death, (2) DNA repair pathways and (3) pathways that result in temporary or permanent cell cycle arrest. Two main repair pathways exist for dealing with DSBs, namely homologous recombination (HR) and non-homologous end joining (NHEJ), that greatly differ in the proteins and enzymes involved, the cell cycle phase they primarily act in and the fidelity of the performed repair (73).

As HR requires the presence of the homologous undamaged DNA on the sister chromosome as a template for repair it is mainly active in late S-phase or G2-phase of the cell cycle and is nearly error free. Briefly, after forming 3' single strand overhangs at both sides of the break Rad51 polymerizes at the resulting ends and strand invasion is initiated. Consequently, helicases expand the resulting crossover bubbles in order to allow DNA polymerases to synthesis across the missing region using the DNA template of the sister chromosome. As a final step, nucleases and ligases cut and then reconnect the restored DNA sections (71, 74).

In contrast, NHEJ is active throughout the phases of the cell cycle as it is independent of homologous DNA sequences and is more error prone compared to HR but faster and simpler. In order to circumvent nuclear digestion of the ends of the break through exonucleases the Ku heterodimer (Ku70, Ku80) rapidly binds to the DNA ends. Subsequently, the protein kinase catalytic subunit DNA–PK is recruited by DNA-bound Ku to the site of damage, resulting in the formation of the DNA–PK complex. In order to maintain a close proximity for the following repair DNA–PK forms a bridge between the DNA ends. Furthermore, DNA-PK often in a complex with Artemis, an endonuclease processing the DNA ends prior to ligation, facilitates the formation of a ligation complex, comprising amongst others XRCC4, DNA ligase 4 and NHEJ1 (75).

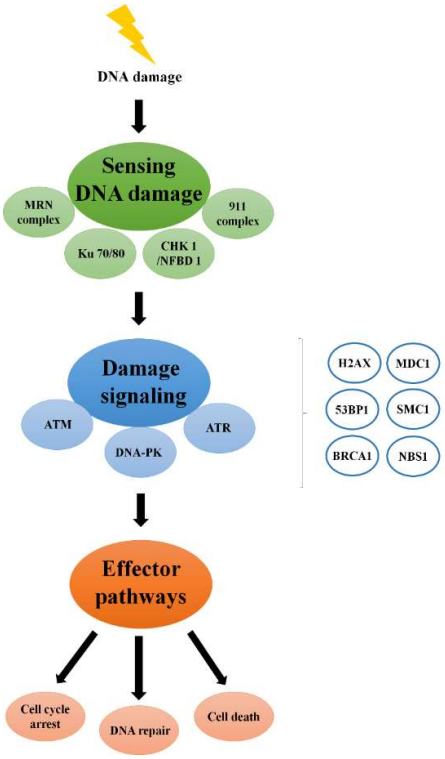

Figure 1: Figure showing proteins involved with the DNA damage response; adapted from Surova et al. Various modes of cell death induced by DNA damage. Oncogene. 2013, 32(33), p. 3789-97 **(76, 77)**

Several of the proteins involved in the DDR have been shown to form sub-nuclear structures when targeted with phosphor-specific antibodies against their activated form and visualized with fluorescent microscopy (72, 78). All have been found to accumulate directly at or in the vicinity of the DSBs, however, the most commonly used is the targeted phosphorylation of the histone H2AX in the residue Ser 139. H2AX is a variant of the highly conserved histone protein H2A, which comprises approximately 2 to 25% of the H2A pool depending on tissue or cell line origin (79). This phosphorylation mainly arises from ATM, although all the main kinases have been shown to potentially being able to phosphorylate H2AX (γH2AX) (80, 81), and spreads within a region of 2 Mb around every DSB amplifying the damage signal and forming distinct foci within few minutes after the induction of damage and reaching a maximum plateau level after 10-30 minutes (80). It was determined that each DSB give rise to one γH2AX focus (82) and that the kinetics of γH2AX disappearance follow the ones of the DSBs rejoining (83). Importantly, the histone H2AX is dephosphorylated upon repair of the DSB and it has been shown that this event marks the ceasing of cell cycling arrest and the progression of the cells in the cell cycle (84). Therefore, the assay offers the possibility to study

persisting residual γH2AX foci which are potentially associated with unrepaired DSBs (79).

1.4 Residual γH2AX foci as an indication of radiation –induced lethal lesions and potential pitfalls

Intrinsic radiosensitivity of cells is closely connected to their efficiency of repairing DNA lesions and the capacity to do so is one of the most important factors determining cellular survival after irradiation. Due to the one to one correlation with the induced DSBs, the rapid appearance even after the low dose of irradiation and the subsequent disappearance upon DSBs rejoining the γH2AX assay has become in the past decades the "gold standard" for the detection of unrepaired DSBs. The assay is simple, sensitive, the formation of γH2AX can be produced in response to a spectrum of genotoxic agents and offers the possibility to study the response of each individual cell in the "natural environment" where the DSB is occurring. Several lines of evidence support the hypothesis that residual γH2AX are indicators of lethal lesions (84, 85). Studies in cell lines that have defects in one of the enzymes involved in the repair of the DNA DSBs showed that in these cell lines retention of DSBs is followed by persisting foci (86). Additional evidence emerges from studies where the residual γH2AX foci were correlated with radiobiological endpoints (86, 87). The fraction of cells lacking foci (less than 3 foci per nucleus) correlates with the clonogenic survival (87) and the kinetics of foci disappearance negatively correlates with surviving fraction after 2 Gy (88). The mean number of residual γH2AX foci correlates with lethal lesions *in vitro* (89). Studies in human tumour cell lines from head and neck region grown as human tumour xenografts indicate that the slope of residual γH2AX foci dose response evaluated in well-oxygenated tumour areas could predict tumour control dose (14).

However, despite the high sensitivity of the assay certain pitfalls of the method have been established. Thus, the presence of microfoci, which are inducible by cellular stress such as hypoxia, but independent of DNA damage induction, may impair accuracy of the method (90). This effect is particularly important when studying tumour cell lines as it appears that the endogenous expression incidence increases with the degree of genomic instability within the cell lines (91). Furthermore, a dependency on cell cycle phases and

the level of chromatin condensation has been demonstrated (79, 92). Evaluation should be also cautious in cases where diverse cytotoxic compounds are used because the formation of γH2AX foci in response to DSBs is not radiation-specific, chemotherapeutic agents and radiomimetic drugs also induce foci (93).

Nevertheless, the detection of γH2AX foci remains the most sensitive and simplest method for monitoring the DDR and a wide range of applications both *in vivo*, *in vitro* and *ex vivo* have been established recently revealing promising results on the way to establish γH2AX as a possible biomarker for radiation sensitivity in patient tumours (94, 95).

1.5 Aim of the study

In previous *in vivo* experiments it was shown that in two hSCC lines (SKX and FaDu as used in the present experiments) grown as xenografts in nude mice, hypoxic tumour areas depicted substantial lower amounts of residual γH2AX foci, a marker of persistent unrepaired DNA DSBs, 24 hours post irradiation suggesting that a hypoxic microenvironment promotes cellular survival after irradiation (1, 14). Despite the fact that the resulted differences could be explained by the lower amount of induced γH2AX foci (30 minutes after irradiation) and the similar foci disappearance kinetics, several scientific questions remained open. The two tumour models under investigation beard pronounced differences in intrinsic radiation sensitivity evaluated previously *in vitro* and *in vivo* (14, 32, 89, 96, 97). Interestingly, these differences were apparently solely expressed in well oxygenated tumour areas, whereas no difference in the mean number of residual γH2AX foci was observed in the hypoxic tumour parts (14). Based on these observations we hypothesized that inter-tumoural heterogeneity in radiation sensitivity under hypoxia is less pronounced compared to well-oxygenated tumour areas, suggesting that hypoxia not only affects cellular survival through reduced induction of DNA damage but potentially also affects the capacity of DNA DSB repair and possibly γH2AX formation and decay (1). Importantly, *in vivo*, it was not possible to systematically assess the oxygenation levels of the cells evaluated over different time periods, but rather the fact that the cells were hypoxic, i.e. positive staining for pimonidazole, at the time of irradiation was considered. In the present *in vitro* study we investigated systematically the effect of

hypoxia exposure on clonogenic cell survival in cells irradiated either prior, post or while being hypoxic in order to functionally characterize the effect of hypoxia exposure on cellular radiosensitivity (1). In addition, we aimed to investigate the role of residual radiation-induced DNA DSBs on cellular survival to provide insights regarding the radiation-induced DNA DSB repair capacity under the different experimental conditions (1).

The understanding of this heterogeneity could be of high clinical relevance in order to establish biomarkers and targeting studies that could specifically address these differences in order to overcome hypoxia mediated treatment resistance.

2 MATERIAL AND METHODS

2.1 Material

2.1.1 Antibodies

antibody	Isotype	clone	blocking	dilution	company
Alexa flour 488 tyramid	goat anti mouse IgG		BSA	1:400	Life technologies (Invitrogen), USA
anti-actin	rabbit, polyclonal	103M4826 V	BSA	1:2000	Sigma Aldrich Co., USA
anti- ATM (phospho Ser 1981)	rabbit IgG, monoclonal	D6H9	BSA	1:1000	cell signaling Technology, Inc., USA
anti- ATM	rabbit IgG, monoclonal	D2E2	BSA	1:1000	cell signaling Technology, Inc., USA
anti -ATR (phospho S428)	rabbit IgG, monoclonal	EPR2184	BSA	1:1000	abcam, Cambridge, UK
anti- ATR	rabbit IgG, polyclonal		BSA	1:1000	biomol GmbH, Germany
anti- CHK1 (phospho Ser345)	rabbit IgG, monoclonal	133D3	BSA	1:1000	cell signaling Technology, Inc., USA
anti- CHK1	mouse IgG1, monoclonal	2G1D5	BSA	1:1000	cell signaling Technology, Inc., USA
anti- CHK2 (phospho Thr68)	rabbit IgG, monoclonal	C13C1	BSA	1:1000	cell signaling Technology, Inc., USA
anti- CHK2	rabbit IgG, monoclonal	D9C6	BSA	1:1000	cell signaling Technology, Inc., USA
anti- DNA PK (phospho S2056)	rabbit IgG, polyclonal		BSA	1:1000	abcam, UK
anti- DNA PK	mouse IgG1, monoclonal	18-2	Milk	1:500	abcam, UK
anti- Hif 1alpha	mouse IgG	54/Hif-1α	BSA	1:500	BD Bioscience, USA
anti- Histone gH2AX (phospho Ser139)	mouse IgG1, monoclonal	JBW301	BSA	1:1000	Merck Millipore, Germany
anti- Rad51	mouse IgG, polyclonal		BSA	1:500	abcam, UK
anti- pimonidazole	mouse, monoclonal		PBS	1:50	Hypoxyprobe Inc., USA
Amersham ECL rabbit IgG, HRP linked whole Ab	rabbit IgG	NA934V	BSA	1:2000	GE Healthcare Life Science, USA
secondary AB anti-mouse	mouse IgG	NAP31V	BSA	1:2000	GE Healthcare Life Science, USA

2.1.2 Devices

Device	**company**
Axiovert 200 inversed fluorescence microscope	Carl Zeiss Microscopy GmbH, Germany
Axio Imager Z1 Apotome fluorescence mircroscope	Carl Zeiss Microscopy GmbH, Germany
Hypoxia incubator	Binder GmbH, Germany
Incubator	Heraeus Instruments, Germany
Kühlzentrifuge Universal 30RF	Hettich GmbH & Co.KG, Germany
Lichtmikroskop Stemi 2000	Carl Zeiss Microscopy GmbH, Germany
monochrome digital camera (AxioCamMRm)	Carl Zeiss Microscopy GmbH, Germany
Monochromkamera (Model: #25.0 2 Mp monochrome w/o IR)	Diagnostic instruments, inc., USA
motorized scanning stage, 400x, EC Plan Neofluar	Märzhäuser Wetzlar GmbH&Co.KG, Germany
objective for Axiovert 200 inversed fluorescence microscope (40x, 1.6 Öl, EC Plan – NEOFLUAR)	Carl Zeiss Microscopy GmbH, Germany
Röntgenbestrahlungseinheit RS 225 research system	Gulmay Medical LTD, UK
Shandon CytoSpin III Zytozentrifuge	Thermo Fisher Scientific Inc., USA
Sterilwerkbank	BDK Luft und Reinraumtechnik, Germany
ledetect 96	LABEXIM Products, Austria
AccuBlock™	Labnet International, Inc, USA
Kühlzentrifuge Mikro 200r	Hettich GmbH & Co.KG, Germany
Sonifier B12	Branson Sonic Power Company, USA
Curix 60	AGFA Healthcare Corporation, USA
Odyssey Fc Imaging System	Li-cor Bioscience, USA
Tankblot	Peqlab Biotechnologie GmbH, Germany
Electrophoresis Power Supply PS 3002	Life technologies (Gibco), USA

2.1.3 Chemicals

Chemicals	**company**
Ark™ kit (animal research kit)	Dako Deutschland GmbH, Germany
BSA	Carl Roth GmbH & Co.KG, Germany
Bromphenolblau	AppliChem GmbH, Germany
complete MINI protease inhibitor cocktail tablets	Roche diagnostics, Swiss
DAPI	Sigma Aldrich Co., USA
Dc™ Protein Assay	BioRad, USA
DL-Dithiothreitol (DTT)	Sig Sigma Aldrich Co., USA
DMEM	Biochrom GmbH, Germany
DMSO	Sigma Aldrich Co., USA
Ethanol 99% (vollst. verh. MEK/BITREX)	SAV-LIQUID PRODUCTION GMBH, Germany
FCS	Sigma Aldrich Co., USA
Flourescence Mounting Medium	Dako Deutschland GmbH, Germany
Formaldehyd Lösung 4%	Merck KGaA, Germany

Formaldehyd min. 37%	Merck KGaA, Germany
Glycerol	AppliChem GmbH, Germany
Glycerol – 2 – phosphat	Sigma Aldrich Co., USA
Glycin	Carl Roth GmbH & Co.KG, Germany
HEPES- buffer	Biochrom GmbH, Germany
2-Propanol	VWR Chemicals International, Germany
KCl	Carl Roth GmbH & Co.KG, Germany
K_2HPO_4	Carl Roth GmbH & Co.KG, Germany
β-Mercaptoethanol	Sigma Aldrich Co., USA
Methanol	VWR Chemicals International, Germany
NaCl (AnalaR Normapur)	VWR Chemicals International, Germany
Na_2HPO_4 x 2 H_2O	AppliChem GmbH, Germany
$NaHCO_3$	Biochrom GmbH, Germany
$NiCl_2$	Sigma Aldrich Co., USA
Non-essential aminoacids	Biochrom GmbH, Germany
Na-pyrovate	Biochrom GmbH, Germany
PBS	Biochrom GmbH, Germany
Penicillin/Streptomycin	Life technologies (Gibco), USA
phosphatasee inhibitor cochtail 2	Sigma Aldrich Co., USA
phosphatase inhibitor cochtail 3	Sigma Aldrich Co., USA
pimonidazole	Natural Pharmacia International, USA
Rotiphorese Gel 30	Carl Roth GmbH & Co.KG, Germany
Dodecylsulfat-Na-Salt	Serva Electrophoresis GmbH, Germany
Super Pap Pen	Life technologies (Gibco), USA
N, N, N‘,N‘ Tetramethylethylenediamide	Sigma Aldrich Co., USA
Triton X 100	Sigma Aldrich Co., USA
Trizma-Base	Sigma Aldrich Co., USA
Trishydrochloride	AppliChem GmbH, Germany
Trypsin	Sigma Aldrich Co., USA
Tween20	Carl Roth GmbH & Co.KG, Germany
DCTM protein assay (Reagent A, Reagent B)	BioRad, USA
Precision Plus Protein Standrds	BioRad, USA
Nitrocellulose Blotting Membrane	GE Healthcare Life Science, USA
Milchpulver	Carl Roth GmbH & Co.KG, Germany
ECL Western Blotting Detection Reagents	GE Healthcare Life Science, USA

2.1.4 Laboratory equipment

laboratory equipment	**company**
Adhäsions-Objektträger SuperFrost Ultra plus/ SuperFrost plus Gold	R. Langenbrinck, Germany
BD-Falcon 10-cm-Schalen	VWR Chemicals International, Germany
BD-Falcon 6- cm Schalen	VWR Chemicals International, Germany
BD-Falcon T-75-Flaschen	VWR Chemicals International, Germany

BD-Falcon T-25-Flaschen	VWR Chemicals International, Germany
BD GasPak^{TM}-EZ- Gas Generating Pouch Systems	Becton, Dickinson and Company, USA
BD-Falcon Röhrchen	VWR Chemicals International, Germany
BD-Falcon Kryoröhrchen	VWR Chemicals International, Germany
Eppendorfreaktionsgefäße	Eppendorf AG, Germany
Filterkarten (Shandon CytoSpin III)	Thermo Fisher Scientific Inc., USA
Fuchs-Rosenthal counting chamber	Glaswarenfabrik Karl Hecht, Germany
Pipettenspitzen	Thermo Fisher Scientific Inc., USA
Röntgenfilme	AGFA, Belgium
96 Well platten	Greiner bio-one International GmbH
Exmire microsyringe	Ito Corporation, Japan
Odyssey Fc Imaging System	LI-COR Biosciences – GmbH, USA

2.1.5 Solutions

DMEM (1 L)	DMEM Trockenmedium	12,04 g
	$NaHCO_3$	3,33 g
	H_2O	890 ml
	pH	7,2
PBS (1 L)	NaCl	8g
	Na_2HPO_4 x 2 H_2O	1,44g
	KCl	0,2g
	K_2HPO_4	0,2g
cristal violet staining solution (1 L)	cristal violet	0,5g
	formaldehyd	27 ml
	PBS	1000ml
separating gel (6%)	resolving gel buffer	5ml
	H_2O	11ml
	Acrylamid	4ml
	APS (10%)	100µl
	Temed	10µl
separating gel (12%)	resolving gel buffer	5ml
	H_2O	7ml
	Acrylamid	8ml
	APS (10%)	100µl
	Temed	10µl
stacking gel (4.5%)	stacking gel buffer	1.25ml
	H_2O	3ml
	Acrylamid	0.75ml
	APS (10%)	100µl
	Temed	5µl

2.1.6 Buffering Solutions

Lysisbuffer (500ml)	Tris-HCL	3.94g
	Glycerol – 2 – phosphat	5.401g
	NaCl	4.383g
	Na_3VO4	0.092g
	Glycerol	50ml
	Tween20	5ml
	NaF	0.021g
	H_2O	440ml
	pH	7.5
Stripping buffer (550ml)	Glycin	4.5g
	10% SDS in PBS	3ml
	Tween 20	3ml
	H_2O	550 ml
	pH	2.2
TBST (2l)	Tris-HCL	3.152g
	NaCl	11.688g
	Twen 20	2ml
	H_2O	2 l
	pH	7.5
Running buffer (5l)	Tris-Base	30g
	Glycin	144g
	SDS	5g
	H_2O	5l
Transfer buffer (8l)	Tris-Base	46.4g
	Glycin	23.2g
	SDS	2.96g
	Methanol	1.6l
	H_2O	8l
separating gel buffer (500ml)	Tris Base	90.85g
	SDS 10%	20ml (bzw. 2g)
	H_2O	500ml
	pH	8.8
stacking gel buffer (500ml)	Tris Base	30.3g
	SDS 10%	20ml (bzw. 2g)
	H_2O	500ml
	pH	6.8
Loading buffer (Lämmli buffer) (100ml)	Glycerol (=Glycerin)	20ml
	SDS	2g
	Bromphenolblau	10mg
	Sammelgelpuffer (4x)	25ml
	H_2O	95ml
washing buffer (1l)	PBS	1l
	Tween 20	1ml

2.2 Cell culture conditions

Cells were reactivated from a cryo-stock (liquid nitrogen) and grown in DMEM supplemented with 10% of FCS, 1% antibiotics (Penicillin/Streptomycin), 1% Non-Essential Amino Acids, 1% Sodium Pyruvate and 2% Hepes Buffer to obtain optimal growth conditions for the cell lines [0] (1). Standard CFAs were performed using DMEM containing 20% FCS supplemented as previously described. During all cultivations, cells were kept in 37 °C under humidified atmosphere (95% humidity) either in 21% oxygen (normoxic conditions) or in 1% oxygen (hypoxic conditions). Cells were routinely passaged once a week upon reaching 90-95% confluency level and kept in culture until 25th passage after reactivation to minimize the possibility of inducing random mutations. All cells were routinely checked for contamination with Mycoplasma (1).

2.3 Cell lines

Three hSCC cell lines from the head and neck region, namely UT SCC-5, FaDu and SKX, were used in the experiments. All cell lines have been previously extensively characterized both in *in vitro* (89, 96, 98) and *in vivo* (14, 32, 96) studies and were kindly donated from Prof. Baumann (University Hospital of Dresden, Department of Radiation Oncology, Oncoray). They are all including a missense-mutation of the tumour suppressor gene TP53 (98) and are growing *in vitro* as adherent cell cultures.

The UT SCC-5 cell line was established from a primary tumour of the mobile tongue at the Department of Otorhinolaryngology – Head and Neck Surgery (Turku University; Turku Finland) and expresses high radiation resistance evaluated both with *in vivo* and *in vitro* endpoints (32) .

The FaDu cell line used is a subline of the original FaDu cell line available in the ATCC. FaDu cells initially arose from an undifferentiated human hypopharyngeal SCC of the head and neck region and are characterized by moderate radiosensitivity (14, 89, 96, 98-101).

The SKX cell line was established from a biopsy of a moderate differentiated SCC of the floor of mouth and alveolar bone (T4 N2 M0) prior to radiotherapy at the University Hospital Hamburg-Eppendorf in 1991. A cell line was consequently established in Dresden from an original tumour xenograft (96). Previous experiments, both *in vitro* and *in vivo*, indicated that SKX cell line is highly radiosensitive (14, 89, 96-98).

2.4 Methods

2.4.1 Validation of hypoxic conditions

For verification of hypoxic conditions, staining with pimonidazole [0], a 2-nitroimidazole hypoxia marker that forms covalent bonds with cellular macromolecules at oxygen levels below 10 mmHg (23), was performed using the ARK^{TM} Kit [0]. For all cell lines confluent cell cultures were incubated with medium containing 20 µmol pimonidazole for 1 hour prior to incubation either in GasPaks for 0, 1, 2, 2.5 and 3 hours or in 1% O_2 for 4 hours within a hypoxic incubator. After fixation of cells with 4% formaldehyde (15 min) and permeabilization of cell membranes (Triton X100, 0.01% in PBS), endogenous activity of peroxidase was blocked (5min, peroxidase bock, ARK^{TM} kit). This was followed by incubation with the primary antibody (1:50, 15min, 37°C according to the manual provided from the manufacturer). Slides were then incubated with the streptavidine-peroxidase complex (15min, RT). Preparation of DAB chromogen was done based on the manufacturer's guidelines (DAB substrate buffer + DAB chromogen solution) with the addition of 30% $NiCl_2$ (1/1000 dilution) and applied to cells (8min, RT) before counterstained with hematoxylin (2min, RT). Between every application, three washing steps with PBS were performed (5 minutes each). Slides were kept in dark and humid atmosphere during all incubations.

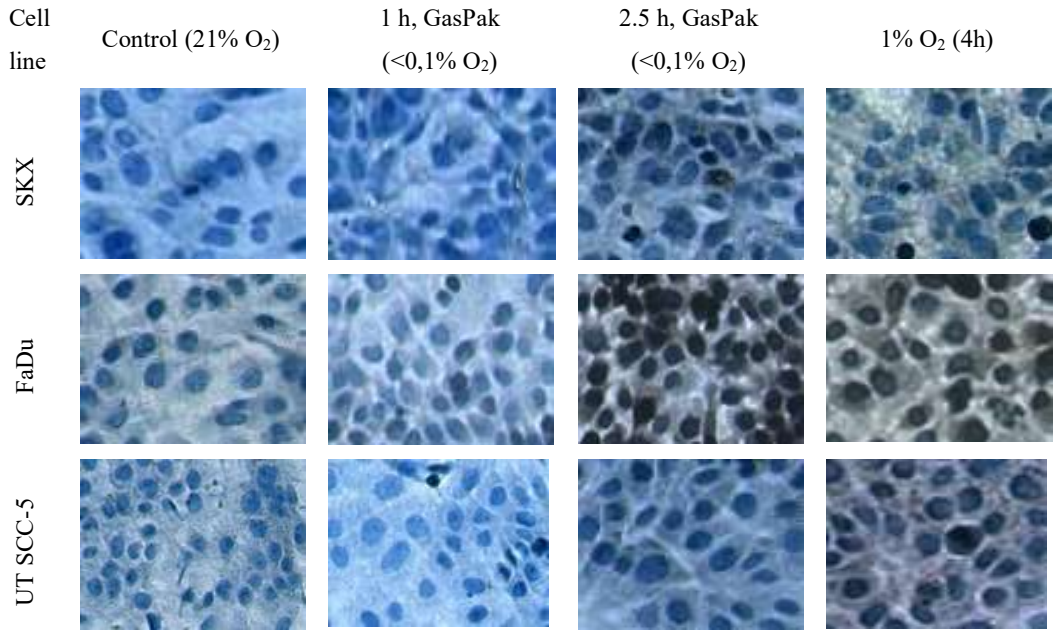

Figure 2: representative images of cells after incubation in GasPaks for 0, 1 and 2.5 hours and after incubation with 1% O_2 for 4 hours for all cell lines und investigation; cytoplasmic staining with pimonidazole increased over incubation time under conditions close to anoxia as well as after long time incubation under moderate hypoxia

2.4.2 Proliferation assay

For all cell lines tumour cells were seeded with a seeding density of 100.000 cells in cell culture dishes (diameter: 6cm) and incubated for 24 hours under normoxic conditions before medium was changed. Cells were subsequently either incubated under normoxic (37°C, 7% CO_2, 21% O_2) or under hypoxic conditions (37°C, 7% CO_2, 1% O_2) and cell numbers were counted daily between day 3 and 7 post seeding. Cell counts were performed manually using a Fuchs-Rosenthal counting chamber [2.1.4].

2.4.3 Colony Formation Assay

After preparation of single cell suspension cells were seeded in cell culture dishes (10 cm diameter) for standard CFA. For each dose, three different seeding densities were used in triplicates (Tabl. 1). Seeding densities varied between cell lines and were adapted for conditions including irradiation under hypoxia, due to expected higher cell survival. For all cell lines, dishes were incubated for 14 days under normoxic conditions, followed by

fixation (formaldehyde, 15min) and staining (cristal violet) [2.1.5]. Colonies with at least 50 cells were counted manually and numbers were recorded.

Table 1: seeding densities for conditions with or without irradiation under hypoxia for different irradiation doses and all cell lines investigated; number of cells seeded was decreased for conditions with irradiation under hypoxia due to the expected higher clonogenic survival under this condition

	SKX		FaDu		UT SCC-5	
O_2 concentration during irradiation	21%	<0.1%	21%	<0.1%	21%	<0.1%
0 Gy	2400	2400	1200	1200	1200	1200
	3000	3000	1500	1500	1500	1500
	3600	3600	1950	1950	1950	1950
1 Gy	3000	3000	1800	1800	1800	1800
	5000	5000	2250	2250	2250	2250
	7000	7000	2400	2400	2400	2400
2 Gy	9000	9000	1800	1800	1800	1800
	12000	12000	2550	2550	2550	2550
	15000	15000	3000	3000	3000	3000
4 Gy	30000	30000	3000	2000	2000	2000
	37500	37500	6000	3000	4000	3000
	45000	45000	9000	4000	6000	4000
6 Gy	120000	40000	24000	3000	10000	3000
	180000	60000	30000	4000	15000	4000
	240000	80000	36000	5000	20000	5000
8 Gy	120000	40000	24000	3000	24000	3000
	180000	60000	30000	4000	30000	4000
	240000	80000	36000	5000	36000	5000

2.4.4 γH2AX-Assay

After preparation of single cell suspension, cells were centrifuged on glass slides (FaDu: 75000 cells/spot; SKX/UT SCC-5: 100000 cells/spot) by cytospin procedure (200 rpm, 2min) [2.1.2] and fixed with 4% formaldehyde (15 min). After permeabilization of the cell membranes (Triton X100, 0.01% in PBS) cells were blocked using BSA (1% in PBS, 30min, RT), in order to block unspecific reactions, and incubated with primary antibody (1:1000 in BSA, Anti-phospho-Histone H2AX, 1h, 37°C). For second antibody Alexa 488 flourescence probe was used (1:400 in BSA, 45min, RT) and nuclei were counterstained with DAPI (1:1000 in PBS, 10 min, RT). Slides were mounted with fluorescent mounting medium and stored at 4°C until image acquisition (1, 14, 89).

2.4.5 Images and image analysis

Images were either generated with Axiovert 200 inversed fluorescence microscope (40x) [2.1.2] using a monochrome camera and VisiVIEW- Imaging software (Visitron Systems GmBH) or with Axio Imager Z1 Apotome fluorescence microscope [2.1.2] using a monochrome digital camera (AxioCamMRm, Carl Zeiss, Jena, Germany; motorized scanning stage, Märzhäuser, Wetzlar, Germany, 400x, EC Plan Neofluar). For both microscopes, at least 8 individual images of different areas were taken per dose group and cell line. For Axio Imager Z1 Apotome fluorescence microscope images were taken as optical sections every 0.5 µm on the Z-axis (z-stack) and individual images were fused into a 2D maximum intensity projections of a single stack image for analysis (1, 14, 89). Images taken with Axiovert 200 inversed fluorescence microscope were evaluated manually using Image J–software (National Institute of Health). For images taken with Axio Imager Z1 Apotome fluorescence microscope evaluation was performed using AxioVision software (LE 64, SP1, version: 4.9.1.0 for Windows) (1). Evaluation of γH2AX foci was restricted to cells with intact nuclei based on DAPI counterstain. Cells exhibiting high background or presenting with pan-nuclear staining were excluded (Fig.3). At least 150 nuclei per dose group were randomly selected and the number of foci per nuclei was recorded.

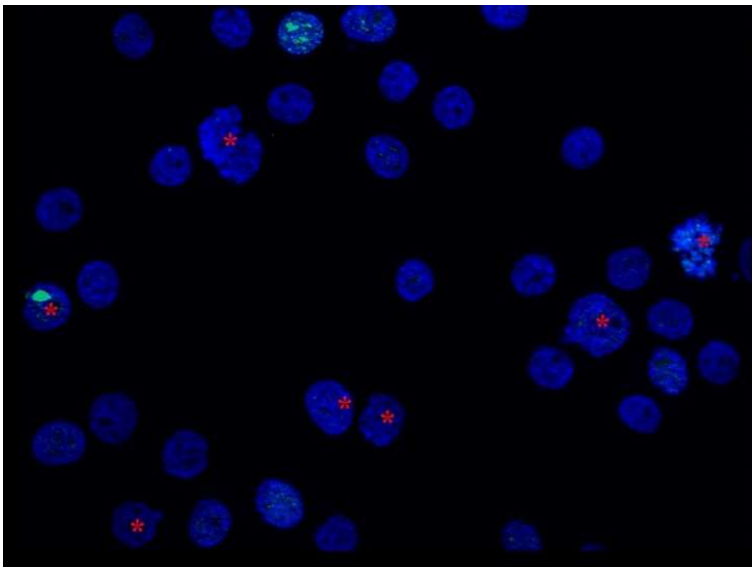

Figure 3: representative image (FaDu, 0Gy, control), excluded cells marked with *; cells without intact nuclei, irregular DAPI staining, overlapping nuclei or cells in mitosis were excluded

2.4.6 Western Blot Analysis

Whole cell lysates were isolated using lysis buffer [2.1.6] with added protease and phosphatase inhibitors [0] and kept on ice. After sonification (intensity: 2.5, 15 sec), samples were centrifuged (14000 rpm, 4 °C, 15 min) [2.1.2] and protein concentration was determined using Lowry assay (DC^{TM} protein assay, BSA-standard, 620nm, ledetect 96). Appropriate amounts of supernatant containing 80-100µg Protein were mixed with Laemmli-buffer (5% β-Mercaptoethanol, 1:1)(102) and mixture was boiled (100°C, 10min) to denaturate proteins. For SDS-PAGE (stacking gel: 4.5%, separating gel: 12%/6% acrylamide, 35 mA/Gel, 4h, RT) samples were loaded using a micro-syringe and a molecular weight marker to determine protein size and progress of electrophoresis was used. Proteins were transferred onto a nitrocellulose membrane through tank blotting procedure (24V, 12-14h, 4°C). Success of protein transfer was assessed with Ponceau staining (2 min, RT). Subsequently, membranes were blocked with BSA (5% BSA in washing buffer [2.1.6], RT, 4h) or milk (5% in washing buffer, RT, 4h, agitation) [2.1.1] and incubated with primary antibodies (overnight, 4°C) [2.1.1]. After washing (washing buffer, 3x5min), membranes were incubated with indicated secondary antibodies (1h, RT) [2.1.1]. For development, membranes were incubated with ECL reagent (2min, RT) and chemiluminescence was detected using Odyssey Fc imaging system [2.1.2]. As required membranes were stripped with stripping buffer (2x 15min, RT) [2.1.6] and reincubated with primary antibodies for further analysis. Digital images were evaluated using Image Studio Software (version 4.0.21, LI-COR Biosciences – GmbH, Lincoln, Nebraska (USA)).

2.5 Experimental design

Over all experiments and for all cell lines used, cells were seeded with the same density (5x 10^5 cells) either in 25 cm² (20000 cells /cm^2) cell culture flasks for CFA and γH2AX Assay or in cell culture dishes (6cm diameter) for western blot analysis (1). After an initial cultivation period for 24 hours to allow cell attachment, culture medium was changed and subsequently, cells were grown until reaching confluency (100 000 cells/cm^2) while being allocated to different conditions according to the respective experimental design. In all experimental settings, cells were exposed to normoxia or hypoxia within three distinct

time frames (in a variety of combinations (Tabl. 2)) namely, pre-irradiation period (growth period) (4-5 days, according to cell line and growth condition), irradiation time and post-irradiation period (repair time 24 h) (Tabl. 2) (1). Irradiation was always performed as single doses of 0, 1, 2, 4, 6 and 8 Gy (200 kV, 15mA X-Rays; dose-rate: 0,91Gy/min; RS 225 research system). For irradiation under hypoxia, cells were kept in GasPaks for 2.5h prior to irradiation and subsequently irradiated in the GasPaks with oxygen concentration of 0.1% (according to the manufacturer's instruction) (1).

Table 2: Table showing the different experimental groups tested with the corresponding abbreviations used; *Adapted from Hauth F.et al. (2017) Cell-line dependent effects of hypoxia prior to irradiation in squamous cell carcinoma lines. Clinical and Translational Radiation Oncology (accepted for publication)*(1)

Oxygen concentration			Experimental condition abbreviation
Growth period (4-5 days)	Irradiation	Post irradiation (24h)	
21%	21%	21%	O-O-O
21%	**0,1%**	21%	O-**H**-O
21%	21%	**1%**	O-O-**H**
21%	**0,1%**	**1%**	O-**H**-**H**
1%	1%	21%	**H**-O-O
1%	21%	**1%**	**H**-O-**H**
1%	**0,1%**	21%	**H**-**H**-O
1%	**0,1%**	**1%**	**H**-**H**-**H**

Seeding for standard CFA and γH2AX assay was always performed from cells of the same flask (for each dose) via division of the single cell suspension. Processing of cells for both assays along with the western blot analysis was always done after the completion of 24 hours post-irradiation period. At least three independent experiments were performed for all cell lines and all conditions for CFA while at least one independent experiment was performed for western blot analysis and γH2AX Assay (1).

2.6 Statistics

All statistical analyses were performed using GraphPad Prism 5 (version: 5.03 for Windows, GraphPad Software, Inc., San Diego, California (USA)). For multiple comparisons of CFA and γH2AX data one way analysis of variance (ANOVA) with Bonferroni correction was used (1). Furthermore, p-values of below 0.05 were considered statistically significant (1).

2.6.1 Proliferation assay

Data obtained by proliferation assay were fitted using the exponential growth model

$$\boldsymbol{y(t) = y(0) * e^{(k*t)}}, (1)$$

where y(0) equals the y-intercept of the curve, t equals the time post seeding in days and k is a growth rate coefficient, resembling the slope of the exponential growth curve.
DTs were calculated based on the formula:

$$\boldsymbol{DT = \frac{\ln 2}{k}}, (2)$$

2.6.2 CFA

For standard CFA PEs and SFs for the different doses were calculated based on the following equations:

$$\boldsymbol{PE}\ [\%] = \frac{\boldsymbol{number\ of\ colonies\ counted}}{\boldsymbol{number\ of\ seeded\ cells}} * \mathbf{100} \qquad (3)$$

$$\boldsymbol{SF}\ [\%] = \frac{\boldsymbol{PE\ (irradiated\ cells)}}{\boldsymbol{PE\ (non-irradiated\ cells, 0Gy)}} \qquad (4)$$

All acquired data was fitted using the linear – quadratic model:

$$\boldsymbol{y(x) = e^{(-\alpha * x - \beta * (x^2))}}, (5)$$

where y(x) equals the surviving fraction, x equals the dose in Gy and α and β are coefficients of dose and dose squared.

2.6.3 γH2AX foci assay

Data obtained by γH2AX foci assay were fitted with the linear regression model. The equation for linear regression used for calculation was:

$$\boldsymbol{y(x) = (a * x + b) - c}, (6)$$

where x equals dose in Gy, y(x) equals the mean number of residual foci and a and b are constants, resembling the slope of the linear regression and the y-intercept, respectively. C resembling the mean value of residual foci counted in 0 Gy.

Based on the Poisson statistics describing the radiation effects on cells, the cellular survival after irradiation is the probability of a cell having zero lethal lesions (7) (1). Therefore, the number of lethal lesions is equal to the –lnSF (8). This is mathematically described by the equations:

$$\boldsymbol{SF_{CFA} = e^{(-mean\ number\ of\ lethal\ lesions)}} (7)$$

$$\boldsymbol{-ln\, SF_{CFA} = mean\ number\ of\ lethal\ lesions} (8)$$

The correlation between –ln SF_{CFA} and the number of residual γH2AX foci were fitted with the linear regression model (1):

$$\boldsymbol{y(x) = c * x + d}, (9)$$

where x equals –ln SF_{CFA}, y(x) equals the mean number of residual foci and c and d are constants, resembling the slope of the linear regression and the y-intercept, respectively. This equation allowed the direct recalculation of survival curves based only on the number of residual γH2AX foci as previously shown (89).

$$\boldsymbol{SF(calculated)} = \boldsymbol{e}^{\left\{-\left(\frac{\boldsymbol{mean\ number\ of\ foci-d}}{\boldsymbol{c}}\right)\right\}} \quad (10)$$

2.6.4 Calculation of OER

The OER for every experimental condition was calculated from the standard CFA based on the following equation:

$$\boldsymbol{OER} = \frac{\boldsymbol{Dose\ normoxia\ (SF{=}0.1)}}{\boldsymbol{Dose\ hypoxia\ (SF{=}0.1)}} \quad (11)$$

Since the number of residual γH2AX foci significantly correlates with the surviving fractions obtained by CFA (8) we were able to recalculate the OERs based only on the linear regression of mean residual foci with –ln SF_{CFA} (9). This was performed by fixing the biological effect at the level of 10% survival (-ln $(0,1)_{CFA}$=2.3) and defining the amount of mean expected residual foci under hypoxia and normoxia using the following equation:

$$\boldsymbol{mean\ number\ of\ residual\ foci} = \boldsymbol{c} * \mathbf{2.3} + \boldsymbol{d}\ , (12)$$

where c and d are constants, resembling the slope of the linear regression and the y-intercept of the equation for either normoxia or hypoxia, respectively $\boldsymbol{y(x)} = \boldsymbol{c} * \boldsymbol{x} + \boldsymbol{d}$, (9). Next, we transferred these values to the equivalent γH2AX dose-response curve and defined the dose levels needed to produce the corresponding amount of residual foci.

$$\boldsymbol{Dose\ (Gy)} = \frac{\boldsymbol{(mean\ number\ of\ residual\ foci - b)}}{\boldsymbol{a}}\ , (13)$$

where a and b are constants, resembling the slope of the linear regression and the y-intercept, respectively $\boldsymbol{y(x) = (a*x+b)}$ – c, (6). As a final step, by dividing the two dose levels, we calculated the OERs (Suppl. Fig. 1).

2.6.5 Calculation of DMF

It is described mathematically as followed:

$$\boldsymbol{DMF = \frac{Dose\ without\ reagent\ (SF{=}0.1)}{Dose\ with\ reagent\ (SF{=}0.1)}}, (14)$$

3 RESULTS

3.1 Effect of hypoxia on cellular growth

As a first approach to our hypothesis, we investigated the impact of hypoxia on cellular growth for all cell lines under investigation. We observed exponential growth of cells under both normoxic and hypoxic conditions with FaDu cells exhibiting the longest doubling time (DT), UT SCC-5 cells showing an intermediate and SKX the shortest DT under normoxic conditions, respectively (**Fig. 4:** *SKX:* DT= 41.3h; *FaDu:* DT= 30.1h; *UT SCC-5:* DT= 39.9h). Incubation under hypoxia increased DT for all cell lines, in a cell line dependent manner (**Fig. 4:** *SKX:* DT= 52.7h; *FaDu:* DT= 39.6h; *UT SCC-5:* DT= 56.5h). Interestingly, we observed the highest deceleration of growth in UT SCC-5 cells, whereas in FaDu cell line exposure to hypoxia resulted in the slightest reduction of growth rate.

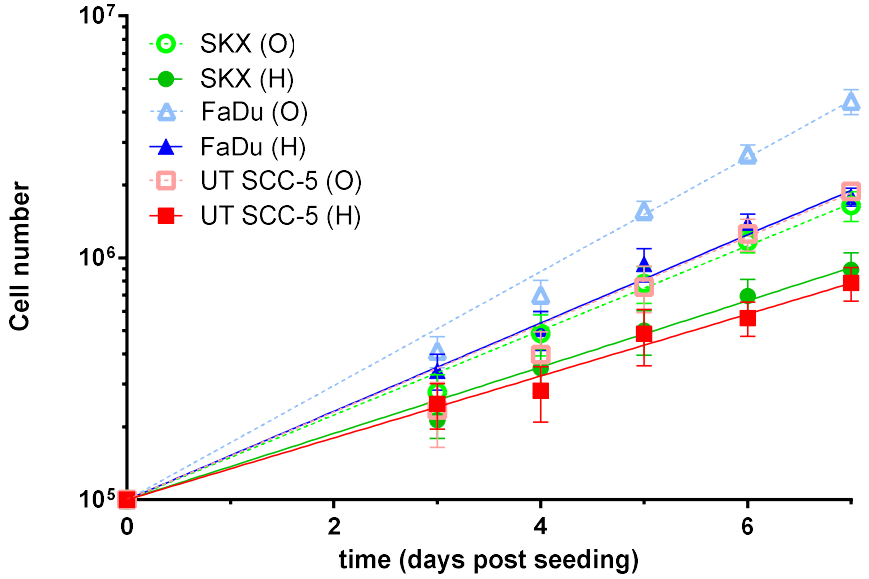

Figure 4: Figure showing exponential growth curves for all cell lines under investigation. Dashed lines and open symbols indicating data obtained under normoxic conditions (O), whereas filled symbols and solid lines indicating data obtained under hypoxic conditions (H). Error bars indication the standard deviation of three independent experiments.

3.2 Normoxia (experimental group: O-O-O)

Figure 5A shows the results of standard CFA under normoxic conditions for the three hSCC cell lines under investigation. Clonogenic cell survival revealed substantial

differences in intrinsic radiosensitivity depicted as differences in the survival fraction after 2 Gy (SF_2) with SKX showing high radiosensitivity (SF_2= 0.14), while FaDu showed moderate radiosensitivity (SF_2= 0.38) and UT SCC-5 low radiosensitivity (SF_2= 0.59) respectively (Supp. Tab. 1) (1). In terms of γH2AX foci assay, for all cell lines residual γH2AX foci were increasing linearly with increasing dose. However, the slope values of the linear dose-response varied among the different cell lines (**Fig. 5B:** *SKX:* slope= 2.13, r^2= 0.3887; *Fa Du:* slope= 1.58, r^2= 0.2623; *UT SCC-5:* slope= 1.13, r^2= 0.2028).

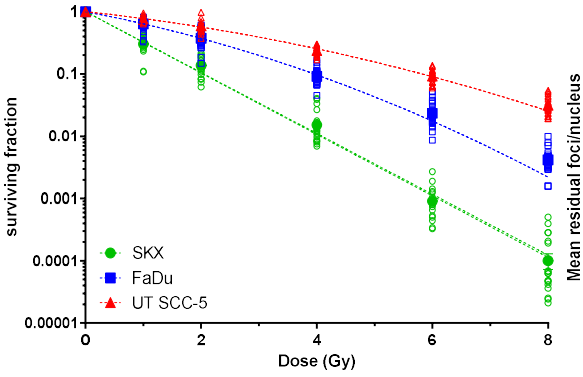

Figure 5A: Standard CFA under normoxic conditions (experimental group: O-O-O) for all cell lines investigated. Shown are the means of 8 (SKX, UT SCC-5) and 11 (FaDu) experiments (closed symbols) with the standard error of the mean. Open symbols indicating single values of individual experiments. Differences in SF_2 values indicate differences in intrinsic radiosensitivity within the cell lines under investigation. *Adapted from Hauth F.et al. (2017) Cell-line dependent effects of hypoxia prior to irradiation in squamous cell carcinoma lines. Clinical and Translational Radiation Oncology (accepted for publication) (1)*

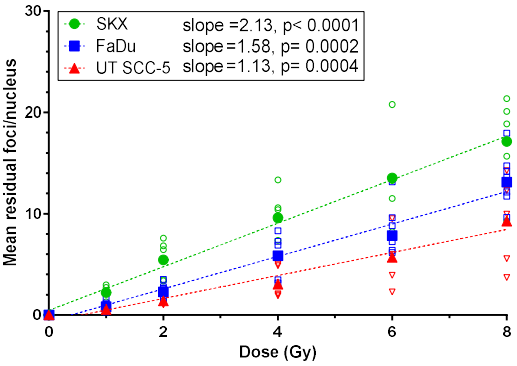

Figure 5B: Linear correlation of residual γH2AX foci number with radiation dose for all cell lines under investigation under normoxic conditions (experimental group: O-O-O). Shown are the means of 5 (SKX, UT SCC-5) and 7 (FaDu) experiments with standard deviation of the mean. Differences in slopes of the linear regressions indicating differences of intrinsic radiation sensitivity between the cell lines used. *Adapted from Hauth F.et al. (2017) Cell-line dependent effects of hypoxia prior to irradiation in squamous cell carcinoma lines. Clinical and Translational Radiation Oncology (accepted for publication)(1)*

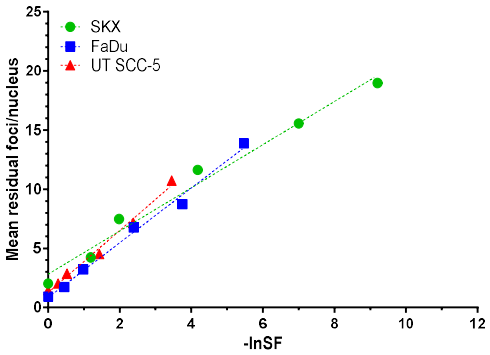

Figure 5C: Correlation of mean number of residual γH2AX foci with the observed –lnSF (mean number of lethal lesions) for all cell lines used under normoxic conditions (experimental group: O-O-O). Error bars indicating standard error of the mean. *Adapted from Hauth F.et al. (2017) Cell-line dependent effects of hypoxia prior to irradiation in squamous cell carcinoma lines. Clinical and Translational Radiation Oncology (accepted for publication)(1)*

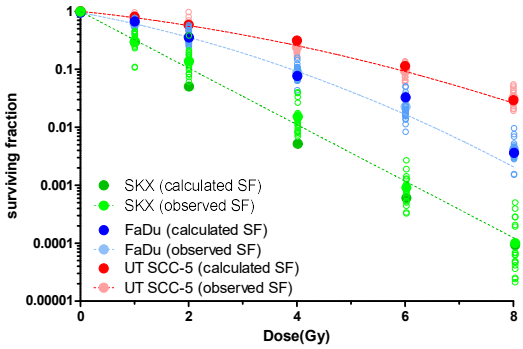

Figure 5D: Figure showing survival curves obtained by CFA data (observed SF) and survival curves recalculated based on data obtained by γH2AX foci assay (calculated SF). For CFA data both single surviving fractions per dose (open symbols) and means of single surviving fractions per dose (closed symbols) are blotted. *Adapted from Hauth F.et al. (2017) Cell-line dependent effects of hypoxia prior to irradiation in squamous cell carcinoma lines. Clinical and Translational Radiation Oncology (accepted for publication) (1)*

Plotting the mean values of residual γH2AX foci against the $-\ln SF_{CFA}$ led to a significant linear correlation (**Fig. 5C:** *SKX:* slope= 2.63, r^2= 0.99; *FaDu:* slope= 1.83, r^2= 0.99; *UT SCC-5:* slope= 2.32, r^2= 0.98) for all cell lines (Suppl. Tab. 1). From the respective linear correlation equations we were able to recalculate the whole survival curves based only on the number of residual foci. For all cell lines no systematic differences were observed between the data obtained by standard CFA and the ones predicted by recalculation through mean γH2AX foci numbers, resulting in overlapping curves (within the expected experimental spread) (**Fig. 5D**).

3.3 Effect of post-irradiation incubation under hypoxia on cellular survival and number of residual γH2AX foci (experimental group: O-O-H)

For FaDu and SKX 24 hours post-irradiation exposure to hypoxia resulted in survival curves that were not significantly different from those obtained under normoxic conditions, whereas for UT SCC-5 cells a slight increase in cellular survival was observed (**Fig. 6A:** *SKX:* SF_2= 0.10, p= 0.20; *FaDu:* SF_2= 0.34, p= 0.48; *UT SCC-5:* SF_2= 0.61, p= 0.004) (**Suppl. Tab. 1**). Consistent with the results of the CFA the slopes of the normoxic dose-γH2AX foci linear regressions were not different compared to the ones obtained

after hypoxia exposure during post irradiation incubation time for both FaDu and SKX cell line (**Fig. 6B:** *SKX:* slope= 1.84, r^2= 0.32; *FaDu:* slope= 1.43, r^2= 0.22). Whereas, for UT SCC-5 cell line 24-hour post-irradiation incubation under hypoxia led to a higher slope compared to normoxic conditions (**Fig. 6B:** *UT SCC-5:* slope= 1.50, r^2= 0.22) (1).

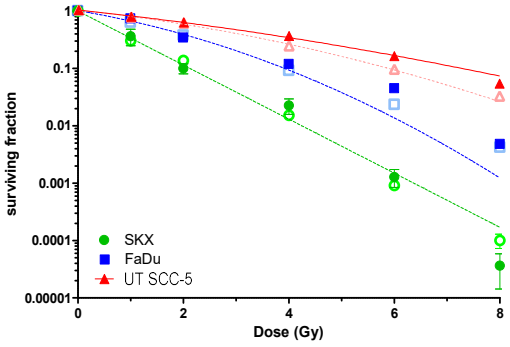

Figure 6A: Figure showing results of standard CFA for normoxic control (O-O-O, open symbols) and 24 hour post-irradiation incubation under hypoxia (O-O-H, filled symbols). For all cell lines results of 3 independant experiments with standard error of the mean are plotted. No significant difference between results for post-irradiation exposure and control condition could be detected. Error bars indicating standard error of the means. *Adapted from Hauth F.et al. (2017) Cell-line dependent effects of hypoxia prior to irradiation in squamous cell carcinoma lines. Clinical and Translational Radiation Oncology (accepted for publication) (1)*

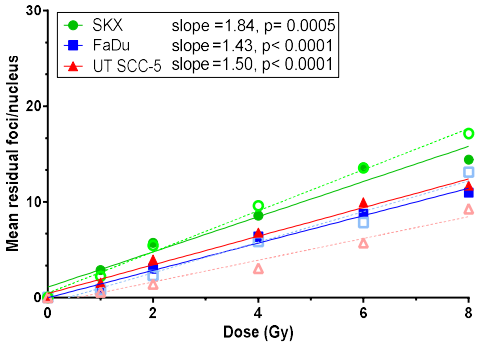

Figure 6B: Linear dose-response of mean number of residual foci for normoxic control (O-O-O, open symbols, dashed line) and post-irradiation incubation under hypoxia (O-O-H, filled symbols, solid line). Shown are the results of 3 (FaDu), 4 (SKX) and 6 (UT SCC-5) independant experiments with standard error of the mean. *Adapted from Hauth F.et al. (2017) Cell-line dependent effects of hypoxia prior to irradiation in squamous cell carcinoma lines. Clinical and Translational Radiation Oncology (accepted for publication)(1)*

In addition, reconstruction of the cell survival curves based on the correlation of γH2AX foci and $-\ln SF_{CFA}$ (**Fig. 6C:** *SKX:* slope= 2.01 r^2= 0.99; *FaDu:* slope= 2.15, r^2= 0.95; *UT SCC-5:* slope= 3.99, r^2= 0.92) resulted in a good approximation for SKX and FaDu cell lines and to a slight underestimation of survival for UT SCC-5 cells (**Fig. 6D**). HMFs, derived from both CFA and γH2AX assay data, revealed values close to one (**Supp. Tab. 1: HMF_{CFA}:** *SKX:* 1.0; *FaDu:* 1.0; *UT SCC-5:* 1.2; **$HMF_{\gamma H2AX}$:** *SKX:* 1.0; *FaDu:* 1.1; *UT SCC-5:* 1.2), indicating no effect of post-irradiation exposure to hypoxia (1) (**Fig. 14**).

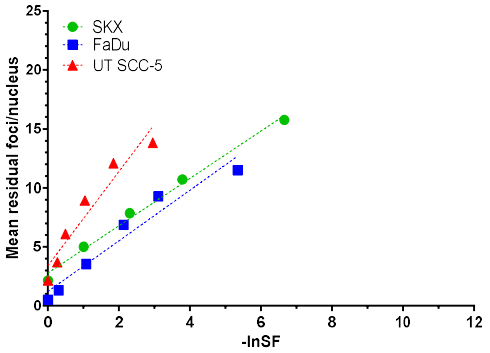

Figure 6C: Linear correlation between –lnSF and mean number of residual γH2AX foci for post-irradiation incubation under hypoxia (experimental group: O-O-H). Shown are results of mean number of residual foci with standard error of the means. *Adapted from Hauth F.et al. (2017) Cell-line dependent effects of hypoxia prior to irradiation in squamous cell carcinoma lines. Clinical and Translational Radiation Oncology (accepted for publication)(1)*

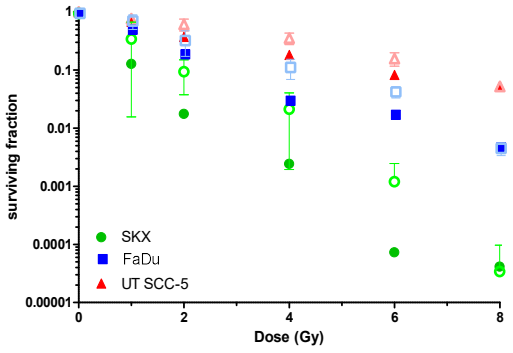

Figure 6D: Figure showing observed and recalculated surviving fractions for all cell lines under investigation for post-irradiation incubation under hypoxia (experimental group: O-O-H). Mean numbers of observed SF are indicated by open symbols, calculated SF values are indicated by filled symbols. Error bars indicating standard deviation. *Adapted from Hauth F.et al. (2017) Cell-line dependent effects of hypoxia prior to irradiation in squamous cell carcinoma lines. Clinical and Translational Radiation Oncology (accepted for publication)(1)*

3.4 Effect of acute hypoxia at the time of irradiation on cellular survival and number of residual γH2AX foci (experimental group: O-H-O)

Application of severe hypoxia at the time of irradiation (acute hypoxia), significantly increased cellular survival in all cell lines over all doses tested (**Fig. 7A:** *SKX:* SF_2= 0.48; *FaDu:* SF_2= 0.71; *UT SCC-5:* SF_2= 0.76) (1). In parallel a significant decrease of the amount of residual γH2AX foci as depicted by the slopes of the linear regression was observed (**Fig. 7B:** *SKX:* slope= 1.31, r^2= 0.29; *FaDu:* slope= 0.41, r^2= 0.42; *UT SCC-5:* slope= 0.41, r^2= 0.03) (1). The survival curves obtained by the correlation of the mean γH2AX foci numbers with $-lnSF_{CFA}$ (**Fig. 7C:** *SKX:* slope= 2.12 r^2= 0.95; *FaDu:* slope= 1.91, r^2= 0.91; *UT SCC-5:* slope= 2.85, r^2= 0.93) did not differ from those observed by standard CFA for FaDu and UT SCC-5 cell lines, whereas for SKX survival was slightly underestimated (**Fig. 7D**) (1). No significant difference was observed in the calculation of OERs based on standard CFA data among the different cell lines with a mean OER of 2.36 (**Supp. Tab. 1:** ***OER_{CFA}:*** *SKX:* 2.3; *FaDu:* 2.4; *UT SCC-5:* 2.3) while calculation of OERs based on data obtained by γH2AX assay resulted in a mean OER of 2.58 over all cell lines (**Supp Tab. 1:** ***$OER_{\gamma H2AX}$:*** *SKX:* 2.0; *FaDu:* 2.9; *UT SCC-5:* 2.8) (**Fig. 14**) (1).

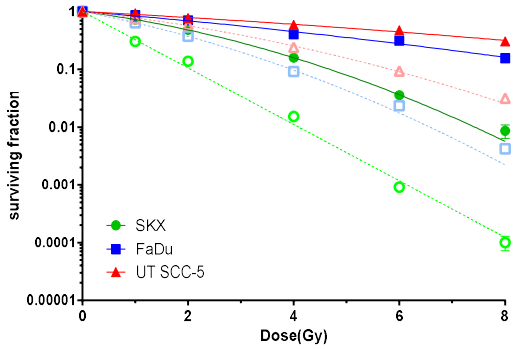

Figure 7A: Standard CFA revealing increased cellular survival for cells exposed to acute hypoxia during irradiation for all cell lines used. Dashed lines and open symbols indicating data obtained under normoxic conditions (experimental group: O-O-O) and filled symbols and solid line indicating data obtained under acute hypoxia (experimental group: O-H-O). Error bars indicate the standard errror of the mean. *Adapted from Hauth F.et al. (2017) Cell-line dependent effects of hypoxia prior to irradiation in squamous cell carcinoma lines. Clinical and Translational Radiation Oncology (accepted for publication)(1)*

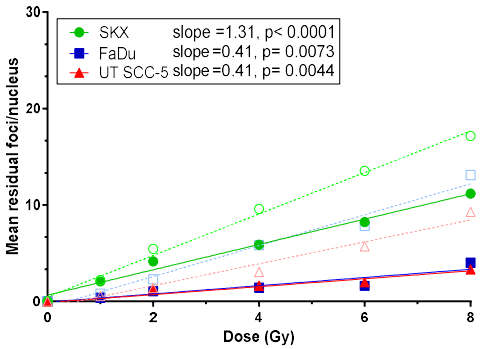

Figure 7B: Figure showing a linerar dose –foci response for all cell lines under investigation. Dashed lines and open symbols indicating data obtained under normoxic conditions (experimental group: O-O-O) and filled symbols and solid line indicating data obtained under acute hypoxia (experimental group: O-H-O). Shown are the means of 3 (SKX, UT SCC-5) and 4 (FaDu) independent experiments with standard error of the mean. *Adapted from Hauth F.et al. (2017) Cell-line dependent effects of hypoxia prior to irradiation in squamous cell carcinoma lines. Clinical and Translational Radiation Oncology (accepted for publication)(1)*

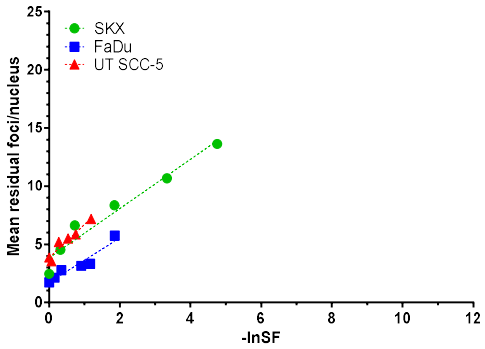

Figure 7C: Correlation between –lnSF$_{CFA}$ and mean number of residual foci followed linear regression for all cell lines under investigation (experimental group: O-H-O). Error bars indicating standard error of the mean.

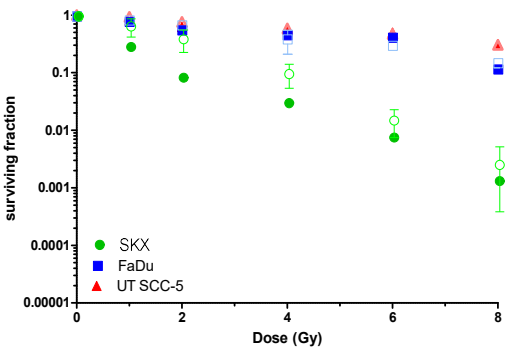

Figure 7D: Figure showing calculated and observed surviving fractions for all cell lines for acute hypoxia at the time of irradiation (experimental group: O-H-O) Mean numbers of observed SF are indicated by open symbols, calculated SF values are indicated by filled symbols. Error bars indicating standard deviation. *Adapted from Hauth F.et al. (2017) Cell-line dependent effects of hypoxia prior to irradiation in squamous cell carcinoma lines. Clinical and Translational Radiation Oncology (accepted for publication) (1)*

3.5 Effect of long term incubation under hypoxia prior to irradiation on cellular survival and number of residual γH2AX foci (experimental group: H-O-O)

Long term exposure to mild hypoxia of 1% O_2 prior to irradiation affected cellular survival compared to control conditions in a cell line dependent manner, namely, induction of radiosensitivity in SKX (**Supp. Tab. 1:** SF_2: 0.05), induction of radioresistance in FaDu (**Supp. Tab. 1:** SF_2: 0.59) and no difference for UT SCC-5 (**Supp. Tab. 1:** SF_2: 0.59) (**Fig. 8A**) (1). Quantification of the magnitude of the effect was performed based on the calculation of HMF values, which were 0.76, 1.54 and 1.10 for SKX, FaDu and UT SCC-5 respectively (**Fig. 14, Supp. Tab. 1**) (1). The slopes of γH2AX foci linear dose response differed from those obtained under normoxic conditions, with decreased slope value for FaDu and SKX cell line and a slight increased slope value for UT SCC-5 cell line (**Fig. 8B:** *SKX:* slope= 0.83, r^2= 0.10; *FaDu:* slope= 0.8, r^2= 0.20; *UT SCC-5:* slope= 1.4, r^2= 0.21) (1). Interestingly, UT SCC-5 and SKX cells expressed an increased amount of background foci in unirradiated controls when cultivated under mild hypoxia (**Suppl. Tab. 2:** mean residual foci (0Gy): *SKX:* 8.7 (H-O-O), 2.0 (O-O-O); *UT SCC-5:* 2.8 (H-O-O), 1.4 (O-O-O)), while no difference was observed for FaDu cell line compared to the control values (**Suppl. Tab. 2:** mean residual foci (0Gy): *FaDu:* 1.1(H-O-O), 0.9 (O-O-O)). Under long term mild hypoxia, recalculation of the cell survival curve could not be performed for the SKX cell line, presumably as a consequence of lack of correlation between mean number of residual γH2AX foci and $-\ln SF_{CFA}$. In contrast, recalculation of survival curves based on the significant linear correlations of γH2AX foci and $-\ln SF_{CFA}$ led to good estimation of the standard CFA curve for FaDu and slight underestimation for UT SCC-5 lines respectively (**Fig. 8C:** *SKX:* slope= 0.58, r^2= 0.14; *FaDu:* slope= 1.58, r^2= 0.99; *UT SCC-5:* slope= 3.86, r^2= 0.97; **Fig. 8D**) (1). Consequently, OERs based on data obtained by γH2AX assay could only be estimated for FaDu and UT SCC-5 cells (**Suppl. Tab. 1:** ***$OER_{\gamma H2AX}$:*** *FaDu:* 1.4; *UT SCC-5:* 1.2) (**Fig. 14**).

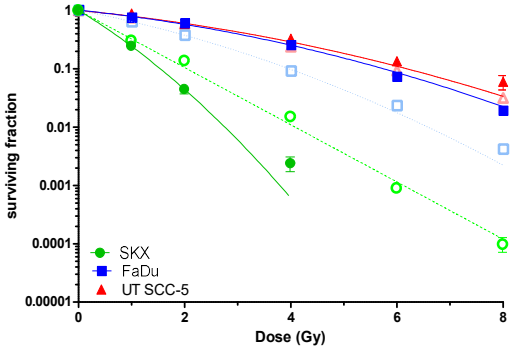

Figure 8A: Application of hypoxia prior to irradiation resulted in three distinct phenotypes for the cell lines under investigation (filled symbols, solid lines; experimental group: H-O-O). Error bars indicating standard error of the mean for three indipendent experiment. Dashed lines and open symbols indicating results obtained under normoxic conditions (experimental group: O-O-O). *Adapted from Hauth F.et al. (2017) Cell-line dependent effects of hypoxia prior to irradiation in squamous cell carcinoma lines. Clinical and Translational Radiation Oncology (accepted for publication)(1)*

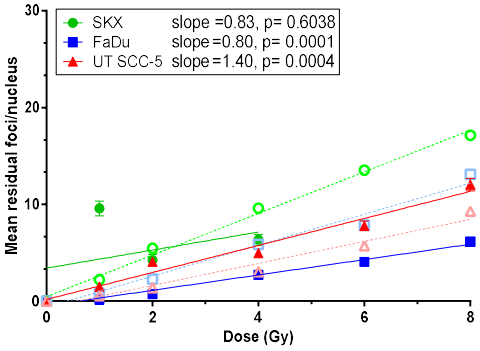

Figure 8B: Figure showing linear dose response of mean number of residual foci for all cell lines used for exposure to hypoxia prior to irradiation (filled symbols, solid lines; experimental group: H-O-O). Error bars indicating standard error of the mean and two indipendent experiments were performed. Open symbols and dashed lines represent data obtained under normoxic conditions (experimental group: O-O-O). *Adapted from Hauth F.et al. (2017) Cell-line dependent effects of hypoxia prior to irradiation in squamous cell carcinoma lines. Clinical and Translational Radiation Oncology (accepted for publication) (1)*

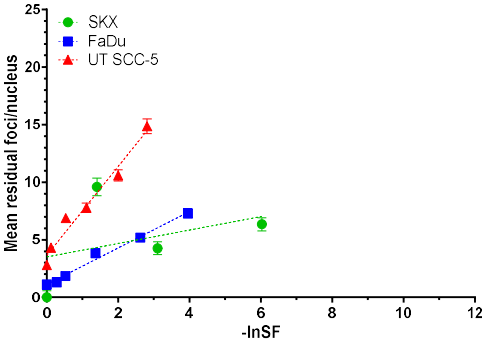

Figure 8C: Figure showing the linear correlation between $-\ln SF_{CFA}$ and mean number of residual γH2AX foci for pre-irradiation incubation under hypoxia (experimental group: H-O-O). Error bars indicating standard error of the mean.

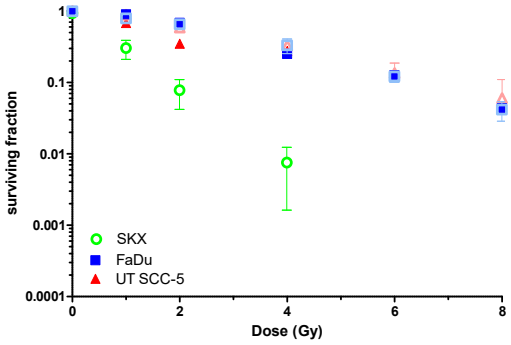

Figure 8D: For FaDu cell line recalculation of surviving fractions led to a survival curve that did not differ from the one observed by standard CFA. For UT SCC-5 cell line recalculation resulted in a slight underestimation of survival, while for SKX cells recalculation was not possible. Mean numbers of observed SF are indicated by open symbols and filled symbols indicating recalculated SF values. Error bars indicating standard deviation. *Adapted from Hauth F.et al. (2017) Cell-line dependent effects of hypoxia prior to irradiation in squamous cell carcinoma lines. Clinical and Translational Radiation Oncology (accepted for publication) (1)*

3.6 Effect of exposure to hypoxia prior and during irradiation on cellular survival and number of γH2AX foci (experimental group: H-H-O)

Application of hypoxia both prior and during the time of irradiation led to a significant increase in cellular survival over all doses and cell lines (**Fig. 9A, Suppl. Tab. 1:** *SKX:* SF_2= 0.46; *FaDu:* SF_2= 0.72; *UT SCC-5:* SF_2= 0.85). For FaDu and UT SCC-5 cells this scenario yielded the maximal increase in cell survival curves, whereas for SKX cell line no differences compared to irradiation under hypoxia alone was observed (**Suppl. Tab. 1:** ***OER_{CFA}:*** *SKX:* 2.45; *FaDu:* 3.73; *UT SCC-5:* 4.22; ***$OER_{\gamma H2AX}$:*** *SKX:* 1.99; *FaDu:* 4.22; *UT SCC-5:* 4.49) (Fig. 14) (1). In parallel, a decrease in slope values was found for the observed linear dose response of residual foci in all cell lines under investigation (**Fig. 9B:** *SKX:* slope= 1.04, r^2= 0.13; *FaDu:* slope= 0.65, r^2= 0.08; *UT SCC-5:* slope= 0.76, r^2= 0.07). For SKX and UT SCC-5 cell line high numbers of residual γH2AX foci were observed in unirradiated cells in this experimental setting (**Suppl. Tab. 2:** mean residual foci (0Gy): *SKX:* 3.9; *UT SCC-5:* 5.1). In contrast, no significant deviation from the background foci values was shown for FaDu cells (**Suppl. Tab. 2:** mean residual foci (0Gy): *FaDu:* 0.9).

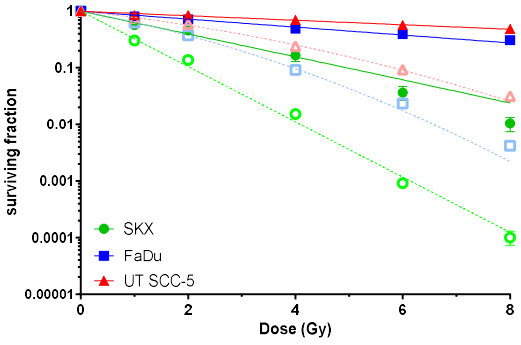

Figure 9A: Application of hypoxia prior and at the time of irradiation increased cellular survival in all cell lines under investigation (filled symbols, experimental group: H-H-O). Dashed lines and open symbolds indicating data obtained under normoxic conditions (experimental group: O-O-O). Error bars indicating standard error of the mean of three independent experiments. *Adapted from Hauth F.et al. (2017) Cell-line dependent effects of hypoxia prior to irradiation in squamous cell carcinoma lines. Clinical and Translational Radiation Oncology (accepted for publication) (1)*

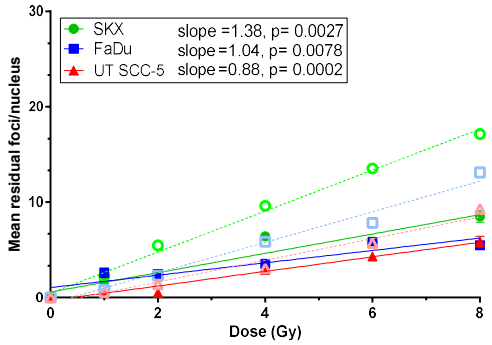

Figure 9B: Figure showing results of γH2AX foci assay for cells kept under hypoxia prior and during irradiation (filled symbols and solid lines; experimental group: H-H-O). A decrease of the linear dose response was observed for all cell lines used. Open symbols and dashed lines indicating data obtained under normoxic conditions (experimental group: O-O-O). Error bars indicating standard error of the mean for two independent experiments. *Adapted from Hauth F.et al. (2017) Cell-line dependent effects of hypoxia prior to irradiation in squamous cell carcinoma lines. Clinical and Translational Radiation Oncology (accepted for publication)(1)*

The correlation between –ln SF_{CFA} and mean residual foci followed linear regression for all cell lines under investigation with remarkably high slope values for UT SCC-5 and FaDu cells (**Fig. 9C:** *SKX:* slope= 1.71 r^2= 0.99; *FaDu:* slope= 4.5, r^2= 0.89; *UT SCC-5:* slope= 8.6, r^2= 0.98). For all cell lines recalculation of survival fractions led to survival curves that did not differ significantly from those obtained under standard CFA conditions (**Fig. 9D**).

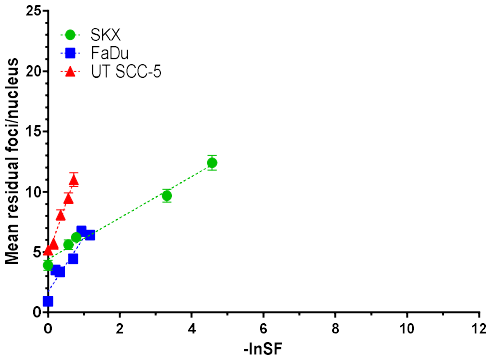

Figure 9C: Figure showing the linear correlation between –ln SF_{CFA} and mean residual foci for all cell lines under investigation. For SKX cell line data obtained after irradiation with 4Gy was excluded. Error bars shown indicating standard error of the mean.

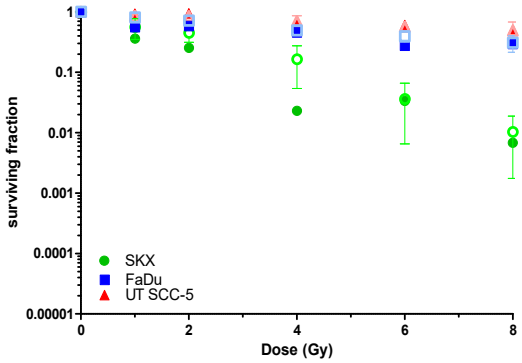

Figure 9D: Recalculation of surviving fractions based on γH2AX foci assay for all cell lines under investigation for cells exposed to hypoxia both prior and at the time of irradiation (experimental group: H-H-O). Mean numbers of observed SF are indicated by open symbols and filled symbols indicating calculated SF values. Error bars indicating standard deviation of the mean. *Adapted from Hauth F.et al. (2017) Cell-line dependent effects of hypoxia prior to irradiation in squamous cell carcinoma lines. Clinical and Translational Radiation Oncology (accepted for publication) (1)*

3.7 Effect of exposure to hypoxia prior and post irradiation on cellular survival and number of γH2AX foci (experimental group: H-O-H)

Hypoxia treatment prior and post irradiation led to radiosensitization in SKX cells compared to normoxic conditions, while in FaDu and UT SCC-5 cells a slight increase of cellular survival was observed (**Fig. 10A, Suppl. Tab. 1:** *SKX:* SF_2= 0.02; *FaDu:* SF_2= 0.49; *UT SCC-5:* SF_2= 0.73). This in turn, resulted in HMFs of 0.7, 1.3 and 1.1 for SKX, FaDu and UT SCC-5 respectively (**Suppl. Tab. 1:** ***$HMF_{\gamma H2AX}$:*** *SKX:* 0.65; *FaDu:* 1.05; *UT SCC-5:* 1.41) (**Fig. 14**) (1). Slope values of the linear regression analysis of residual

foci number and radiation dose did not differ systematically from those obtained under normoxic conditions, with SKX and UT SCC-5 cell line showing a slight increase, while for FaDu cell line a slight decrease was observed (**Fig. 10B:** *SKX:* slope= 2.57, r^2= 0.20; *FaDu:* slope= 1.33, r^2= 0.16; *UT SCC-5:* slope= 1.23, r^2= 0.98). Furthermore, for SKX and UT SCC-5 high values of foci were observed in non-irradiated cells compared to normoxic controls, while for FaDu cell line no significant difference was shown (**Suppl. Tab. 2:** mean residual foci (0Gy): *SKX:* 4.8; *FaDu:* 1.9; *UT SCC-5:* 3.0).

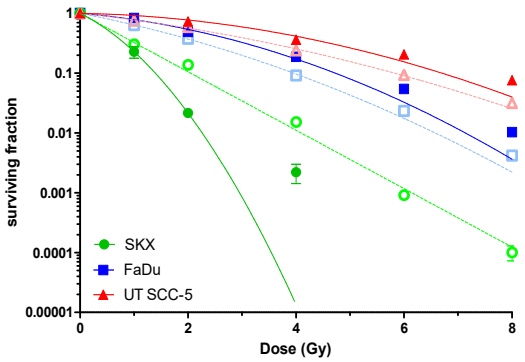

Figure 10A: Figure showing results of standard CFA for cells incubated under hypoxia both prior and post irradiation (filled symbols, solid lines; experimental group: H-O-H). For SKX cell line a decrease in cellular survival could be observed, while for UT SCC-5 and FaDu cells increase of radioresistance was shown under this condition. For SKX cells no survival was observed for cells irradiated with higher doses than 4 Gy. Dashed lines and open symbols indicating data obtained under normoxic conditions (experimental group: O-O-O) and error bars indicating standard error of three independent experiment. *Adapted from Hauth F.et al. (2017) Cell-line dependent effects of hypoxia prior to irradiation in squamous cell carcinoma lines. Clinical and Translational Radiation Oncology (accepted for publication) (1)*

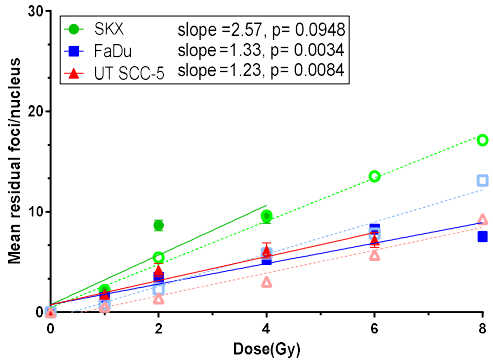

Figure 10B: Application of hypoxia prior and post irradiation (experimental group: H-O-H) resulted in slopes of the linear regression of γH2AX foci assay that differed only minimally from those obtained under normoxic conditions (experimental group: O-O-O), with SKX and UT SCC-5 cell lines showing a slight increase and FaDu showing a slight decrease, respectively. Error bars indicate standard error of the mean of two (SKX, FaDu) and one (UT SCC-5) independent experiments. For UT SCC-5 cell line no data could be collected for cells irradiated with 8 Gy due to poor sample quality. Dashed lines and open symbols indicating data obtained under normoxic conditions. *Adapted from Hauth F.et al. (2017) Cell-line dependent effects of hypoxia prior to irradiation in squamous cell carcinoma lines. Clinical and Translational Radiation Oncology (accepted for publication) (1)*

Based on the linear regression equations derived from the correlation between mean residual γH2AX foci and -lnSF_{CFA} (**Fig. 10C:** *SKX:* slope= 1.66 r^2= 0.92; *FaDu:* slope= 2.64, r^2= 0.97; *UT SCC-5:* slope= 3.95, r^2= 0.86) we could estimate the cell survival

curves accurately compared to the observed ones for SKX and FaDu cell lines and with a slight underestimation for UT SCC-5 cells (**Fig. 10D**).

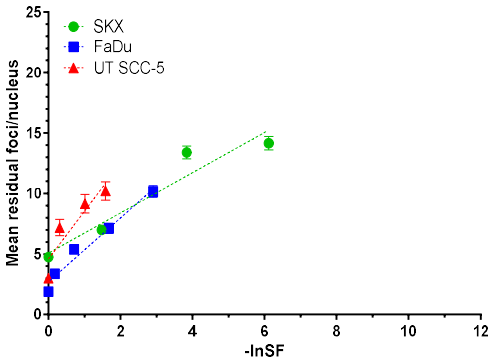

Figure 10C: Linear correlation between –ln SF_{CFA} and mean number of residual foci for all cell lines under investigation and pre- and post irradiation incubation under hypoxia (experimental group: H-O-H). Error bars indicating standard error of the mean.

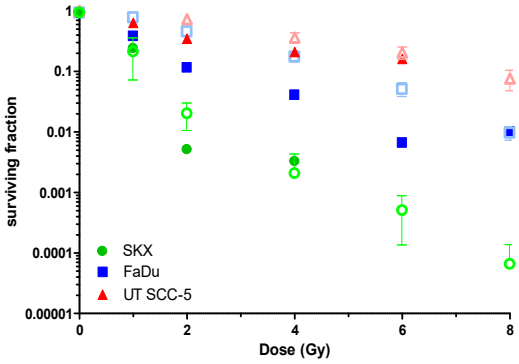

Figure 10D: Recalculation of SFs revealed no significant differences compared to SFs observed by standard CFA for SKX and FaDu cell lines and resulted in a slight underestimation of survival for UT SCC-5 cells (experimental group: H-O-H). Mean numbers of observed SF are indicated by open symbols and recalculated SF values by filled symbols. Error bars indicating standard deviation. *Adapted from Hauth F.et al. (2017) Cell-line dependent effects of hypoxia prior to irradiation in squamous cell carcinoma lines. Clinical and Translational Radiation Oncology (accepted for publication)(1)*

3.8 Effect of exposure to hypoxia at the time of and post irradiation on cellular survival and number of γH2AX foci (experimental group: O-H-H)

Exposure of cells to hypoxia acutely at the time of irradiation and during repair time (24h post-irradiation) led to increased cellular survival (**Fig. 11A, Suppl. Tab. 1:** *SKX:* SF_2= 0.34; *FaDu:* SF_2= 0.89; *UT SCC-5:* SF_2= 0.90) with a mean OER of 2.56 over all cell lines (**Suppl. Tab. 1: *OER_{CFA}:*** *SKX:* 2.6; *FaDu:* 2.4; *UT SCC-5:* 2.8*;* ***$OER_{\gamma H2AX}$:*** *SKX:* 2.3; *FaDu:* 2.9; *UT SCC-5:* 4.6) (Fig. 14) (1). As expected, linear dose response of the mean number of residual foci resulted in lower slope values compared to normoxic conditions (**Fig. 11B:** *SKX:* slope= 1.38, r^2= 0.33; *FaDu:* slope= 1.04, r^2= 0.16; *UT SCC-5:* slope= 0.88, r^2= 0.10). For UT SCC-5 cell line we observed a high amount of residual γH2AX foci in unirradiated cells under this condition compared to the normoxic controls, however no significant differences were shown for FaDu and SKX cells (**Suppl. Tab. 2:**

mean residual foci (0Gy): *SKX:* 1.8; *FaDu:* 1.3; *UT SCC-5:* 6.1). Subsequently, plotting the mean number of residual foci against the –ln SF_{CFA} resulted in a significant linear correlation, with surprisingly high slope values for FaDu and UT SCC-5 cells (**Fig. 11C:** *SKX:* slope= 2.84, r^2= 0.91; *FaDu:* slope= 4.53, r^2= 0.95; *UT SCC-5:* slope= 9.66, r^2= 0.03). Recalculation of survival fractions based on the γH2AX mean foci numbers led to survival curves that were not significantly different from those obtained by standard CFA and data could be fitted with a single curve (**Fig. 11D**).

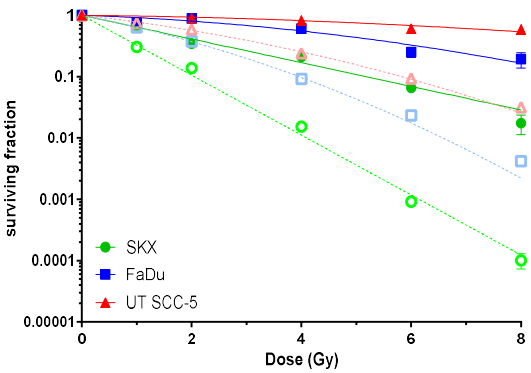

Figure 11A: Results of standard CFA revealed increased cellular survival after application of hypoxia both at the time of irradiation and during repair time (filled symbols, solid lines; experimental group: O-H-H) for all cell lines under investigation. Error bars indicating standard error of the means of 3 individual experiments and dashed lines and open symbols indicating data obtained under normoxic conditions (experimental group: O-O-O). *Adapted from Hauth F.et al. (2017) Cell-line dependent effects of hypoxia prior to irradiation in squamous cell carcinoma lines. Clinical and Translational Radiation Oncology (accepted for publication)(1)*

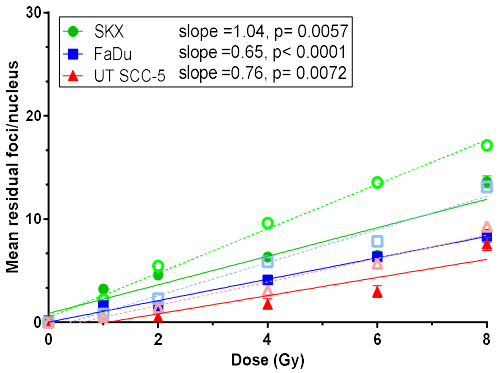

Figure 11B: For all cell lines exposure to hypoxia both during and after irraidation (filled symbols, solid lines; experimental group: O-H-H) let to a decrease of slopes of the linear correlation compared to the normoxic controls. Error bars indicate standard error of the mean. Dashed lines and open symbols indicate data obtained under normoxic conditions (experimental group: O-O-O). *Adapted from Hauth F.et al. (2017) Cell-line dependent effects of hypoxia prior to irradiation in squamous cell carcinoma lines. Clinical and Translational Radiation Oncology (accepted for publication)(1)*

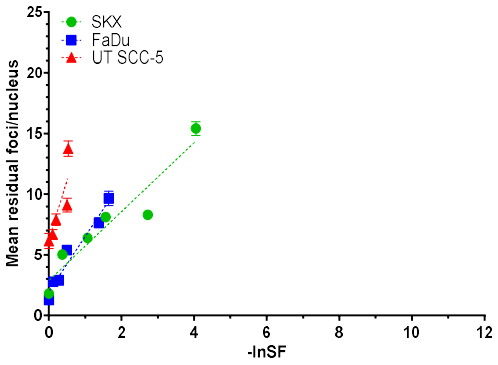

Figure 11C: Figure indicating linear correlation between –ln SF_{CFA} and mean residual foci for exposure to hypoxia at the time and after irradiation (experimental group: O-H-H). Error bars showing standard error of the mean.

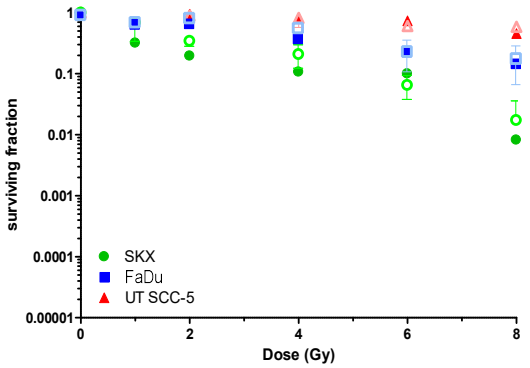

Figure 11D: Calculation of SFs based on the correlation between –ln SF_{CFA} and residual foci resulted in survival curves that did not differ from those obtained by standard CFA foci for exposure to hypoxia at the time and after irradiation (experimental group: O-H-H). Mean numbers of observed SF are indicated by open symbols and calculated SF values indicated by open symbols. Error bars indicating standard deviation. *Adapted from Hauth F.et al. (2017) Cell-line dependent effects of hypoxia prior to irradiation in squamous cell carcinoma lines. Clinical and Translational Radiation Oncology (accepted for publication) (1)*

3.9 Effect of chronic hypoxia on cellular survival and number of γH2AX foci (experimental group: H-H-H)

Continuous incubation of cells under hypoxia (chronic hypoxia), during all the experimental time frames, prior, during and post irradiation, led to an increase in cellular survival for all three cell lines (**Fig. 12A, Suppl. Tab. 1:** *SKX:* SF_2= 0.33; *FaDu:* SF_2= 0.86; *UT SCC-5:* SF_2= 0.85). In parallel a significant decrease of the amount of residual foci as depicted by the slopes of the linear regression of data obtained by γH2AX assay was observed (**Fig. 12B:** *SKX:* slope= 1.39, r^2= 0.21; *FaDu:* slope= 0.98, r^2= 0.12; *UT SCC-5:* slope= 0.86, r^2= 0.05). Interestingly, under this condition we observed a significant increase in numbers of residual foci in non-irradiated controls for FaDu and UT SCC-5 cell line, whereas for SKX only slightly higher numbers were recorded (**Suppl. Tab. 2:** mean residual foci (0Gy): *SKX:* 3.7; *FaDu:* 3.9; *UT SCC-5:* 4.9). In addition, estimation of OERs both based on standard CFA data and γH2AX assay revealed increased survival for cells incubated under chronic hypoxia (**Suppl. Tab.1:** ***OER_{CFA}:*** *SKX:* 1.7; *FaDu:* 2.8; *UT SCC-5:* 2.4; ***$OER_{\gamma H2AX}$:*** *SKX:* 1.7; *FaDu:* 3.9; *UT SCC-5:* 3.5) (Fig. 14) (1).

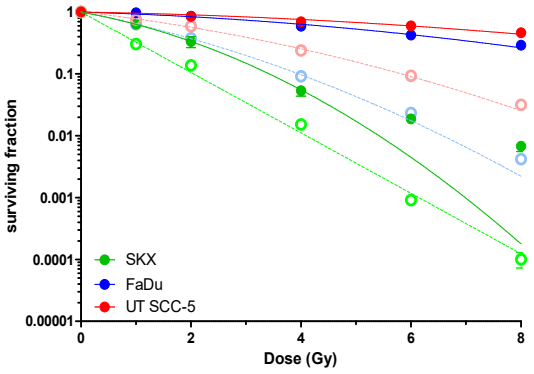

Figure 12A: Application of chronic hypoxia led to an increase in cellular survival for all cell lines under investigation. Error bars indicate standard error of the mean. Dashed lines and open symbols indicating data obtained under normoxic conditions (experimental condition: O-O-O) and solid lines and filled symbols indicating data obtained under chronic hypoxia (experimental condition: H-H-H). *Adapted from Hauth F.et al. (2017) Cell-line dependent effects of hypoxia prior to irradiation in squamous cell carcinoma lines. Clinical and Translational Radiation Oncology (accepted for publication) (1)*

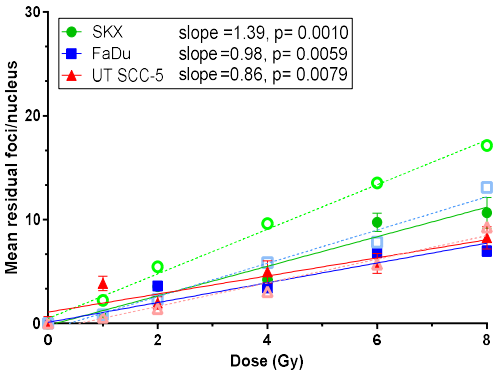

Figure 12B: Continuous incubation of cells under hypoxia led to a significant decrease of slopes of the observed linear regression between mean residual foci and dose for all cell lines under investigation. Dashed lines and open symbols indicating data obtained under normoxic conditions (experimental group: O-O-O) and solid lines and filled symbols indicating data obtained under chronic hypoxia (experimental group: H-H-H). Error bars indicating standard deviation of the means of two (FaDu) and one (SKX, UT SCC-5) indipendant experiments, respectively. *Adapted from Hauth F.et al. (2017) Cell-line dependent effects of hypoxia prior to irradiation in squamous cell carcinoma lines. Clinical and Translational Radiation Oncology (accepted for publication) (1)*

For all cell lines mean number of residual γH2AX foci were linearly correlated with –ln SF_{CFA}, with surprisingly high slope values for FaDu and UT SCC-5 cell lines (**Fig. 12C:** *SKX:* slope= 2.14 r^2= 0.93; *FaDu:* slope= 5.73, r^2= 0.84; *UT SCC-5:* slope= 6.96, r^2= 0.66). Recalculation of survival curves based on the respective equations led to survival curves that were not significantly different from those observed by standard CFA (**Fig. 12 D**).

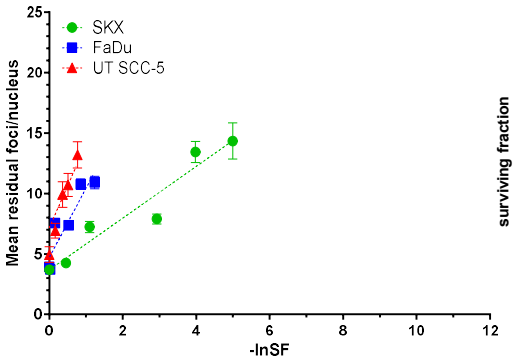

Figure 12C: Figure showing the correlation between mean number of residual foci and –ln SF_{CFA} (mean lethal lesions) for all cell lines used. Error bars indicating standard error of the mean.

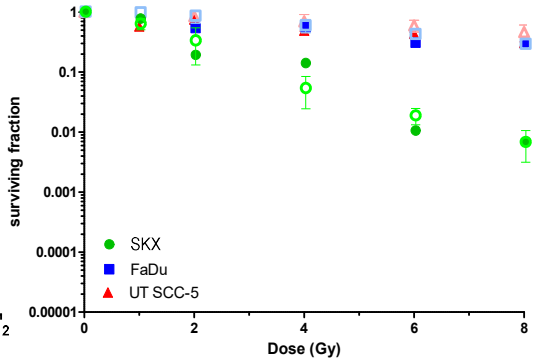

Figure 12D: Recalculation of SFs based on data obtained by γH2AX foci assay resulted in survival curves that did not differ from those observed by standard CFA (experimental group: H-H-H). Open symbols indicating observed SF values and filled symbols indicating calculated SF values. Error bars indicating standard deviation. *Adapted from Hauth F.et al. (2017) Cell-line dependent effects of hypoxia prior to irradiation in squamous cell carcinoma lines. Clinical and Translational Radiation Oncology (accepted for publication) (1)*

3.10 Recalculation of OERs and HMFs

As an approach to our hypothesis, that OERs and HMFs could be recalculated based solely on the mean number of residual γH2AX foci, we correlated OERs and HMFs observed by standard CFA with the corresponding data obtained by γH2AX assay [2.6.4] (Suppl. Fig. 1). As hypothesized, the fit of these parameters resulted in a significant linear correlation for 10% survival with a slope very close to 1, indicating the accuracy of the method.

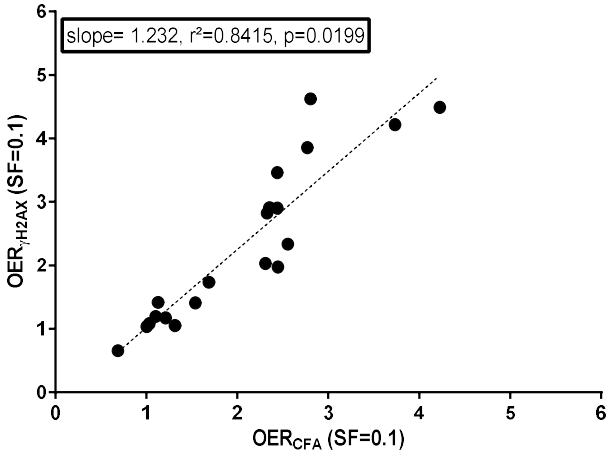

Figure 13: Figure showing the linear correlation between OERs/HMFs observed by standard CFA and OERs/HMFs calculated based on data obtained by γH2AX assay. OERs and HMFs are calculated for 10% survival (SF= 0.1). *Adapted from Hauth F.et al. (2017) Cell-line dependent effects of hypoxia prior to irradiation in squamous cell carcinoma lines. Clinical and Translational Radiation Oncology (accepted for publication)(1)*

3.11 Comparison OER and HMF values for all conditions under investigation

Comparison of OER and HMF values over all conditions and cell lines tested clearly revealed a pattern for experimental groups, where cells were incubated under hypoxic conditions prior to irradiation. Thus, SKX showed an OER value below 1 (experimental groups: H-O-O, H-O-H), or for chronic hypoxic cells (experimental group: H-H-H) an OER value below the OER for acute hypoxia (experimental group: O-H-O) alone, indicating a decrease in cellular survival under these conditions (**Suppl. Tab. 1**). For FaDu cell line we observed an OER value above 1 for cell exposed to hypoxia prior to irradiation (experimental groups: H-O-O, H-O-H) and for chronic hypoxic cells a higher value than expected from exposure to acute hypoxia alone (experimental group: O-H-O) respectively. In contrast, we observed OER/HMF values close to 1 for UT SCC-5 cells (experimental groups: H-O-O, H-O-H) and no significant difference between OER values obtained for acute and chronic hypoxia (experimental groups: O-H-O, H-H-H). Interestingly, for cells exposed to hypoxia both prior and at the time of irradiation we observed exceptional high OER values for all cell lines under investigation with the highest OER value for UT SCC-5 cells (**Suppl. Tab.1: *OER_{CFA}:*** *SKX:* 2.45; *FaDu:* 3.73;

UT SCC-5: 4.22). However, for SKX we still observed the lowest OER value as expected (1).

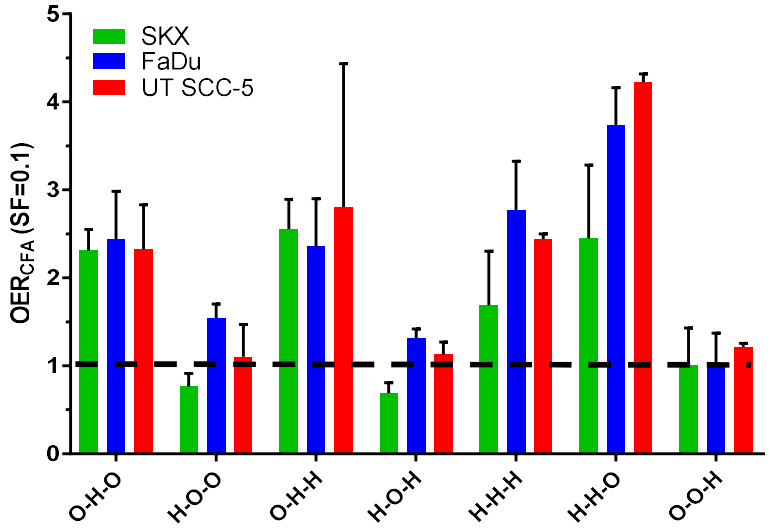

Figure 14: Figure showing OER and HMF values for all conditions and all cell lines tested. Black bar indicating an OER of 1, e.g. no significant difference between condition tested and control (experimental group: O-O-O). Error bars indicating standard deviation of the mean of three individual experiments. *Adapted from Hauth F.et al. (2017) Cell-line dependent effects of hypoxia prior to irradiation in squamous cell carcinoma lines. Clinical and Translational Radiation Oncology (accepted for publication) (1)*

3.12 Effect of acute hypoxia on protein expression and phosphorylation status of proteins (experimental group: O-H-O)

In order to investigate the underline mechanisms leading to the increased cellular survival when cells were irradiated under hypoxic conditions, we performed western blot analysis focused on DNA repair enzymes. Application of acute hypoxia at the time of irradiation led to a strong activation of Hif-1α immediately after irradiation (**Fig. 15A, B, C**) (**Suppl. Fig. 2**). The phenomenon was also observed in the non-irradiated controls, which were only incubated under hypoxia at the same time. Expression level of Rad51, was not changed neither after irradiation nor after exposure to hypoxia for all cell lines investigated (**Fig. 15A, B, C**) (**Suppl. Fig. 2**). As expected, 4Gy irradiation induced a strong upregulation of protein levels and phosphorylation of ATM (Ser 1981) in both FaDu and UT SCC-5 cell lines (**Fig. 15A, B, C**) immediately upon irradiation remaining up to the 6 hours time point, while no difference was recorded after application of acute

hypoxia alone (**Suppl. Fig. 2**). For SKX cell line, no traces of ATM protein could be detected (**Fig. 15A**). Furthermore, for all cell lines we observed induction of DNA-PK phosphorylation (Ser 2056) after irradiation (30 min), with a delayed peak of enzyme activity in SKX cells after 6 hours (**Fig. 15A, B, C**). Under conditions of acute hypoxia a slight reduction of phosphorylation was shown in all cell lines under investigation (**Suppl. Fig. 2**).

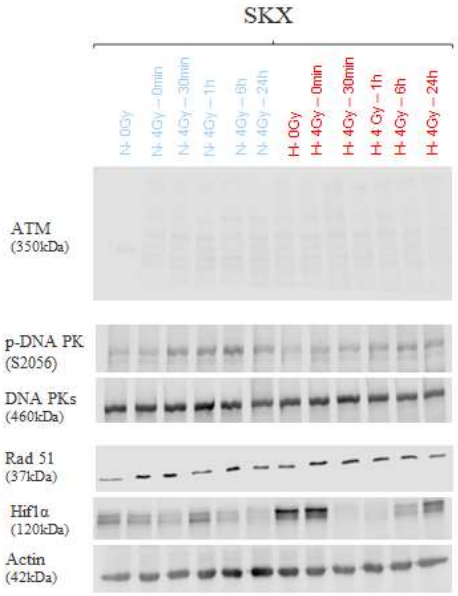

Figure 15A: Figure showing results of western blot analysis for SKX cell line under either normoxic conditions (N, experimental condition: O-O-O) or irradiation under hypoxia (H, experimental condition: O-H-O). Lysates were extracted at the indicated time points post irradiation with 4 Gy (0min, 30min, 1h, 6h, 24h). As a loading control β-Actin was used as shown. For phosphorylated proteins corresponding unphosphorylated proteins served as loading controls. One experiment was performed.

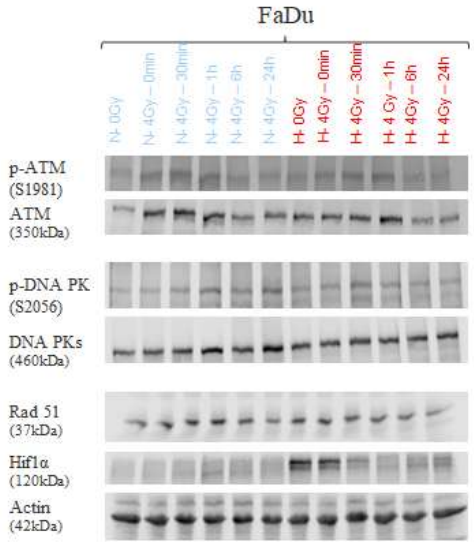

Figure 15B: Figure showing results of western blot analysis for FaDu cell line under either normoxic conditions (N, experimental condition: O-O-O) or irradiation under hypoxia (H, experimental condition: O-H-O). Lysates were extracted at the indicated time points post irradiation with 4 Gy (0min, 30min, 1h, 6h, 24h). As a loading control β-Actin was used as shown. For phosphorylated proteins corresponding unphosphorylated proteins served as loading controls. Two experiments were performed.

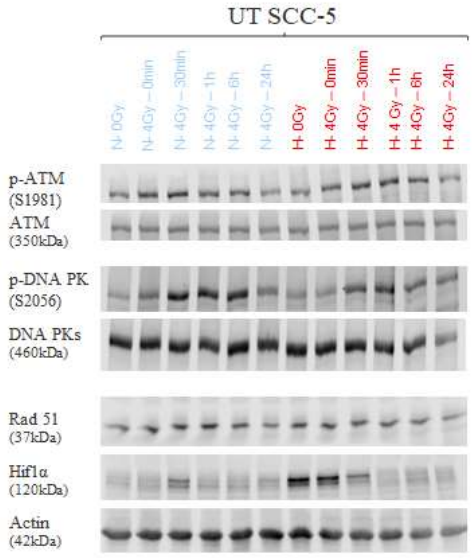

Figure 15C: Figure showing results of western blot analysis for UT SCC-5 cell line under either normoxic conditions (N, experimental condition: O-O-O) or irradiation under hypoxia (H, experimental condition: O-H-O). Lysates were extracted at the indicated time points post irradiation with 4 Gy (0min, 30min, 1h, 6h, 24h). As a loading control β-Actin was used as shown. For phosphorylated proteins corresponding unphosphorylated proteins served as loading controls. One experiment was perfomed.

3.13 Effect of exposure to hypoxia prior to irradiation on protein expression and phosphorylation status of proteins (experimental group: H-O-O)

Exposure to hypoxia prior to irradiation led to an impairment of HR repair pathway compared to normoxic controls as revealed by the downregulation of Rad51 protein levels, an HR-key regulator, for all cell lines under investigation (**Fig. 16A, B, C**) (**Suppl. Fig. 3**) (1). This observation was irrespective of additional irradiation with 4Gy. Phosphorylation of ATM protein at Serine 1981 was increased when cells were not only irradiated but also exposed to hypoxia prior to irradiation for UT SCC-5 cells and to a lesser extent also for FaDu cells (**Fig. 16B, C**) (**Suppl. Fig. 3**) (1). Both ATM and its phosphorylated form (p-ATM) could not be detected in SKX cell line under both conditions (**Fig. 16A)** (1). Phosphorylation of DNA-PKcs at the site of Serine 2056 after irradiation was observed for all cell lines and no differences were recorded between samples kept under normoxic conditions compared to pre-irradiation incubation under hypoxia (**Fig. 16A, B, C**). For SKX a slightly delayed phosphorylation of DNA-PKcs was observed after irradiation with 4 Gy (**Fig. 16A, Suppl. Fig. 3)** (1).

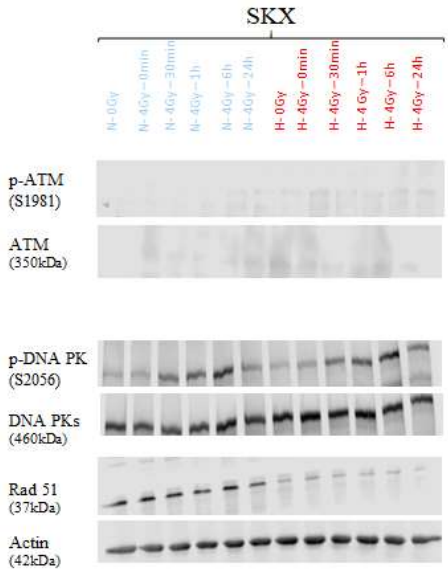

Figure 16A: Figure showing results of western blot analysis for SKX cell line under either normoxic conditions (N, experimental group: O-O-O) or under pre-irradiation incubation under hypoxia (H, experimental group: H-O-O). Lysates were extracted at the indicated time points post irradiation with 4 Gy (0min, 30min, 1h, 6h, 24h). As a loading control β-Actin was used as shown. For phosphorylated proteins corresponding unphosphorylated proteins served as loading controls. Two experiments were perfomed. *Adapted from Hauth F.et al. (2017) Cell-line dependent effects of hypoxia prior to irradiation in squamous cell carcinoma lines. Clinical and Translational Radiation Oncology (accepted for publication) (1)*

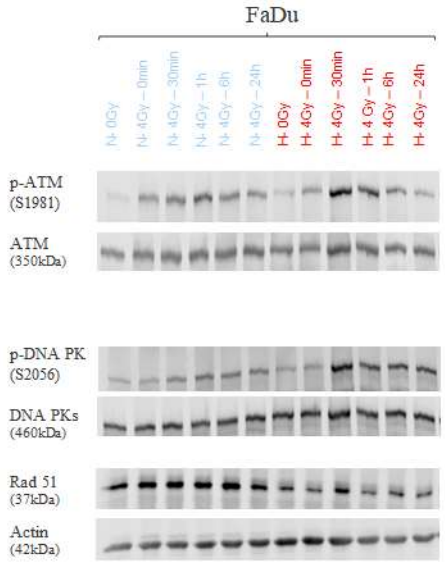

Figure 16B: Figure showing results of western blot analysis for FaDu cell line under either normoxic conditions (N, experimental group: O-O-O) or under pre-irradiation incubation under hypoxia (H, experimental group: H-O-O). Lysates were extracted at the indicated time points post irradiation with 4 Gy (0min, 30min, 1h, 6h, 24h). As a loading control β-Actin was used as shown. For phosphorylated proteins corresponding unphosphorylated proteins served as loading controls. Two experiments were perfomed. *Adapted from Hauth F.et al. (2017) Cell-line dependent effects of hypoxia prior to irradiation in squamous cell carcinoma lines. Clinical and Translational Radiation Oncology (accepted for publication) (1)*

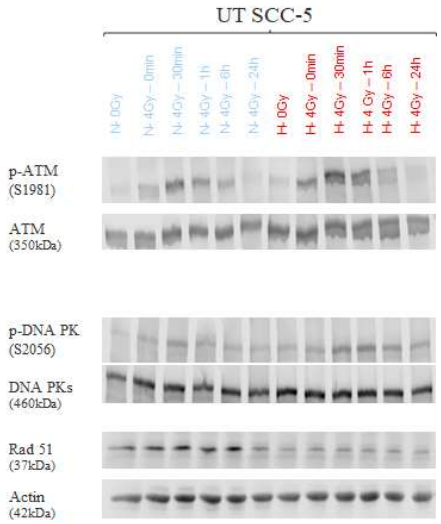

Figure 16C: Figure showing results of western blot analysis for UT SCC-5 cell line under either normoxic conditions (N, experimental group: O-O-O) or under pre-irradiation incubation under hypoxia (H, experimental group: H-O-O). Lysates were extracted at the indicated time points post irradiation with 4 Gy (0min, 30min, 1h, 6h, 24h). As a loading control β-Actin was used as shown. For phosphorylated proteins corresponding unphosphorylated proteins served as loading controls. Two experiments were perfomed. *Adapted from Hauth F.et al. (2017) Cell-line dependent effects of hypoxia prior to irradiation in squamous cell carcinoma lines. Clinical and Translational Radiation Oncology (accepted for publication) (1)*

3.14 Effect of exposure to hypoxia prior to and at the time of irradiation on protein concentration and phosphorylation of proteins (experimental group: H-H-O)

Application of hypoxia prior and at the time of irradiation led to a downregulation of Rad51 protein in UT SCC-5 cell line, with a reduction on 51% for Rad51 (**Fig. 17, Suppl. Fig. 4)**. This impairment of the protein was independent of irradiation with 4 Gy. For ATM a phosphorylation of the protein at the site of Serin 1981 following irradiation was observed with no significant difference between incubation under normoxia and exposure to hypoxia both prior to and at the time of irradiation (**Fig. 17, Suppl. Fig. 4)**. Also testing for phosphorylation of DNA PK (Ser 2056) revealed only an increase after irradiation as expected, but no difference compared to normoxia was detected (**Fig. 17, Suppl. Fig. 4)**.

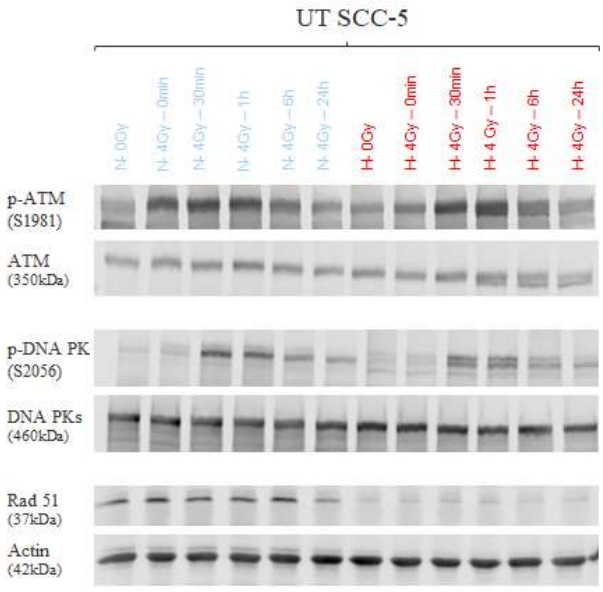

Figure 17: Figure showing results of western blot analysis for UT SCC-5 under either normoxic conditions (N, experimental group: O-O-O) or for exposure to hypoxia both prior and at the time of irradiation (H, experimental group: H-H-O). Lysates were extracted at the indicated time points post irradiation with 4 Gy (0min, 30min, 1h, 6h, 24h). As a loading control β-Actin was used as shown. For phosphorylated proteins corresponding unphosphorylated proteins served as loading controls. One experiment was performed.

4 DISCUSSION

In previous experiments it was shown that hypoxic subvolumes of tumours grown as xenografts in nude mice exhibited less residual DNA DSBs, depicted as residual γH2AX foci, 24 hours after irradiation. Furthermore, differences in intrinsic radiosensitivity between the two cell lines under investigation were solely expressed in well oxygenated tumour areas (14). Based on these observations we hypothesized that irradiation of tumour cell lines under hypoxia leads to less pronounced differences in radiation sensitivity compared to the one observed when irradiation occurs under ambient conditions and that exposure to hypoxia at different timepoints regarding irradiation alters the radiation response of cells both in terms of cellular survival as well as the expression profile of DNA damage response enzymes (1). Therefore, the aim of the current study was to functionally characterize the effect of hypoxia exposure on cellular survival and DNA damage repair in three hSCC lines of the head and neck region with pronounced differences in intrinsic radiosensitivity, namely SKX (radiosensitive), FaDu (moderate sensitivity) and UT SCC-5 (radioresistant) (1).

Our findings indicate that the most important factor determining cellular survival is the presence of oxygen during irradiation as this condition resulted in significantly higher cellular survival and significantly lower amounts of residual γH2AX foci. However, since the survival increase was rather homogeneous as depicted from the OER values, hypoxia exposure did not alter the overall pattern of radiation sensitivity across the respective cell lines. Therefore, our results do not support the initial hypothesis (1). Furthermore, our observations, suggest that post-irradiation hypoxia exposure does not affect cellular survival whereas pre-irradiation hypoxia exposure yields differential radiation response in a cell line dependent manner indicating differences in intrinsic hypoxia tolerance (1).

All experiments were performed 24 hours after irradiation, a time point, which has been previously shown to be adequate for DNA DSB repair completion in SKX and FaDu cells (85, 88, 96). Only confluent cell cultures were irradiated as Hammond et al. reported in their paper from 2004 that for RKO cell line S-phase cells were more sensitive to both hypoxia (<0.02% O_2) and reoxygenation (1, 103). Additionally, several reports points out

the cell cycle dependent and DNA damage independent expression of H2AX, which can in turn affect the evaluation of phosphorylated histone through the appearance of so-called microfoci (79, 90). By using confluent cultures, cells are enriched in the G1 phase and therefore the cell cycle dependent effects can be minimized. In the past many studies by different groups focused on survival and differences in DNA DSB repair under conditions of severe hypoxia or even anoxia (104-106), but not much is known about alterations under mild or moderate hypoxia. This is intriguing as cells that are moderate hypoxic may exhibit a radioresistant phenotype while not suffering from the cytotoxic effects of severe hypoxia. This phenomenon was demonstrated in a paper by Menegakis et al. where they observed a significant decline on the residual γH2AX foci with increasing distance form perfused vessels in human tumour xenografts, indicative of an intratumoural oxygen gradient, suggesting that a large number of tumour cells might be constantly exposed to conditions of intermediate hypoxia and such condition might affect their radiation response (14). Consequently, for our experiments we decided to set oxygen cultivation levels to 1% (1). This oxygen concentration has been shown previously to be adequate for binding of pimonidazole, a 2-nitroimidazole exogenous hypoxia marker that is bioreduced via formation of covalent bonds with cellular macromolecules at oxygen levels below 10 mmHg and has been extensively used previously in many studies both *in vivo* and *in vitro* (14, 23, 34, 94, 107).

Three different hSCC cell lines of the head and neck region with pronounced differences in intrinsic radiosensitivity were investigated in the study. These differences were reported earlier both after *in vitro* and *in vivo* testing (14, 32, 89, 96, 97, 99) and were confirmed in our study by terms of clonogenic survival (standard CFA) as well as by terms of residual DNA DSBs marked as residual γH2AX foci under normoxic conditions (SKX: sensitive; FaDu: moderate sensitivity; UT SCC-5: resistant) (1). However, in comparison to previous studies we observed lower SF_2 values for FaDu cells with regard to standard CFA. This effect can be explained by the atypically high PE for this cell line in the non-irradiated petri-dishes, which led respectively to lower SF_2 values as PE acts as numerator during calculation of surviving fractions [2.6.2]. For SKX and UT SCC-5 cells, surviving fractions after 2 Gy did not significantly differ from data obtained in previous studies (89, 96, 97). Extensive radiosensitivity in SKX cell line has been recently

reported by Mansour et al. to be mediated by overexpression of a micro-RNA (miR-421) leading to downregulation of ATM expression (97). In line with previously published data of Menegakis et al. (89), ratio of slopes of linear γH2AX foci dose response between SKX and FaDu cell lines was consistent although slope values differed within the two studies. This discrepancy can be explained by differences in evaluation technique as in the former study foci where counted manually under the microscope whereas in our study evaluation was performed on a PC-screen after acquisition of images. As in evaluation of cells under the microscope assessment of different focus planes of single cells is feasible, this potentially results in higher or at least different counting of numbers of foci per nucleus.

Among the DNA lesions induced by ionizing irradiation, DNA DSBs are of outmost significance, since if these lesions remain unrepaired can potentially lead to genetic instability or loss of genetic material through chromosomal aberrations, deletions or translocations resulting in mitotic catastrophe (68, 72, 108). The probability of survival for a single cell after irradiation is determined by the probability that this cell has no residual lethal lesion, respectively residual unrejoined DNA DSBs (1). There is good supporting evidence that survival post –irradiation is closely linked to residual DSBs (109) and that the number of unrepaired DSBs correlate with residual γH2AX foci. MacPhail et al. showed that higher rates of foci loss correlated with higher clonogenic survival in ten different cancer cell lines, indicating a close relation between the two parameters (110). Similarly, Banath et al. showed that residual γH2AX foci are indicative of lethal lesions after exposure of SiHa cells to various types of DNA damaging agents (85). Results of several other groups supported the observations of these two studies (109, 111). The probability of radiation-induced cell death for a single cell can be described by the Poisson distribution of lethal lesions. Based on this, it has been shown that γH2AX residual foci correlate significantly with the lethal lesions expected by the Poisson model (87, 89) (1). We were able to reproduce this observation in our study and found strong correlations between number of residual DNA DSBs, marked as residual γH2AX foci, and –ln SF, indicating mean number of lethal lesions predicted by Poisson statistics. Furthermore, as previously published we also showed that cell survival curves could be reconstructed based only on the mean number of residual γH2AX foci (1, 89). These

correlations demonstrate the close connection of intrinsic radiation sensitivity (measured as SF) and number of unrepaired DSBs (evaluated as residual γH2AX foci).

As a first approach to our hypothesis, we evaluated the effect of hypoxia on cellular growth and observed a significant increase of DTs for all cell lines investigated, with UT SCC-5 cell line showing the highest, SKX an intermediate and FaDu cell line showing the slightest delay of cellular growth, respectively. In contrast, in terms of PE of standard CFA for cells incubated under hypoxia prior to irradiation we observed an increase for FaDu cell line, whereas a decrease of PE compared to normoxic conditions was shown for SKX and UT SCC-5 cells. The impact of hypoxia on cellular growth and clonogenicity has been extensively tested under different experimental conditions, however the reference data are very much variable and often contradictory. While it has been demonstrated that severe hypoxia downregulates overall protein synthesis through diverse mechanisms affecting cell cycle progression and growth stimulation (52, 112-114), it appears that the outcome of different studies is very much dependent on the cell line origin (tumour or normal tissue), on genetic background (e.g. p53 status), the oxygen concentration applied to the cells (severe or moderate hypoxia) and to the duration of hypoxia exposure. Spiro et al. reported already in 1984 a decline of PE in a cell cycle dependent manner for V-79 Chinese hamster lung fibroblasts incubated under conditions close to anoxia (gassing with 100% N_2) for 20 hours prior to plating (115). Interestingly, another report showed no significant alteration of PE for several cell lines of various tissue origins, namely HT1080 (fibrosarcoma), RKO (colon carcinoma cell line), HeLa (cervix carcinoma cell line) and RCC4 (renal clear cell carcinoma cell line), for cells grown under moderate hypoxia (2% and 0.5% O_2) during colony formation (116). Hammond et al. reported no significant decrease of DNA synthesis measured by [^{3}H]thymidine incorporation for RKO cells grown for up to 24 hours at 2% oxygen, whereas incubation at 0.02% oxygen lead to a substantial decrease (117). Chan et al. only observed a slight decrease in proliferation after 72 hours of continuous gassing with 0.02% oxygen in H1299 lung cancer cells (118), while Kumareswaran et al. observed a significant decrease of cellular proliferation for asynchronously growing fibroblasts exposed to 0.02% oxygen for up to 7 days (106).

In the present study, we applied hypoxia in three different time frames with regard to radiation exposure. Post irradiation hypoxia did not have a significant impact on neither cellular survival nor the amount of residual γH2AX foci for all cell lines under investigation and accordingly let to HMF values close to one (1). This observation is consistent with previously published data *in vivo* for FaDu and SKX xenografted tumours in nude mice where no difference was observed in γH2AX dephosphorylation kinetics between oxic and hypoxic cells within the first 24 hours after irradiation (14).

Irradiation of cells under hypoxia led to a significant increase of cellular survival and lower number of residual γH2AX foci in all cell lines (1). This result demonstrates the well-established oxygen effect and probably arises from the lower induction of damage in hypoxic cells (46, 119). The magnitude of the oxygen effect can generally be expressed by the OER, which is defined as the ratio of dose under hypoxia versus normoxia leading to the same biological effect, e.g. 1% survival (46, 118, 119). The OER values were similar within the cell lines investigated and thus irrespective of the observed differences in intrinsic radiosensitivity. This observation suggests that induction of damage under hypoxic conditions at the time of irradiation did not differ between the cell lines. This finding is contradictory to what was previously suggested from FaDu and SKX *in vivo* experiments, where the slope of residual γH2AX dose response was similar between hypoxic cells (at the time of irradiation) of FaDu and SKX tumour cells (14). The disparity between the results of the two studies is most probably arising from the fact that the conditions *in vivo* cannot be fully reproduced *in vitro*. Cells in tumours might be subjected to metabolic changes, and exposed not only to different degrees of hypoxia but also to cycles of hypoxia and reoxygenation (cycling hypoxia) leading to different biological behaviors (46, 120, 121). In contrast, in cell cultures used in this set of experiments, tumour cells were exposed to one hypoxia level, generating a completely different microenvironment than that observed in tumours. On the other hand, *in vitro* experiments allow for standardized conditions, such as level and duration of hypoxia, which cannot be fully controlled under *in vivo* conditions (1). Nevertheless, the reason for this discrepancy is not fully understood and it is a matter of further investigation. Kumareswaran et al. reported in their study from 2012 OERs for fibroblasts synchronized in G0-G1 phase of 1.81±0.31 for cells kept under hypoxia (0.02% O_2) and 2.01±0.13 for

cells exposed to anoxia (0.0% O_2) for 16 hours, respectively (106). Similarly, Chan et al. reported for H1299 lung carcinoma cells an OER of 2.61 under anoxic conditions and an OER of 2.19 under 0.2% O_2 (118). These results are very much in line with the mean OER of 2.36 observed in our study, indicating that the oxygen concentration reached in the Gas-Paks (BD GasPak^{TM}-EZ-Gas Generating Pouch System) after 2 hours cultivation was very close to anoxic levels.

For experimental conditions without irradiation under hypoxia HMFs instead of OERs were calculated for quantification of effect of hypoxia on cellular survival. Calculation was performed similar to calculation of OER as the ratio of dose of the experimental condition and co-effective dose under normoxic conditions. Interestingly, we were also able to calculate OERs and HMFs by the use of the mean number of residual γH2AX foci alone and found a strong correlation between recalculated values and values obtained by standard CFA. To our knowledge, this is the first demonstration that OERs could be directly calculated from the mean number of residual foci, further strengthening our hypothesis that cellular survival is very closely connected to the amount of residual DNA DSBs (1). This correlation could be used for the calculation of radiobiological endpoints in the future and is especially important for the establishment of γH2AX as a biomarker in clinical and preclinical studies (94).

Surprisingly, cultivation of cells under hypoxia prior to irradiation revealed three different radiation responses for the three cell lines under investigation (1). In UT SCC-5 cells hypoxia was well tolerated and no significant difference was observed in cellular survival post irradiation compared to normoxic conditions. In FaDu cells hypoxia treatment prior to irradiation, led to significantly higher cellular survival. Hypoxia-induced radioresistance, might arise from upregulation of pro-survival signaling pathways or from upregulation of DNA radiation response pathways (12, 46, 54). In contrast, hypoxia exposure prior to irradiation led to a significant decrease in cellular survival in SKX cells (1). The differential radiation response of cells cultivated under hypoxia prior to irradiation, implies that besides of hypoxia induced radiation resistance, cells from different tumour cell lines might express pronounced differences in their intrinsic tolerance to hypoxia, which might affect radiation treatment outcome *in vivo*. This is

further supported by the experimental data where the local tumour control of xenografted tumours from the three cell lines were shown to be significantly different (32, 99). The histological examination revealed that SKX and UT SCC-5 tumours are both moderately well differentiated SCC tumours (98). However, despite the histological similarity, these two cell lines differ dramatically in their *Tumour Control Dose of 50%* (TCD_{50}) with UT SCC-5 having the highest hypoxic fraction and the highest TCD_{50} values after both single and fractionated irradiation whereas SKX had the lowest (32, 99).

Cell line dependent response to hypoxia exposure prior to irradiation and the effects on radiation sensitivity have been previously published. Similar to the survival curves observed for UT SCC-5 cells, Spiro et al. reported that pre irradiation incubation for 20 hours under anoxia followed by reoxygenation prior to irradiation led to no alteration of survival curves for V-79 chinese hamster lung fibroblasts (115). In their review from 2006 Freiberg et al. showed reduced relative survival measured by PE and increased sensitivity of cells lacking ATM after exposure to hypoxia for up to 25 hours followed by reoxygenation due to suppression of G-2 mediated cell cycle arrest mediated by ATM-CHK2 signaling pathway (122, 123). These results are in line with our observation that the SKX cell line, which lacks functional ATM protein, is highly sensitive to prolonged hypoxia treatment (1). In support to our hypothesis, in a publication from Zölzer et al. authors reported an increase of radiosensitivity in one cell line after incubation under conditions close to anoxia (0.2 mmHg O_2) for 24 hours prior to irradiation, whereas no difference could be shown in the other three cell lines under investigation (124). These results indicate that effects of pre-irradiation incubation under hypoxia might already be present after shorter time periods than the ones observed in our study.

Interestingly, besides the increased radiation sensitivity of SKX cells when pre-cultivated under hypoxia prior to irradiation we also observed significant increase in the γH2AX foci number in unirradiated controls. Bencokova et al. reported in their study from 2009 that RKO cells accumulated γH2AX foci in an oxygen dependent manner, with the most significant increase at oxygen levels below 0.02% (125). Using a fluorescence-activated cell sorter, they also showed that U2OS cells in G2/M phase did not form γH2AX foci, indicating a cell cycle dependency of foci formation under hypoxic conditions. However,

they were able to show that cells, which accumulated RPA foci, confirming the occurrence of replication fork stalling, also accumulated γH2AX foci in untreated cells for any DNA damaging agent (125). These results were further verified by a study from Hammond et al., who reported formation of γH2AX foci under conditions close to anoxia (0.02% O_2, 16 h) in 28% of the treated RKO cells (126), indicating that foci are not solely formed at the site of DNA damage under these circumstances. In addition, in a study conducted by Tsuchimoto et al. authors showed an increase of 50% of average γH2AX foci numbers in M059K cells (human glioma cell line) in unirradiated controls after pre-irradiation incubation and irradiation under hypoxia (95% N_2, 5% CO_2, 0% O_2) for 24 hours followed by 24 hours of reoxygenation (127).

Application of hypoxia treatment at two different time-frames did not change the overall observations from the single-time frame application (1). Combination of hypoxia treatment during and post irradiation, or prior and post irradiation led to survival curves that were not significantly different from the corresponding curves when hypoxia was applied during irradiation or prior to irradiation alone. This finding is in line with our previous observation that post-irradiation hypoxia does not have any impact on cellular survival (1).

Irradiation under hypoxia of cells which have also been grown under hypoxia yielded the maximal increase in cellular survival for FaDu and UT SCC-5 cells, suggesting that prolonged hypoxia exposure in combination with hypoxia during irradiation leads to very resistant phenotypes overcoming even the reduced hypoxia tolerance of SKX cell line (1). The surprisingly high increase in radiation resistance under these conditions in UT SCC-5 cells might partly explain the observation of high TCD_{50} values in combination with high hypoxic fractions in xenograft tumours of this cell line in *in vivo* experiments (32, 99). This phenomenon might have very important implications on radiation treatment outcome of chronically hypoxic cells in tumours that might either be reoxygenated during repair of radiation induced DNA damage or exposed to cycles of hypoxia and reoxygenation. In contrast to our observation, it has been shown that reoxygenation after continuous exposure of RKO cells to 0.02% oxygen for 16 hours resulted in significant levels of DNA damage, measured by comet assay, whereas hypoxia alone did not yield a

significant effect (126). In another report, 24 hours pre-irradiation incubation under conditions close to anoxia in combination with irradiation under hypoxia led to survival curves that did not significantly differ from those obtained under more acutely hypoxic conditions (3 hours pre-irradiation incubation) for two p53 wild type cell lines and one p53 mutant cell line. Interestingly, under these conditions they observed an increase of radiosensitivity in one other p53 mutant cell line (124). The discrepancy of the previously mentioned studies to ours is most probably arising from differences in oxygen concentration, period of pre-irradiational exposure to hypoxia and differences in the level of applied hypoxia yielding to differential microenvironmental adaptation and consequently cellular radiation response.

Chronically hypoxic cells kept continuously under hypoxia, prior, during and post irradiation, were significantly more radioresistant compared to their normoxic counterparts. For FaDu and UT SCC-5 cells the effect was comparable to the one observed under acute hypoxia alone. In contrast, the magnitude of the effect was significantly lower in SKX cell line suggesting that in this cell line the effect of hypoxia induced radioresistance was counteracted by hypoxia induced cellular toxicity. Increase of residual γH2AX foci 24 hours after irradiation for synchronized fibroblast (G0-G1) exposed to either anoxia or severe hypoxia (0.02% O_2) for 16 hours prior and 24 hours post irradiation has been also reported previously (106). In line with these results, we as well observed higher numbers of residual γH2AX foci in non-irradiated cells after exposure to chronic hypoxia in all cell lines under investigation.

In order to test the hypothesis that the observed effects of prolonged incubation under mild hypoxia prior to irradiation on cellular survival are due to alterations in level or activity of DNA repair enzymes we performed western blot analysis.
Incubation in GasPaks for 2.5 hours either with or without irradiation led to an equal induction of Hif 1α expression, verifying hypoxic conditions of oxygen concentration close to 0.1% O_2 after this period of time. This observation is in line with results from many other studies, showing induction of Hif 1α, an important hypoxia-induced transcription factor, stabilized as a response to low oxygen levels, after incubation of cells under conditions close to anoxia (117, 118, 123). Under conditions of acute hypoxia

(experimental group: O-H-O) no significant difference to normoxic conditions in phosphorylation of neither ATM nor DNA-PKcs could be detected after irradiation. In contrast, Bencokova et al. showed in 2009 hypoxia mediated phosphorylation of ATM independent of other DNA damaging agents (125). However, the earliest time point analyzed was exposure to hypoxia for 3 hours and conditions very close to anoxia were tested. The discrepancy to our study might arise both from the lesser exposure time to hypoxia and the added effect of irradiation on phosphorylation of ATM protein, thus overlapping the effect hypoxia alone might promote on phosphorylation status of the protein. Similarly, Um et al. observed an increase of DNA-PKcs activity after 4 hours of exposure to 1% O_2 (128). Yet, DNA-PKcs activity was measured by a DNA-dependent protein kinase assay system and oxygen concentration was considerably higher than in our study, thus explaining the inconsistency with our study. Furthermore, no difference of Rad51 protein levels was observed after irradiation alone or in combination with exposure to hypoxia at the time of irradiation. In line, Bindra et al. observed no difference in Rad 51 expression after 24h of exposure to hypoxia whereas a significant downregulation was shown after 48 hours of hypoxia exposure (105).

Pre-irradiation incubation under hypoxia led to downregulation of Rad51 in all cell lines under investigation, irrespective of additional radiation treatment. The observed downregulation of Rad51 was also independent of reoxygenation up to 24 hours after exposure to hypoxia (1). These results are in line with previously published data by other groups, who reported hypoxia mediated decrease in the expression of Rad51 in various cancer cell lines from diverse origin. Interestingly, this effect appears to be independent of cell cycle phases, Hif 1α expression and p53 status resulting in decreased HR for both hypoxic and reoxygenated cells, indicating functional depletion of the protein (1, 129). Notably, when cells were reoxygenated prior to irradiation a radiosensitizing effect was observed (105, 118, 130). Kumareswaran et al. observed decreased Rad51 protein expression at oxygen concentrations of 1% O_2 in a lung and a cervical cancer cell line after chronic hypoxia while exposure to cycles of hypoxia led to a non-significant alteration of protein expression (131). Potential mechanisms involved in the suppression of the HR pathway under hypoxia have been proposed either through a Hif 1α mediated downregulation of MYC activity leading to downregulation of BRCA1 and other

important HR proteins (132, 133) or through a Hif 1α independent pathway by suppression of Rad51 through binding of repressive E2F4/p130 complexes to an E2F site of the promotor of the Rad51 gene (104, 105, 130). Sprong et al. showed that mutation of homologous recombination results in radiosensitisation and lower OERs compared to wild type counterpart cell lines, when cells were irradiated under conditions close to anoxia. In contrast, although observing an increase of radiosensitivity for DNA-PKs deficient cells after irradiation under normoxia, irradiation under hypoxia did not result in alteration of OERs (134).

As expected, for FaDu and UT SCC-5 cell lines we observed phosphorylation of ATM protein after irradiation and hypoxia induced increase in phosphorylation for UT SCC-5 cells and to a lesser extent also for FaDu cell line (1). In a study conducted by Freiberg et al., authors observed phosphorylation of ATM on serine 1981 after incubation of lymphoblastoid cells under anoxic conditions after 4 and 9 hours, whereas exposure of cells to 2% O_2 for 9 hours revealed no significant effect on phosphorylation levels (122). Bencokova et al. reported that ATM is autophosphorylated on serine 1981 and active both under hypoxic conditions close to anoxia and during reoxygenation in GM0536 cells (125). However, no significant phosphorylation was observed for cells incubated under higher oxygen concentrations. The discrepancy to our study could be explained by differences in oxygen concentration and duration of exposure to hypoxia as well as in the fact that cells were exposed both to hypoxia and irradiation. In contrast, for SKX cell line ATM protein could not be detected in all western blot analysis performed (1). This result is in line with a recently published study by Mansour et al., where authors demonstrated that depletion of ATM in SKX cells is due to post-transcription regulation through overexpression of a micro-RNA leading to downregulation of ATM– mediated DDR (97). In turn, this leads to increased genetic instability and thus explains the extreme radiosensitivity of this cell line. In their paper from 2010, Cam et al. reported that inhibition of mTORC1 by hypoxia is dependent on an intact ATM activity in mouse embryonic fibroblasts (MEF) (135). Inhibition of mTORC1, the mammalian target of rapamycin, is crucial for proliferation and cellular survival under hypoxic conditions through restriction of cellular processes with high-energy consumption such as mRNA translation (52, 53, 136, 137). Based on these results, we hypothesized that the extreme

hypoxia sensitivity of SKX cell line is partly due to depletion of functional ATM and thus inappropriate downregulation of mTORC1 signaling and its downstream effective pathways.

Consequently, we performed analysis of DNA-PKcs, an important component of NHEJ repair pathway in DNA damage response. For all cell lines under investigation we observed increase phosphorylation of DNA-PKcs on Serine 2056 after irradiation, with a slightly delayed phosphorylation in SKX cells. Interestingly, under conditions of pre-irradiation incubation under hypoxia we observed an increased phosphorylation of DNA PKcs for FaDu and UT SCC-5 cells whereas no difference could be shown for SKX cell line. In line, Um et al. reported an increase of DNA-PKcs and DNA-PK activity in nuclear extracts of HepaC1C7 cells after exposure to hypoxia (1% O_2) in a time dependent manner (128) and Madan et al. also reported increased activity of DNA-PKcs in MEF-7 cells after exposure of cells to 1.8% oxygen for 24 hours (138). In contrast, Wirthner et al. reported downregulation of DNA-PKcs mRNA levels after long time incubation under hypoxia for up to 256 hours in MEF cells (139). The use of long term severe hypoxia without irradiation along with the fact that the impact of mRNA downregulation on DNA repair protein levels was not assessed systematically does not allow direct comparison to our data.

In order to further elucidate the extreme radiosensitivity of SKX cell line under pre-irradiation incubation under hypoxia we hypothesized that the increase of radiosensitivity might be based on the increase of reproductive cell death though induction of senescence. Graeber et al. reported already in 1996 that p53 mutant cells exposed to hypoxia undergo apoptosis in a highly extenuated manner compared to p53 wild type cells under the same conditions (57). However, we did not observe morphological signs of apoptosis in our cultures but rather elevated number of γH2AX foci in non-irradiated controls of SKX cell line after pre-irradiation incubation under hypoxia. In line with our observation, Sedelnikova et al. showed accumulation of γH2AX foci in co-localization with DNA repair factors in human cell culture cells undergoing senescence (140). However, this was not tested in our experimental design. Another possible pathway of cell death after exposure to hypoxia is hypoxia-induced autophagy. This hypothesis is supported by

Papandreou et al., who reported induction of autophagy in RKO and SiHa cells incubated under conditions close to anoxia (<0.01% O2) for up to 24 hours (59). Interestingly, Chaachouay et al. reported increased radioresistance mediated through AMPK independent stimulation of autophagy already at oxygen levels of 1% O_2 (60). Several reviews suggest that hypoxia-induced autophagy might have an important role in hypoxia mediated cell death (141, 142).

Collectively, our proposal regarding the extreme hypoxia intolerance of SKX cell line is based on a combination of downregulation of HR-repair pathway after long term pre-irradiation incubation under hypoxia on the basis of an intrinsic functional defect of ATM and thus reduced efficiency of DDR repair in this cell line (1). For UT SCC-5 cell line and FaDu cell line in particular, deficiency in HR was well tolerated and did not lead to radiosensitization. We hypothesize that downregulation of Rad51 in FaDu cells triggers an alternative pathway of DDR and thus explain increase of radioresistance observed under prolonged hypoxia treatment. This hypothesis is further supported by the observed increase in ATM and DNA PKcs phosphorylation under this condition for both cell lines (1). Our data therefore suggests a significant role for ATM protein concerning cellular survival and the capability of cells to adapt to the hypoxic microenvironment for cells exposed to moderate hypoxia for prolonged periods of time. An alternative hypothesis, which was not tested, is that the heterogeneity of cellular radiosensitivity phenotypes observed under prolonged hypoxia might reflect the heterogeneity of metabolic adaptation of the cell lines to hypoxia (54, 55).

In summary, our data support the hypothesis that time dependent exposure of hypoxia leads to differential cellular phenotypes affecting cellular survival after irradiation. This phenomenon might have important implications in the interpretation of studies aiming to develop predictive biomarkers for radiation response (143). Understanding the impact of hypoxia exposure on repair and radiation sensitivity appears to be important for recognition and discovery of novel targets to overcome radiation resistance in hypoxic tumours.

5 SUMMARY

Hypoxia has been shown to be a negative prognostic marker for survival and the occurrence of metastatic disease for patients with various kinds of tumours. It has been shown previously that for two SCC tumors grown as xenografts in nude mice hypoxic tumour cells showed a significantly lower amount of residual DNA double strand breaks (DSB) compared to normoxic cells. However, it was not possible to assess the duration and exact timing of hypoxia exposure in relation to irradiation in this experimental setting. Therefore, we aimed to study the influence of hypoxia exposure at different timeframes in relation to irradiation on cellular survival and the amount of residual DNA double strand breaks. Three human squamous cell carcinoma cell lines with differences in their intrinsic radiation sensitivity were exposed to hypoxia prior, during or 24 hours after irradiation and consequently either seeded in parallel for colony formation assay (CFA) and for γH2AX assay or processed for western blot analysis.

For normoxic conditions we were able to reproduce the observed differences in intrinsic radiosensitivity both in terms of CFA and in terms of γH2AX assay. Irradiation under hypoxic conditions led to an increase in cellular survival and a decrease of residual DSBs with similar oxygen enhancement ratios (OER) for all cell lines (OER_{mean} =2.36). Based on the mean number of residual foci we were able to recalculate the observed survival curves and accurately estimate the OER values. Exposure to hypoxia after irradiation did neither alter cellular survival nor the amount of residual γH2AX foci. Interestingly, long term incubation under hypoxia prior to irradiation resulted in diverse effects on cellular survival, namely radiosensitization in SKX (HMF=0.76), induction of radioresistance in FaDu (HMF=1.54) and no effect in UT SCC-5 cells (HMF=1.10). These phenotypic behaviors were consistent when cells were exposed to hypoxia either during or after irradiation additionally or were chronically hypoxic. Under this condition, western blot analysis revealed increased phosphorylation of ATM and DNA PKcs after irradiation for UT SCC-5 and to a lesser extent also for FaDu cell line. Interestingly, we observed homogenous downregulation of Rad51 after pre-irradiation incubation under hypoxia.

In conclusion, our data indicates a significant role for hypoxia tolerance on cellular radiation sensitivity for cells exposed to hypoxia prior to irradiation for prolonged periods of time. Furthermore, our data suggests that ATM might have an important impact on

cellular adaptation and cellular survival in a hypoxic microenvironment. Enhancing our knowledge on hypoxia is important to overcome treatment resistance of hypoxic tumors.

6 ZUSAMMENFASSUNG

Die Tumorhypoxie ist ein weit verbreitetes Phänomen, das zu Metastasierung sowie Therapieresistenz führen kann und so einen negativen Prognosefaktor für das Überleben von Patienten darstellt. Vorarbeiten *in vivo* zeigten, dass hypoxische Tumorzellen gegenüber normoxischen Tumorzellen signifikant weniger residuelle DNA Doppelstrangbrüche (DSB) nach Bestrahlung aufweisen, wobei die Heterogenität zwischen verschiedenen Tumorlinien abhängig von der Oxygenierung erscheint. Das Ziel dieser Arbeit war die Abhängigkeit der Strahlensensitivität und des Zellüberlebens vom Zeitpunkt der Hypoxieexposition in Bezug auf den Bestrahlungszeitpunkt in verschiedenen Tumorlinien *in vitro* zu untersuchen. Hierzu wurden drei humane Plattenepithelkarzinomzelllinien des Kopf- und Halsbereiches mit Unterschieden in ihrer intrinsischen Strahlensensitivität ausgewählt. Diese wurden vor, während oder nach der Bestrahlung Hypoxie ausgesetzt und anschließend entweder parallel für die Koloniebildungsassays ausgesät und für den γH2AX Foci Assay gefärbt oder für die Western Blot Analyse vorbereitet.

Die Bestrahlung von Zellen unter hypoxischen Bedingungen führte zu einem Anstieg der Überlebensfraktion sowie zu einer signifikanten Reduktion der Anzahl residualer γH2AX Foci (MW OER: 2,36). Hypoxie nach Bestrahlung führte hingegen zu keiner signifikanten Veränderung des Zellüberlebens. Interessanterweise zeigte die Inkubation unter Hypoxie vor Bestrahlung unterschiedliche Effekte in den drei Zelllinien: Strahlensensibilisierung in SKX (HMF: 0.76), Verstärkung von Strahlenresistenz in FaDu (HMF: 1.54) und keinen Effekt in UT SCC-5 (HMF: 1.10). Diese Phänotypen zeigten sich ebenfalls bei zusätzlicher Hypoxieexposition während oder nach Bestrahlung. Unter dieser Bedingung konnte in der Western Blot Analyse in allen Zellen eine verminderte Expression von Rad51 nachgewiesen werden. Für UT SCC-5 Zellen und zu einem geringeren Anteil auch für FaDu Zellen beobachteten wir eine verstärkte, bestrahlungsbedingte Phosphorylierung von ATM und DNA-PKcs.

Zusammenfassend weisen die Daten dieser Studie darauf hin, dass die intrinsische Hypoxietoleranz einen wichtigen Einfluss auf die zelluläre Strahlensensitivität haben könnte und deuten auf eine wichtige Rolle von ATM für das Zellüberleben und die

Anpassung von Zellen an hypoxische Bedingungen hin. Die vorliegenden Ergebnisse sind bedeutend für die Entwicklung von neuen Strategien zur Überwindung der Strahlenresistenz hypoxischer Zellen.

7 APPENDIX

Suppl. Tab. 1: table showing SF_2 values obtained by CFA and slope of yH2AX foci assay as well as p-values of the linear correlation between -ln SF_{CFA} and mean number of residual foci for all cell lines and conditions under investigation; *Adapted from Hauth F.et al. (2017) Cell-line dependent effects of hypoxia prior to irradiation in squamous cell carcinoma lines. Clinical and Translational Radiation Oncology (accepted for publication) (1)*

Condition	Cell line	OER (SF= 0.1)		SF_2	Slope of γH2AX foci assay	P-value of linear correlation (-lnSF vs. mean residual foci)
		CFA	γH2AX-assay			
O-O-O (21%-21%-21%)	SKX			0.14	2.13	0.0001
	FaDu			0.38	1.58	< 0.0001
	UT SCC-5			0.59	1.13	< 0.0001
O-O-**H** (21%-21%-1%)	SKX	1.00	1.03	0.10	1.84	0.0003
	FaDu	1.03	1.08	0.34	1.43	0.0011
	UT SCC-5	1.21	1.17	0.61	1.50	0.0022
O-**H**-O (21%-0.1%-21%)	SKX	2.31	2.03	0.48	1.31	0.0008
	FaDu	2.44	2.90	0.71	0.41	0.0028
	UT SCC-5	2.32	2.82	0.76	0.41	0.0019
H-O-O (1%-21%-21%)	SKX	0.76		0.05	0.82	0.6238
	FaDu	1.54	1.41	0.59	0.80	< 0.0001
	UT SCC-5	1.10	1.19	0.59	1.40	0.0003
O-**H**-**H** (21%-0.1%-1%)	SKX	2.55	2.33	0.34	1.38	0.0034
	FaDu	2.35	2.91	0.89	1.04	0.0008
	UT SCC-5	2.8	4.62	0.90	0.88	0.0261
H-O-**H** (1%-21%-1%)	SKX	0.69	0.65	0.02	2.57	0.0421
	FaDu	1.32	1.05	0.49	1.33	0.0025
	UT SCC-5	1.13	1.41	0.73	1.23	0.0246
H-**H**-**H** (1%-0.1%-1%)	SKX	1.69	1.73	0.33	1.39	0.002
	FaDu	2.77	3.85	0.86	0.98	0.0104
	UT SCC-5	2.44	3.46	0.85	0.86	0.0490
H-**H**-O (1%-0.1%-21%)	SKX	2.45	1.98	0.46	1.04	0.0008
	FaDu	3.73	4.22	0.72	0.65	0.0048
	UT SCC-5	4.22	4.49	0.85	0.76	0.0002

Suppl. Tab. 2: Table showing plating efficiencies (PE) and number of mean residual foci after 0 Gy irradiation for all cell lines and all conditions under investigation.

cell line	condition	PE	mean residual foci 0 Gy
SKX	O-O-O	16.65	2.02
	O-O-**H**	7.50	2.15
	O-**H**-O	15.03	2.45
	H-O-O	10.19	8.75
	O-**H**-**H**	12.18	1.81
	H-O-**H**	11.26	4.75
	H-**H**-O	12.44	3.91
	H-**H**-**H**	10.48	3.69
FaDu	O-O-O	43.71	0.91
	O-O-**H**	18.34	0.52
	O-**H**-O	35.42	1.72
	H-O-O	49.77	1.12
	O-**H**-**H**	28.72	1.29
	H-O-**H**	38.05	1.90
	H-**H**-O	43.76	0.92
	H-**H**-**H**	39.12	3.94
UT SCC-5	O-O-O	31.1	1.44
	O-O-**H**	17.95	2.14
	O-**H**-O	20.11	3.86
	H-O-O	26.16	2.81
	O-**H**-**H**	18.19	6.14
	H-O-**H**	22.7	3.01
	H-**H**-O	28.97	5.16
	H-**H**-**H**	27.32	4.94

OER based on **1% Survival**: -ln (0.01)=4.605

-ln (SF) vs. Foci: y=m*x + c

y= mean number of residual foci
x= -ln (SF)
m= Slope of linear regression
c= y- intercept

m (control)= 2.252
c (control)= 1.463

y= 2.252*4.605 + 1.463
y= 11.833

m (O-H-O)= 2.408
c (O-H-O)= 0.9053

y= 2.408*4.605 + 0.9053
y= 11.99

Für x=4.605 gilt damit:

y = m*4.605 + c

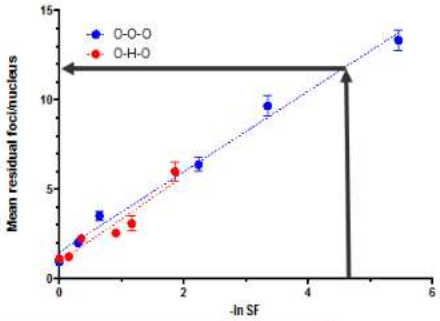

Foci vs. Dose: y=m*x + c

y= mean number of residual foci
x= Dose (Gy)
m= Slope of linear regression
c= y- intercept

m (control)= 1.556
c (control)= 0.5218

y= 1.556*x + 0.5218
11.833= 1.566*x + 0.5218 /-0.5218
11.3112= 1.566* /:1.566
7.27=x

Für x (Dose) =? Gilt damit:

x= (y-c) / m

m (O-H-O)= 0.5147
c (O-H-O)= 0.8712
y= 0.5147*x + 0.8712
11.99 = 0.5147*x + 0.8712 /-0.8712
11.12= 0.5147*x /:0.5147

21.61=x

OER= x(Experiment)/ x(control)

OER= 21.61/7.27 =2.97

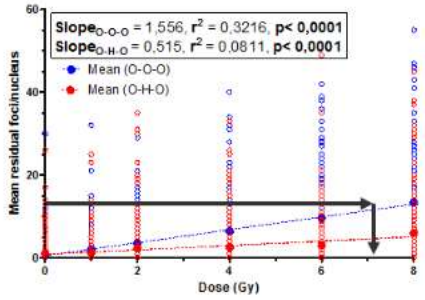

Suppl. Fig. 1: Figure showing exemplarily mathematical process of recalculation of OER/HMF based on number of residual foci

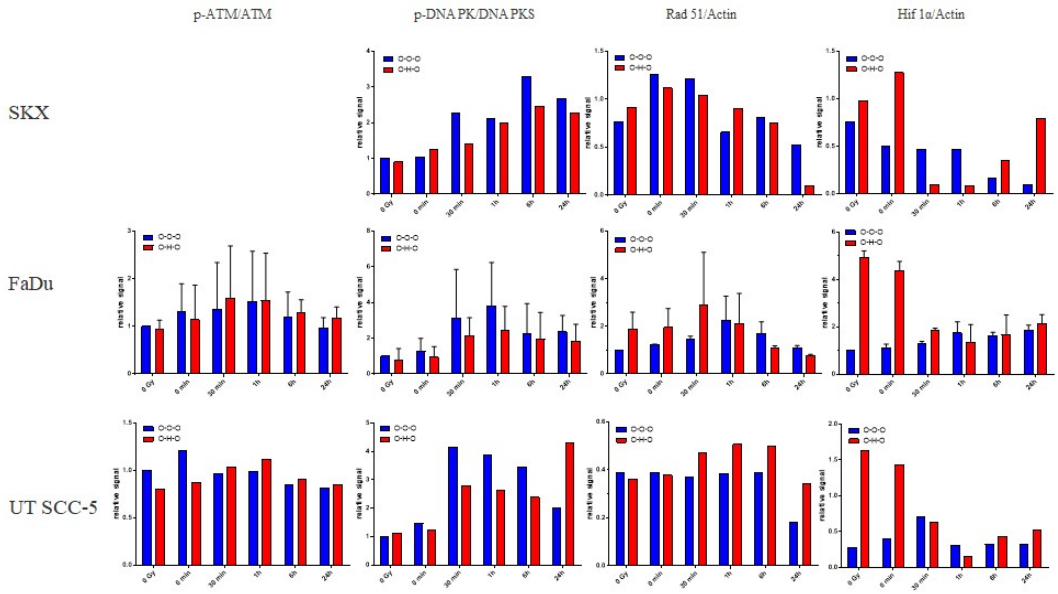

Suppl. Fig. 2: Bar diagrams showing relative signal of protein levels for all cell lines under investigation for conditions of irradiation under hypoxia (experimental group: O-H-O). Shown are results of 1 (SKX, UT SCC-5) and 2 (FaDu) individual experiments respectively. Error bars indicating standard deviation of the mean.

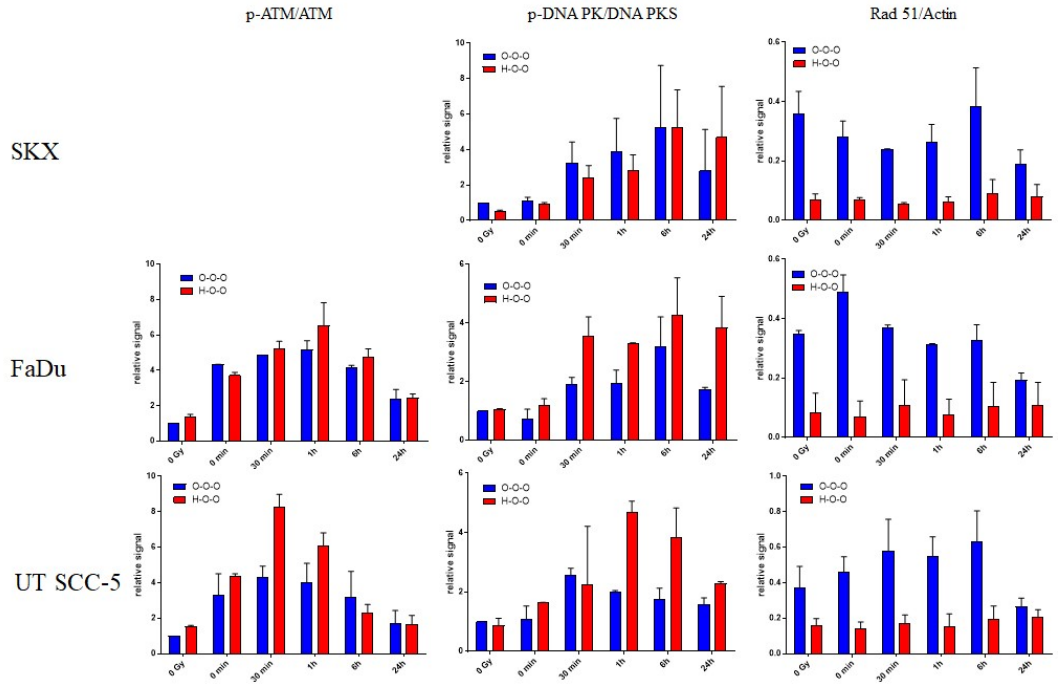

Suppl. Fig. 3: Bar diagrams showing relative signal of protein levels for all cell lines under investigation for long term exposure to hypoxia prior to irradiation (experimental group: H-O-O). Shown are results of 2 individual experiments. Error bars indicating standard deviation of the mean.
Adapted from Hauth F.et al. (2017) Cell-line dependent effects of hypoxia prior to irradiation in squamous cell carcinoma lines. Clinical and Translational Radiation Oncology (accepted for publication) (1)

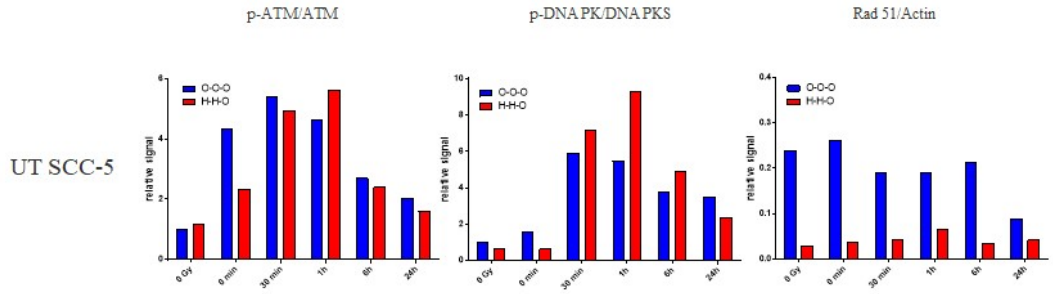

Suppl. Fig. 4: Bar diagrams showing relative signal of protein levels for UT SCC-5 cell line under investigation for exposure to hypoxia both prior and at the time of irradiation (experimental group: H-H-O). Shown are results of 1 individual experiment

8 LITERATURVERZEICHNIS

1. Hauth F, Toulany M, Zips D, Menegakis A. Cell-line dependent effects of hypoxia prior to irradiation in squamous cell carcinoma lines. Clinical and Translational Radiation Oncology. 2017:accepted for publication.
2. Hanahan D, Weinberg RA. Hallmarks of cancer: the next generation. Cell. 2011;144(5):646-74.
3. Bindra RS, Glazer PM. Genetic instability and the tumor microenvironment: towards the concept of microenvironment-induced mutagenesis. Mutation research. 2005;569(1-2):75-85.
4. Carmeliet P, Jain RK. Molecular mechanisms and clinical applications of angiogenesis. Nature. 2011;473(7347):298-307.
5. Kerbel RS. Tumor angiogenesis. The New England journal of medicine. 2008;358(19):2039-49.
6. Colliez F, Gallez B, Jordan BF. Assessing Tumor Oxygenation for Predicting Outcome in Radiation Oncology: A Review of Studies Correlating Tumor Hypoxic Status and Outcome in the Preclinical and Clinical Settings. Frontiers in oncology. 2017;7:10.
7. Horsman MR, Overgaard J. The impact of hypoxia and its modification of the outcome of radiotherapy. Journal of radiation research. 2016;57 Suppl 1:i90-i8.
8. Nordsmark M, Bentzen SM, Rudat V, Brizel D, Lartigau E, Stadler P, et al. Prognostic value of tumor oxygenation in 397 head and neck tumors after primary radiation therapy. An international multi-center study. Radiotherapy and oncology : journal of the European Society for Therapeutic Radiology and Oncology. 2005;77(1):18-24.
9. Roussos ET, Condeelis JS, Patsialou A. Chemotaxis in cancer. Nature reviews Cancer. 2011;11(8):573-87.
10. Ferrara N, Kerbel RS. Angiogenesis as a therapeutic target. Nature. 2005;438(7070):967-74.
11. Zips D, Le K, Yaromina A, Dorfler A, Eicheler W, Zhou X, et al. Triple angiokinase inhibition, tumour hypoxia and radiation response of FaDu human squamous cell carcinomas. Radiotherapy and oncology : journal of the European Society for Therapeutic Radiology and Oncology. 2009;92(3):405-10.
12. Hill RP, Bristow RG, Fyles A, Koritzinsky M, Milosevic M, Wouters BG. Hypoxia and Predicting Radiation Response. Seminars in radiation oncology. 2015;25(4):260-72.
13. Vaupel P, Kallinowski F, Okunieff P. Blood flow, oxygen and nutrient supply, and metabolic microenvironment of human tumors: a review. Cancer research. 1989;49(23):6449-65.
14. Menegakis A, Eicheler W, Yaromina A, Thames HD, Krause M, Baumann M. Residual DNA double strand breaks in perfused but not in unperfused areas determine different radiosensitivity of tumours. Radiotherapy and oncology : journal of the European Society for Therapeutic Radiology and Oncology. 2011;100(1):137-44.
15. Ljungkvist AS, Bussink J, Rijken PF, Kaanders JH, van der Kogel AJ, Denekamp J. Vascular architecture, hypoxia, and proliferation in first-generation xenografts of human head-and-neck squamous cell carcinomas. International journal of radiation oncology, biology, physics. 2002;54(1):215-28.
16. Dewhirst MW. Relationships between cycling hypoxia, HIF-1, angiogenesis and oxidative stress. Radiation research. 2009;172(6):653-65.
17. Pries AR, Hopfner M, le Noble F, Dewhirst MW, Secomb TW. The shunt problem: control of functional shunting in normal and tumour vasculature. Nature reviews Cancer. 2010;10(8):587-93.
18. Thomlinson RH, Gray LH. The histological structure of some human lung cancers and the possible implications for radiotherapy. British journal of cancer. 1955;9(4):539-49.
19. Adam MF, Gabalski EC, Bloch DA, Oehlert JW, Brown JM, Elsaid AA, et al. Tissue oxygen distribution in head and neck cancer patients. Head & neck. 1999;21(2):146-53.
20. Koukourakis MI, Bentzen SM, Giatromanolaki A, Wilson GD, Daley FM, Saunders MI, et al. Endogenous markers of two separate hypoxia response pathways (hypoxia inducible factor 2 alpha and carbonic anhydrase 9) are associated with radiotherapy failure in head and neck cancer patients recruited in the CHART randomized trial. Journal of clinical oncology : official journal of the American Society of Clinical Oncology. 2006;24(5):727-35.
21. Rademakers SE, Hoogsteen IJ, Rijken PF, Oosterwijk E, Terhaard CH, Doornaert PA, et al. Pattern of CAIX expression is prognostic for outcome and predicts response to ARCON in patients with laryngeal cancer treated in a phase III randomized trial. Radiotherapy and oncology : journal of the European Society for Therapeutic Radiology and Oncology. 2013;108(3):517-22.
22. Mellanen P, Minn H, Grenman R, Harkonen P. Expression of glucose transporters in head-and-neck tumors. International journal of cancer Journal international du cancer. 1994;56(5):622-9.

23. Wilson WR, Hay MP. Targeting hypoxia in cancer therapy. Nature reviews Cancer. 2011;11(6):393-410.
24. Ragnum HB, Vlatkovic L, Lie AK, Axcrona K, Julin CH, Frikstad KM, et al. The tumour hypoxia marker pimonidazole reflects a transcriptional programme associated with aggressive prostate cancer. British journal of cancer. 2015;112(2):382-90.
25. Schutze C, Bergmann R, Bruchner K, Mosch B, Yaromina A, Zips D, et al. Effect of [(18)F]FMISO stratified dose-escalation on local control in FaDu hSCC in nude mice. Radiotherapy and oncology : journal of the European Society for Therapeutic Radiology and Oncology. 2014;111(1):81-7.
26. Thorwarth D, Alber M. [Individualised radiotherapy on the basis of functional imaging with FMISO PET]. Zeitschrift fur medizinische Physik. 2008;18(1):43-50.
27. Horsman MR, Mortensen LS, Petersen JB, Busk M, Overgaard J. Imaging hypoxia to improve radiotherapy outcome. Nature reviews Clinical oncology. 2012;9(12):674-87.
28. Nordsmark M, Loncaster J, Aquino-Parsons C, Chou SC, Gebski V, West C, et al. The prognostic value of pimonidazole and tumour pO2 in human cervix carcinomas after radiation therapy: a prospective international multi-center study. Radiotherapy and oncology : journal of the European Society for Therapeutic Radiology and Oncology. 2006;80(2):123-31.
29. Winther M, Alsner J, Tramm T, Nordsmark M. Hypoxia-regulated gene expression and prognosis in loco-regional gastroesophageal cancer. Acta oncologica. 2013;52(7):1327-35.
30. Mortensen LS, Johansen J, Kallehauge J, Primdahl H, Busk M, Lassen P, et al. FAZA PET/CT hypoxia imaging in patients with squamous cell carcinoma of the head and neck treated with radiotherapy: results from the DAHANCA 24 trial. Radiotherapy and oncology : journal of the European Society for Therapeutic Radiology and Oncology. 2012;105(1):14-20.
31. Zips D, Zophel K, Abolmaali N, Perrin R, Abramyuk A, Haase R, et al. Exploratory prospective trial of hypoxia-specific PET imaging during radiochemotherapy in patients with locally advanced head-and-neck cancer. Radiotherapy and oncology : journal of the European Society for Therapeutic Radiology and Oncology. 2012;105(1):21-8.
32. Yaromina A, Thames H, Zhou X, Hering S, Eicheler W, Dorfler A, et al. Radiobiological hypoxia, histological parameters of tumour microenvironment and local tumour control after fractionated irradiation. Radiotherapy and oncology : journal of the European Society for Therapeutic Radiology and Oncology. 2010;96(1):116-22.
33. Overgaard J. Hypoxic radiosensitization: adored and ignored. Journal of clinical oncology : official journal of the American Society of Clinical Oncology. 2007;25(26):4066-74.
34. Kaanders JH, Wijffels KI, Marres HA, Ljungkvist AS, Pop LA, van den Hoogen FJ, et al. Pimonidazole binding and tumor vascularity predict for treatment outcome in head and neck cancer. Cancer research. 2002;62(23):7066-74.
35. Janssens GO, Rademakers SE, Terhaard CH, Doornaert PA, Bijl HP, van den Ende P, et al. Improved recurrence-free survival with ARCON for anemic patients with laryngeal cancer. Clinical cancer research : an official journal of the American Association for Cancer Research. 2014;20(5):1345-54.
36. Eustace A, Mani N, Span PN, Irlam JJ, Taylor J, Betts GN, et al. A 26-gene hypoxia signature predicts benefit from hypoxia-modifying therapy in laryngeal cancer but not bladder cancer. Clinical cancer research : an official journal of the American Association for Cancer Research. 2013;19(17):4879-88.
37. Buffa FM, Harris AL, West CM, Miller CJ. Large meta-analysis of multiple cancers reveals a common, compact and highly prognostic hypoxia metagene. British journal of cancer. 2010;102(2):428-35.
38. Helbig L, Koi L, Bruchner K, Gurtner K, Hess-Stumpp H, Unterschemmann K, et al. Hypoxia-inducible factor pathway inhibition resolves tumor hypoxia and improves local tumor control after single-dose irradiation. International journal of radiation oncology, biology, physics. 2014;88(1):159-66.
39. Fokas E, Im JH, Hill S, Yameen S, Stratford M, Beech J, et al. Dual inhibition of the PI3K/mTOR pathway increases tumor radiosensitivity by normalizing tumor vasculature. Cancer research. 2012;72(1):239-48.
40. Vaupel P, Mayer A. Hypoxia in cancer: significance and impact on clinical outcome. Cancer metastasis reviews. 2007;26(2):225-39.
41. Cvetkovic D, Movsas B, Dicker AP, Hanlon AL, Greenberg RE, Chapman JD, et al. Increased hypoxia correlates with increased expression of the angiogenesis marker vascular endothelial growth factor in human prostate cancer. Urology. 2001;57(4):821-5.
42. Semenza GL. The hypoxic tumor microenvironment: A driving force for breast cancer progression. Biochimica et biophysica acta. 2016;1863(3):382-91.

43. Brizel DM, Scully SP, Harrelson JM, Layfield LJ, Bean JM, Prosnitz LR, et al. Tumor oxygenation predicts for the likelihood of distant metastases in human soft tissue sarcoma. Cancer research. 1996;56(5):941-3.
44. Jung HY, Fattet L, Yang J. Molecular pathways: linking tumor microenvironment to epithelial-mesenchymal transition in metastasis. Clinical cancer research : an official journal of the American Association for Cancer Research. 2015;21(5):962-8.
45. Zhang L, Hill RP. Hypoxia enhances metastatic efficiency by up-regulating Mdm2 in KHT cells and increasing resistance to apoptosis. Cancer research. 2004;64(12):4180-9.
46. Bristow RG, Hill RP. Hypoxia and metabolism. Hypoxia, DNA repair and genetic instability. Nature reviews Cancer. 2008;8(3):180-92.
47. Luoto KR, Kumareswaran R, Bristow RG. Tumor hypoxia as a driving force in genetic instability. Genome integrity. 2013;4(1):5.
48. Lalonde E, Ishkanian AS, Sykes J, Fraser M, Ross-Adams H, Erho N, et al. Tumour genomic and microenvironmental heterogeneity for integrated prediction of 5-year biochemical recurrence of prostate cancer: a retrospective cohort study. The Lancet Oncology. 2014;15(13):1521-32.
49. Witsch E, Sela M, Yarden Y. Roles for growth factors in cancer progression. Physiology. 2010;25(2):85-101.
50. Chen EY, Mazure NM, Cooper JA, Giaccia AJ. Hypoxia activates a platelet-derived growth factor receptor/phosphatidylinositol 3-kinase/Akt pathway that results in glycogen synthase kinase-3 inactivation. Cancer research. 2001;61(6):2429-33.
51. Caniggia I, Mostachfi H, Winter J, Gassmann M, Lye SJ, Kuliszewski M, et al. Hypoxia-inducible factor-1 mediates the biological effects of oxygen on human trophoblast differentiation through TGFbeta(3). The Journal of clinical investigation. 2000;105(5):577-87.
52. Koumenis C, Naczki C, Koritzinsky M, Rastani S, Diehl A, Sonenberg N, et al. Regulation of protein synthesis by hypoxia via activation of the endoplasmic reticulum kinase PERK and phosphorylation of the translation initiation factor eIF2alpha. Molecular and cellular biology. 2002;22(21):7405-16.
53. Bi M, Naczki C, Koritzinsky M, Fels D, Blais J, Hu N, et al. ER stress-regulated translation increases tolerance to extreme hypoxia and promotes tumor growth. The EMBO journal. 2005;24(19):3470-81.
54. Wouters BG, Koritzinsky M. Hypoxia signalling through mTOR and the unfolded protein response in cancer. Nature reviews Cancer. 2008;8(11):851-64.
55. Wouters BG, van den Beucken T, Magagnin MG, Koritzinsky M, Fels D, Koumenis C. Control of the hypoxic response through regulation of mRNA translation. Seminars in cell & developmental biology. 2005;16(4-5):487-501.
56. Parks SK, Cormerais Y, Marchiq I, Pouyssegur J. Hypoxia optimises tumour growth by controlling nutrient import and acidic metabolite export. Molecular aspects of medicine. 2016;47-48:3-14.
57. Graeber TG, Osmanian C, Jacks T, Housman DE, Koch CJ, Lowe SW, et al. Hypoxia-mediated selection of cells with diminished apoptotic potential in solid tumours. Nature. 1996;379(6560):88-91.
58. Dong Z, Venkatachalam MA, Wang J, Patel Y, Saikumar P, Semenza GL, et al. Up-regulation of apoptosis inhibitory protein IAP-2 by hypoxia. Hif-1-independent mechanisms. The Journal of biological chemistry. 2001;276(22):18702-9.
59. Papandreou I, Lim AL, Laderoute K, Denko NC. Hypoxia signals autophagy in tumor cells via AMPK activity, independent of HIF-1, BNIP3, and BNIP3L. Cell death and differentiation. 2008;15(10):1572-81.
60. Chaachouay H, Fehrenbacher B, Toulany M, Schaller M, Multhoff G, Rodemann HP. AMPK-independent autophagy promotes radioresistance of human tumor cells under clinical relevant hypoxia in vitro. Radiotherapy and oncology : journal of the European Society for Therapeutic Radiology and Oncology. 2015;116(3):409-16.
61. Valko M, Leibfritz D, Moncol J, Cronin MT, Mazur M, Telser J. Free radicals and antioxidants in normal physiological functions and human disease. The international journal of biochemistry & cell biology. 2007;39(1):44-84.
62. Koch CJ, Stobbe CC, Bump EA. The effect on the Km for radiosensitization at 0 degree C of thiol depletion by diethylmaleate pretreatment: quantitative differences found using the radiation sensitizing agent misonidazole or oxygen. Radiation research. 1984;98(1):141-53.
63. Grimes DR, Partridge M. A mechanistic investigation of the oxygen fixation hypothesis and oxygen enhancement ratio. Biomedical physics & engineering express. 2015;1(4):045209.
64. Horsman MR, Wouters B, Joiner MC, Overgaard J. Basic Clinical Radiobiology. In: Joiner M, Van der Kogel AJ, editors. 4: Hodder Arnold; 2009. p. 207-16.

65. Spitz DR, Azzam EI, Li JJ, Gius D. Metabolic oxidation/reduction reactions and cellular responses to ionizing radiation: a unifying concept in stress response biology. Cancer metastasis reviews. 2004;23(3-4):311-22.
66. Li C, Jackson RM. Reactive species mechanisms of cellular hypoxia-reoxygenation injury. American journal of physiology Cell physiology. 2002;282(2):C227-41.
67. Hoeijmakers JH. Genome maintenance mechanisms for preventing cancer. Nature. 2001;411(6835):366-74.
68. Helleday T, Lo J, van Gent DC, Engelward BP. DNA double-strand break repair: from mechanistic understanding to cancer treatment. DNA repair. 2007;6(7):923-35.
69. Paull TT, Lee JH. The Mre11/Rad50/Nbs1 complex and its role as a DNA double-strand break sensor for ATM. Cell cycle. 2005;4(6):737-40.
70. Ward I, Chen J. Early events in the DNA damage response. Current topics in developmental biology. 2004;63:1-35.
71. Pallis AG, Karamouzis MV. DNA repair pathways and their implication in cancer treatment. Cancer metastasis reviews. 2010;29(4):677-85.
72. Harper JW, Elledge SJ. The DNA damage response: ten years after. Molecular cell. 2007;28(5):739-45.
73. Wouters B, Begg AC. Basic Clinical Radiobiology. In: Joiner M, Van der Kogel AJ, editors. 4. UK: Hodder Arnold; 2009. p. 11-26.
74. Sonoda E, Hochegger H, Saberi A, Taniguchi Y, Takeda S. Differential usage of non-homologous end-joining and homologous recombination in double strand break repair. DNA repair. 2006;5(9-10):1021-9.
75. Lieber MR. The mechanism of human nonhomologous DNA end joining. The Journal of biological chemistry. 2008;283(1):1-5.
76. Hosoya N, Miyagawa K. Targeting DNA damage response in cancer therapy. Cancer science. 2014;105(4):370-88.
77. Surova O, Zhivotovsky B. Various modes of cell death induced by DNA damage. Oncogene. 2013;32(33):3789-97.
78. van Attikum H, Gasser SM. Crosstalk between histone modifications during the DNA damage response. Trends in cell biology. 2009;19(5):207-17.
79. Kinner A, Wu W, Staudt C, Iliakis G. Gamma-H2AX in recognition and signaling of DNA double-strand breaks in the context of chromatin. Nucleic acids research. 2008;36(17):5678-94.
80. Rogakou EP, Pilch DR, Orr AH, Ivanova VS, Bonner WM. DNA double-stranded breaks induce histone H2AX phosphorylation on serine 139. The Journal of biological chemistry. 1998;273(10):5858-68.
81. Burma S, Chen BP, Murphy M, Kurimasa A, Chen DJ. ATM phosphorylates histone H2AX in response to DNA double-strand breaks. The Journal of biological chemistry. 2001;276(45):42462-7.
82. Sedelnikova OA, Rogakou EP, Panyutin IG, Bonner WM. Quantitative detection of (125)IdU-induced DNA double-strand breaks with gamma-H2AX antibody. Radiation research. 2002;158(4):486-92.
83. Rothkamm K, Lobrich M. Evidence for a lack of DNA double-strand break repair in human cells exposed to very low x-ray doses. Proceedings of the National Academy of Sciences of the United States of America. 2003;100(9):5057-62.
84. Keogh MC, Kim JA, Downey M, Fillingham J, Chowdhury D, Harrison JC, et al. A phosphatase complex that dephosphorylates gammaH2AX regulates DNA damage checkpoint recovery. Nature. 2006;439(7075):497-501.
85. Banath JP, Klokov D, MacPhail SH, Banuelos CA, Olive PL. Residual gammaH2AX foci as an indication of lethal DNA lesions. BMC cancer. 2010;10:4.
86. Lobrich M, Shibata A, Beucher A, Fisher A, Ensminger M, Goodarzi AA, et al. gammaH2AX foci analysis for monitoring DNA double-strand break repair: strengths, limitations and optimization. Cell cycle. 2010;9(4):662-9.
87. Klokov D, MacPhail SM, Banath JP, Byrne JP, Olive PL. Phosphorylated histone H2AX in relation to cell survival in tumor cells and xenografts exposed to single and fractionated doses of X-rays. Radiotherapy and oncology : journal of the European Society for Therapeutic Radiology and Oncology. 2006;80(2):223-9.
88. Banath JP, Macphail SH, Olive PL. Radiation sensitivity, H2AX phosphorylation, and kinetics of repair of DNA strand breaks in irradiated cervical cancer cell lines. Cancer research. 2004;64(19):7144-9.
89. Menegakis A, Yaromina A, Eicheler W, Dorfler A, Beuthien-Baumann B, Thames HD, et al. Prediction of clonogenic cell survival curves based on the number of residual DNA double strand breaks measured by gammaH2AX staining. International journal of radiation biology. 2009;85(11):1032-41.

90. McManus KJ, Hendzel MJ. ATM-dependent DNA damage-independent mitotic phosphorylation of H2AX in normally growing mammalian cells. Molecular biology of the cell. 2005;16(10):5013-25.
91. Yu T, MacPhail SH, Banath JP, Klokov D, Olive PL. Endogenous expression of phosphorylated histone H2AX in tumors in relation to DNA double-strand breaks and genomic instability. DNA repair. 2006;5(8):935-46.
92. Goodarzi AA, Noon AT, Deckbar D, Ziv Y, Shiloh Y, Lobrich M, et al. ATM signaling facilitates repair of DNA double-strand breaks associated with heterochromatin. Molecular cell. 2008;31(2):167-77.
93. Banath JP, Olive PL. Expression of phosphorylated histone H2AX as a surrogate of cell killing by drugs that create DNA double-strand breaks. Cancer research. 2003;63(15):4347-50.
94. Menegakis A, von Neubeck C, Yaromina A, Thames H, Hering S, Hennenlotter J, et al. gammaH2AX assay in ex vivo irradiated tumour specimens: A novel method to determine tumour radiation sensitivity in patient-derived material. Radiotherapy and oncology : journal of the European Society for Therapeutic Radiology and Oncology. 2015.
95. Ivashkevich A, Redon CE, Nakamura AJ, Martin RF, Martin OA. Use of the gamma-H2AX assay to monitor DNA damage and repair in translational cancer research. Cancer letters. 2012;327(1-2):123-33.
96. Kasten-Pisula U, Menegakis A, Brammer I, Borgmann K, Mansour WY, Degenhardt S, et al. The extreme radiosensitivity of the squamous cell carcinoma SKX is due to a defect in double-strand break repair. Radiotherapy and oncology : journal of the European Society for Therapeutic Radiology and Oncology. 2009;90(2):257-64.
97. Mansour WY, Bogdanova NV, Kasten-Pisula U, Rieckmann T, Kocher S, Borgmann K, et al. Aberrant overexpression of miR-421 downregulates ATM and leads to a pronounced DSB repair defect and clinical hypersensitivity in SKX squamous cell carcinoma. Radiotherapy and oncology : journal of the European Society for Therapeutic Radiology and Oncology. 2013;106(1):147-54.
98. Eicheler W, Zips D, Dorfler A, Grenman R, Baumann M. Splicing mutations in TP53 in human squamous cell carcinoma lines influence immunohistochemical detection. The journal of histochemistry and cytochemistry : official journal of the Histochemistry Society. 2002;50(2):197-204.
99. Koch U, Hohne K, von Neubeck C, Thames HD, Yaromina A, Dahm-Daphi J, et al. Residual gammaH2AX foci predict local tumour control after radiotherapy. Radiotherapy and oncology : journal of the European Society for Therapeutic Radiology and Oncology. 2013;108(3):434-9.
100. Suit HD, Zietman A, Tomkinson K, Ramsay J, Gerweck L, Sedlacek R. Radiation response of xenografts of a human squamous cell carcinoma and a glioblastoma multiforme: a progress report. International journal of radiation oncology, biology, physics. 1990;18(2):365-73.
101. Petersen C, Baumann M, Dubben HH, Arps H, Melenkeit A, Helfrich J. Linear-quadratic analysis of tumour response to fractionated radiotherapy: a study on human squamous cell carcinoma xenografts. International journal of radiation biology. 1998;73(2):197-205.
102. Laemmli UK. Cleavage of structural proteins during the assembly of the head of bacteriophage T4. Nature. 1970;227(5259):680-5.
103. Hammond EM, Dorie MJ, Giaccia AJ. Inhibition of ATR leads to increased sensitivity to hypoxia/reoxygenation. Cancer research. 2004;64(18):6556-62.
104. Bindra RS, Schaffer PJ, Meng A, Woo J, Maseide K, Roth ME, et al. Alterations in DNA repair gene expression under hypoxia: elucidating the mechanisms of hypoxia-induced genetic instability. Annals of the New York Academy of Sciences. 2005;1059:184-95.
105. Bindra RS, Schaffer PJ, Meng A, Woo J, Maseide K, Roth ME, et al. Down-regulation of Rad51 and decreased homologous recombination in hypoxic cancer cells. Molecular and cellular biology. 2004;24(19):8504-18.
106. Kumareswaran R, Ludkovski O, Meng A, Sykes J, Pintilie M, Bristow RG. Chronic hypoxia compromises repair of DNA double-strand breaks to drive genetic instability. Journal of cell science. 2012;125(Pt 1):189-99.
107. Janssen HL, Haustermans KM, Sprong D, Blommestijn G, Hofland I, Hoebers FJ, et al. HIF-1A, pimonidazole, and iododeoxyuridine to estimate hypoxia and perfusion in human head-and-neck tumors. International journal of radiation oncology, biology, physics. 2002;54(5):1537-49.
108. Helleday T, Petermann E, Lundin C, Hodgson B, Sharma RA. DNA repair pathways as targets for cancer therapy. Nature reviews Cancer. 2008;8(3):193-204.
109. Wada S, Van Khoa T, Kobayashi Y, Funayama T, Ogihara K, Ueno S, et al. Prediction of cellular radiosensitivity from DNA damage induced by gamma-rays and carbon ion irradiation in canine tumor cells. The Journal of veterinary medical science / the Japanese Society of Veterinary Science. 2005;67(11):1089-95.

110. MacPhail SH, Banath JP, Yu TY, Chu EH, Lambur H, Olive PL. Expression of phosphorylated histone H2AX in cultured cell lines following exposure to X-rays. International journal of radiation biology. 2003;79(5):351-8.
111. Mirzayans R, Severin D, Murray D. Relationship between DNA double-strand break rejoining and cell survival after exposure to ionizing radiation in human fibroblast strains with differing ATM/p53 status: implications for evaluation of clinical radiosensitivity. International journal of radiation oncology, biology, physics. 2006;66(5):1498-505.
112. Koritzinsky M, Magagnin MG, van den Beucken T, Seigneuric R, Savelkouls K, Dostie J, et al. Gene expression during acute and prolonged hypoxia is regulated by distinct mechanisms of translational control. The EMBO journal. 2006;25(5):1114-25.
113. Baxter GC, Stanners CP. The effect of protein degradation on cellular growth characteristics. Journal of cellular physiology. 1978;96(2):139-45.
114. Blais JD, Filipenko V, Bi M, Harding HP, Ron D, Koumenis C, et al. Activating transcription factor 4 is translationally regulated by hypoxic stress. Molecular and cellular biology. 2004;24(17):7469-82.
115. Spiro IJ, Rice GC, Durand RE, Stickler R, Ling CC. Cell killing, radiosensitization and cell cycle redistribution induced by chronic hypoxia. International journal of radiation oncology, biology, physics. 1984;10(8):1275-80.
116. Papandreou I, Krishna C, Kaper F, Cai D, Giaccia AJ, Denko NC. Anoxia is necessary for tumor cell toxicity caused by a low-oxygen environment. Cancer research. 2005;65(8):3171-8.
117. Hammond EM, Denko NC, Dorie MJ, Abraham RT, Giaccia AJ. Hypoxia links ATR and p53 through replication arrest. Molecular and cellular biology. 2002;22(6):1834-43.
118. Chan N, Koritzinsky M, Zhao H, Bindra R, Glazer PM, Powell S, et al. Chronic hypoxia decreases synthesis of homologous recombination proteins to offset chemoresistance and radioresistance. Cancer research. 2008;68(2):605-14.
119. Hall EJ, Giaccia AJ. Oxygen effect and reoxygenation. 7 ed. Radiobiology for the Radiologist: Lippincott Williams & Wilkins; 2012.
120. Kimura H, Braun RD, Ong ET, Hsu R, Secomb TW, Papahadjopoulos D, et al. Fluctuations in red cell flux in tumor microvessels can lead to transient hypoxia and reoxygenation in tumor parenchyma. Cancer research. 1996;56(23):5522-8.
121. Reynolds TY, Rockwell S, Glazer PM. Genetic instability induced by the tumor microenvironment. Cancer research. 1996;56(24):5754-7.
122. Freiberg RA, Krieg AJ, Giaccia AJ, Hammond EM. Checking in on hypoxia/reoxygenation. Cell cycle. 2006;5(12):1304-7.
123. Gibson SL, Bindra RS, Glazer PM. Hypoxia-induced phosphorylation of Chk2 in an ataxia telangiectasia mutated-dependent manner. Cancer research. 2005;65(23):10734-41.
124. Zolzer F, Streffer C. Increased radiosensitivity with chronic hypoxia in four human tumor cell lines. International journal of radiation oncology, biology, physics. 2002;54(3):910-20.
125. Bencokova Z, Kaufmann MR, Pires IM, Lecane PS, Giaccia AJ, Hammond EM. ATM activation and signaling under hypoxic conditions. Molecular and cellular biology. 2009;29(2):526-37.
126. Hammond EM, Dorie MJ, Giaccia AJ. ATR/ATM targets are phosphorylated by ATR in response to hypoxia and ATM in response to reoxygenation. The Journal of biological chemistry. 2003;278(14):12207-13.
127. Tsuchimoto T, Sakata K, Someya M, Yamamoto H, Hirayama R, Matsumoto Y, et al. Gene expression associated with DNA-dependent protein kinase activity under normoxia, hypoxia, and reoxygenation. Journal of radiation research. 2011;52(4):464-71.
128. Um JH, Kang CD, Bae JH, Shin GG, Kim DW, Kim DW, et al. Association of DNA-dependent protein kinase with hypoxia inducible factor-1 and its implication in resistance to anticancer drugs in hypoxic tumor cells. Experimental & molecular medicine. 2004;36(3):233-42.
129. Harris AL. Hypoxia--a key regulatory factor in tumour growth. Nature reviews Cancer. 2002;2(1):38-47.
130. Bindra RS, Glazer PM. Repression of RAD51 gene expression by E2F4/p130 complexes in hypoxia. Oncogene. 2007;26(14):2048-57.
131. Kumareswaran R, Chaudary N, Jaluba K, Meng A, Sykes J, Borhan A, et al. Cyclic hypoxia does not alter RAD51 expression or PARP inhibitor cell kill in tumor cells. Radiotherapy and oncology : journal of the European Society for Therapeutic Radiology and Oncology. 2015.
132. Koshiji M, Kageyama Y, Pete EA, Horikawa I, Barrett JC, Huang LE. HIF-1alpha induces cell cycle arrest by functionally counteracting Myc. The EMBO journal. 2004;23(9):1949-56.

133. To KK, Sedelnikova OA, Samons M, Bonner WM, Huang LE. The phosphorylation status of PAS-B distinguishes HIF-1alpha from HIF-2alpha in NBS1 repression. The EMBO journal. 2006;25(20):4784-94.
134. Sprong D, Janssen HL, Vens C, Begg AC. Resistance of hypoxic cells to ionizing radiation is influenced by homologous recombination status. International journal of radiation oncology, biology, physics. 2006;64(2):562-72.
135. Cam H, Easton JB, High A, Houghton PJ. mTORC1 signaling under hypoxic conditions is controlled by ATM-dependent phosphorylation of HIF-1alpha. Molecular cell. 2010;40(4):509-20.
136. Liu L, Cash TP, Jones RG, Keith B, Thompson CB, Simon MC. Hypoxia-induced energy stress regulates mRNA translation and cell growth. Molecular cell. 2006;21(4):521-31.
137. Arsham AM, Howell JJ, Simon MC. A novel hypoxia-inducible factor-independent hypoxic response regulating mammalian target of rapamycin and its targets. The Journal of biological chemistry. 2003;278(32):29655-60.
138. Madan E, Gogna R, Pati U. p53 Ser15 phosphorylation disrupts the p53-RPA70 complex and induces RPA70-mediated DNA repair in hypoxia. The Biochemical journal. 2012;443(3):811-20.
139. Wirthner R, Wrann S, Balamurugan K, Wenger RH, Stiehl DP. Impaired DNA double-strand break repair contributes to chemoresistance in HIF-1 alpha-deficient mouse embryonic fibroblasts. Carcinogenesis. 2008;29(12):2306-16.
140. Sedelnikova OA, Horikawa I, Zimonjic DB, Popescu NC, Bonner WM, Barrett JC. Senescing human cells and ageing mice accumulate DNA lesions with unrepairable double-strand breaks. Nature cell biology. 2004;6(2):168-70.
141. Mathew R, Karantza-Wadsworth V, White E. Role of autophagy in cancer. Nature reviews Cancer. 2007;7(12):961-7.
142. Hoyer-Hansen M, Jaattela M. Connecting endoplasmic reticulum stress to autophagy by unfolded protein response and calcium. Cell death and differentiation. 2007;14(9):1576-82.
143. Yaromina A, Krause M, Baumann M. Individualization of cancer treatment from radiotherapy perspective. Mol Oncol. 2012;6(2):211-21.

9 ERKLÄRUNG ZUM EIGENANTEIL DER DISSERTATIONSSCHRIFT

Die Arbeit wurde in der Universitätsklinik für Radioonkologie unter Betreuung von Herrn Prof. Dr. Daniel Zips und Herrn Dr. Apostolos Menegakis durchgeführt.

Die Konzeption der Studie erfolgte durch Herrn Prof. Dr. Daniel Zips, Doktorvater, Herrn apl. Prof. Dr. Mahmoud Toulany, und Herrn Dr. Apostolos Menegakis, Postdoktorand und Betreuer der Dissertation. Sämtliche Versuche wurden nach Einarbeitung durch Herrn Dr. Apostolos Menegakis, und Herrn Klaus Meyer von mir eigenständig durchgeführt. Die statistische Auswertung erfolgte eigenständig durch mich nach Anleitung durch Dr. Apostolos Menegakis.

Ich versichere, das Manuskript selbständig verfasst zu haben und keine weiteren als die von mir angegebenen Quellen verwendet zu haben.

Die Publikation, welche auf den Daten dieser Doktorarbeit basiert, wurde von mir unter Anleitung von Herrn Prof. Dr. Zips, Herrn Dr. Apostolos Menegakis und Herrn apl. Prof. Dr. Mahmoud Toulany selbstständig verfasst. Die Korrektur des Manuskripts erfolgte ebenfalls durch Herrn Prof. Dr. Zips, Herrn Dr. Apostolos Menegakis und Herrn apl. Prof. Dr. Mahmoud Toulany.

Tübingen, den 14.06.2017 Franziska Hauth

10 VERÖFFENTLICHUNGEN

Teile der vorliegenden Dissertationsschrift wurden bereits veröffentlicht:

Authors:	Hauth, F; Toulany, M; Zips, D; Menegakis, A
Titel:	Cell-line dependent effects of hypoxia prior to irradiation in squamous cell carcinoma lines
Journal:	Clinical and Translational Radiation Oncology
Year:	2017

11 DANKSAGUNG

Mein besonderer Dank gilt meinem Doktorvater Herrn Prof. Dr. med. Daniel Zips und meinem Betreuer Herrn Dr. sc. hum. Apostolos Menegakis für die intensive Betreuung meiner Doktorarbeit, das spannende Thema und das exzellente Betreuungsverhältnis.

Bei Herrn Prof. Dr. Rodemann und dem Team der Sektion für Strahlenbiologie und molekularer Umweltforschung möchte ich mich sehr für die gute Arbeitsatmosphäre und die guten fachlichen Diskussionen bedanken. Insbesondere möchte ich mich hier bei Herrn apl. Prof. Dr. Mahmoud Toulany für die Einarbeitung in die Arbeit mit Western Blot Assays und die Betreuung dieser Arbeiten bedanken. Dank gilt auch dem Team der experimentellen Radioonkologie unter der Leitung von Prof. Dr. Huber.

Danken möchte ich auch Frau Prof. Dr. Marlies Knippers und Frau Dr. Inka Montero vom Interdisziplinären Zentrum für Klinische Forschung (IZKF) der medizinischen Fakultät der Universität Tübingen für die Betreuung während des Promotionskollegs und die finanzielle Unterstützung meiner Doktorarbeit.

Herrn Prof. Dr. Michael Baumann (ehemals: Direktor der Klinik für Strahlentherapie und Radioonkologie, Universitätsklinikum Carl Gustav Carus Dresden; Direktor am Institut für Radioonkologie, Helmholz-Zentrum Dresden-Rossendorf; Direktor des OncoRay-Zentrum, Dresden; aktuell: Vorstandsvorsitzender und wissenschaftlicher Vorstand, DKFZ, Heidelberg) und Frau Prof. Dr. Mechthild Krause (Direktorin der Klinik für Strahlentherapie und Radioonkologie, Universitätsklinikum Carl Gustav Carus Dresden; Direktorin am Institut für Radioonkologie, Helmholz-Zentrum Dresden-Rossendorf; Direktorin des OncoRay-Zentrum, Dresden) möchte ich für die Bereitstellung der in dieser Doktorarbeit verwendeten Zelllinien danken.

Besonders möchte ich mich natürlich noch bei meiner Familie und meinen Freunden bedanken, die mich in dieser Zeit begleitet und unterstützt haben.